Characterisation of bioactive proteins present in *Actinidia* species

A thesis submitted in partial fulfilment
of the requirements for the degree of

Master of Science

at the

School of Biological Sciences,
University of Canterbury

by

Eric William Richards

2014

Table of Contents

Acknowledgements

Foremost, I would like to thank my two supervisors, Grant Pearce and Andrew Muscroft-Taylor, for questioning and critiquing my results and ideas. Although hard at times, your guidance has moulded me into a better scientist, for which I am grateful for. You were always willing to talk to me and showed me that being pro-active and independent are rewarding.

Equally, I thank Dion Thompson whom I regarded as a third supervisor. The guidance that you gave helped immensely. I enjoyed discussing results and theories with you.

Jackie, thank you for taking the time to assist me with laboratory protocols and etiquette. I would also like to especially thank Amy Yewdall, Jeremy Keown, Moritz Lassé, and Antonia Miller who helped me with technical problems I had throughout the project. Countless others in the School of Biological Sciences have guided me and this was much appreciated. Without all of you my time here would not have been as enjoyable and I wish you all the best for your own research projects.

A special mention must go to everyone who was a part of room 625. I certainly did not anticipate that my time as a research student would be as much fun as what it was. Without your outgoing personalities and quirky conversations the memories would not have been as great.

I would like to acknowledge Ultimate Frisbee. I have spent many evenings and study breaks playing, training, and thinking about this peculiar sport. The team attitude and community has made me strive to be better both on and off the field (injury permitting).

Having a balanced life could not have been possible without my friends and flatmates. Discussing aspects of life other than science kept me sane, which was much appreciated. I look forward to sharing more time with you all in the future.

Lastly to my family, thank you for your patience and support. It was always comforting to know that you were there if I needed help. I truly appreciated it.

Abstract

Kiwifruit consumption is well known to have a positive impact on digestive health. Actinidin and kiwellin, two kiwifruit proteins have been characterised because of their importance in Actazin™ that is produced from kiwifruit to aid digestion. A biophysical characterisation was carried out for both proteins and the catalytic activity of actinidin was measured during the production of Actazin™ to assess if kiwifruit processing was detrimental to the catalytic rate.

Actinidin, purified from *A. deliciosa* cultivar showed that a decrease in enzymatic activity could be from partially inactivated actinidin. Similarly actinidin from Actazin™ became inactivated when the powder was solubilised in buffer. Most of the lost activity could be recovered when a reductant was added and it is hypothesised that the catalytically important cysteine residue was becoming oxidised by a chemical species that was present in the solubilised kiwifruit powder.

Freezing, thawing, and storing the processed kiwifruit pulp resulted in the largest drop of total actinidin activity of 46%. Freeze drying the frozen pulp surprisingly did not significantly affect the retention of actinidin despite incurring prolonged heat stress. Further studies that assess the effects that freezing and thawing have on the stability of actinidin is therefore suggested.

Kiwellin was characterised using a number of analytical techniques and was shown to be a monomeric protein in solution that had a high melting point. It was suggested that disulfide bonds and salt bridges could be stabilising kiwellin, which was also highly dynamic in solution. Kiwellin did not show the presence of any secondary structures, which is in contrast to previous studies and small angle X-ray scattering revealed that kiwellin had an elongated shape. The dynamic nature of the protein may have implications for the interactions between kiwellin and actinidin, which has been previously shown and this could be related to the physiological function of kiwellin.

Abbreviations

2ACT	PDB classified crystal structure of actinidin
9PAP	PDB classified crystal structure of papain
Å	Angstrom
A_{280}	absorbance at 280 nm
Asn-182	asparagine residue at position 182
AUC	analytical ultracentrifugation
BLAST	basic local alignment sequence tool
BSA	bovine serum albumin
^{o}C	degrees Celsius
CBZ-Lys-ONP	N-α-carbobenzoxy-L-lysine-*p*-nitrophenyl ester
CD	circular dichroism spectroscopy
c(*M*)	continuous mass distribution
Cys-25	cysteine residue at position 25
Da	Daltons
D_{max}	maximum distance
DSF	differential scanning fluorimetry
DTT	dithiothreitol
EDTA	ethylenediaminetetraacetic acid
ESI-MS	electro spray ionisation mass spectroscopy
EST	expressed sequence tag
GrK	green kiwifruit (*Actinidia deliciosa* cv. Hayward)
GoK	gold kiwifruit (*Actinidia chinensis*)
His-162	histidine residue at position 162
K_m	Michaelis-Menten constant

k_{cat}	catalytic constant
MALDI-TOF	matrix-assisted laser desorption/ionization time-of-flight mass spectrometry
p </> 0.05/1	probability of statistical significance
PDB	protein data bank
pI	isoelectric point
P(*r*)	pair distribution function plot
Psa	*Pseudomonas syringae* pv. *actinidiae*
RALS	right angle light scattering
rcf	relative centrifugal force
R_g	radius of gyration
RI	refractive index
room temperature	20^oC
r.m.s.d.	root mean square deviation
S	Svedburgs
SAXS	small angle X-ray scattering
SDS-PAGE	sodium dodecyl sulfate polyacrylamide gel electrophoresis
SEC/SLS	size exclusion chromatography static light scattering
SSC	soluble solid content
T_m	melting temperature
UV	ultraviolet
vitamin C	ascorbate dibasic sodium salt
V_{max}	maximum velocity
Q-Q plot	quartile-quartile plot

Table of Figures

List of Tables

List of Equations

Chapter One : Introduction

1.1 Overview

Since the introduction of kiwifruit vines to New Zealand in the 1900's the industry has grown and is now a major contributor to the economy. Improved growing practices and a unified global marketing campaign from Zespri International Ltd has allowed New Zealand growers to produce large quantities of fruit each season and export this to a global market. A significant portion of the fruit produced is classified as 'process grade' and can be used to develop kiwifruit products, such as those in the health food industry. The growing awareness of consumers to the nutritional value of foods has increased the demand for naturally derived food products that have a beneficial impact on health. Kiwifruit consumption has been shown to have positive impacts on health and can relieve symptoms of disease states, such as those involving the digestive system. Fibre, bulking, and bioactive proteins, that are unique to kiwifruit are attributed to the improvements seen in digestive health.

This Master's thesis is a collaborative research project with the biotechnology company Anagenix Ltd which produces the kiwifruit product, Actazin™, which is sold as a digestive aid. The aim of this thesis is to understand how various factors during the production of Actazin™ affect the activity and stability of the bioactive protein, actinidin. Additionally we aim to further characterise actinidin and kiwellin, another kiwifruit protein.

1.2 Introduction to the kiwifruit industry in New Zealand

1.2.1 Kiwifruit production in New Zealand

Kiwifruit or Chinese gooseberry, is the fruit from a woody vine that is native to China. Seeds were first introduced into New Zealand in 1904 and these plants were used to develop cultivars that were grown in commercial orchards, which became established in the 1930's (Ferguson, 2004). Production in New Zealand has increased substantially since the first orchards were established. In 2012 New Zealand produced 376,400 tonnes of kiwifruit, which, when compared to other countries rated highly (Figure 1). In recent years, the

production has, however, declined and this has been the result of the widespread prevalence of the kiwifruit pathogen, *Pseudomonas syringae* pv. *actinidiae* (Psa) (Kiwifruit-Vine-Health, 2014). New cultivars that are resistant to Psa are expected to return the production to pre-Psa levels and will be important for the recovery of the kiwifruit industry (MPI, 2014). Europe and Asia are major export markets for kiwifruit produced in New Zealand (Zespri, 2013-2014) and the fruit is largely sold as fresh fruit during the kiwifruit off-season in the Northern Hemisphere.

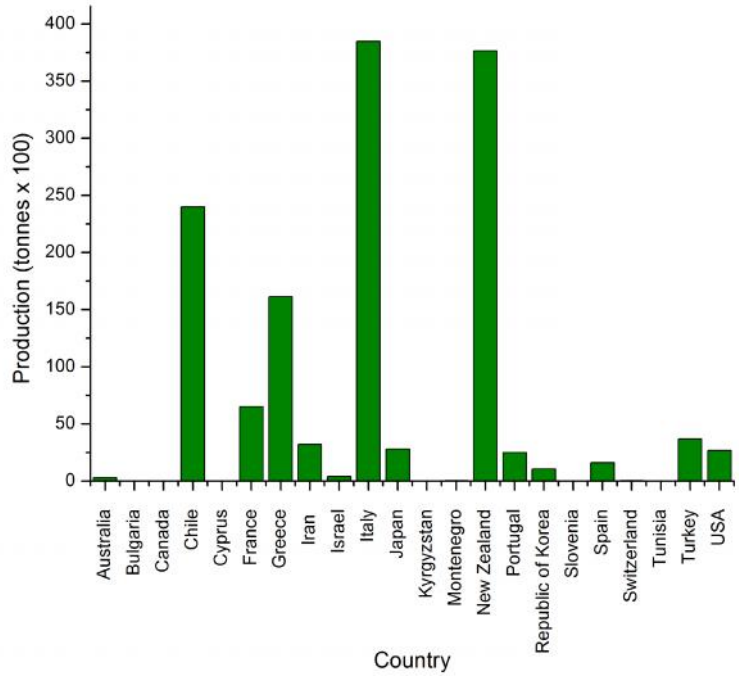

Figure 1: Global kiwifruit production in 2012 (FAOSTAT, 2012).

1.2.2 *Actinidia* genus

Kiwifruit belong to the genus *Actinidia*. There are 55 species recognised in this genus and several species are commercial grown, such as *A. deliciosa, A, chinensis, A. arguta, A. eriantha, A. kolomikta,* and *A. polygama* (Datson *et al.*, 2011). *A. deliciosa* cv. Hayward is the most widely grown cultivar and is often referred to as green kiwifruit. *A. chinensis* cultivars are also widely distributed and new cultivars like Zespri® Hort16a and SunGold (gold kiwifruit) are increasingly popular due to the desirable flavour and textural properties that these cultivars have. Overall green kiwifruit accounts for approximately 85% of commercial kiwifruit grown in New Zealand, while gold kiwifruit accounts for the remaining 15% (Datson *et al.*, 2011). The diversity of species in the *Actinidia* genus has contributed to a

strong selective breeding program, which continually introduces new varieties that have desirable characteristics. One example of this is the introduction of Zespri® SunGold, which has an increased resistance to Psa when compared to other cultivars. This has had important economic implications for the kiwifruit industry in New Zealand after the pathogen devastated the Zespri® Hort16a crops (Zespri, 2013-2014).

1.2.3 Growing kiwifruit as a horticulture crop

Kiwifruit vines favour warm, moist and sheltered growing conditions, not unlike those experienced in regions of China that have a high presence of kiwifruit vines. The distribution of kiwifruit orchards in New Zealand reflect these growing conditions. The Bay of Plenty in the North Island of New Zealand is responsible for producing 77% of the total kiwifruit in the country (NZ-Statistics, 2007) and these growing conditions combined with improved growing practices which have resulted in substantial yields of kiwifruit. Kiwifruit yields per hectare in New Zealand are the highest in the world. This has resulted in a large national production of kiwifruit which is sold as fresh fruit or a processed product.

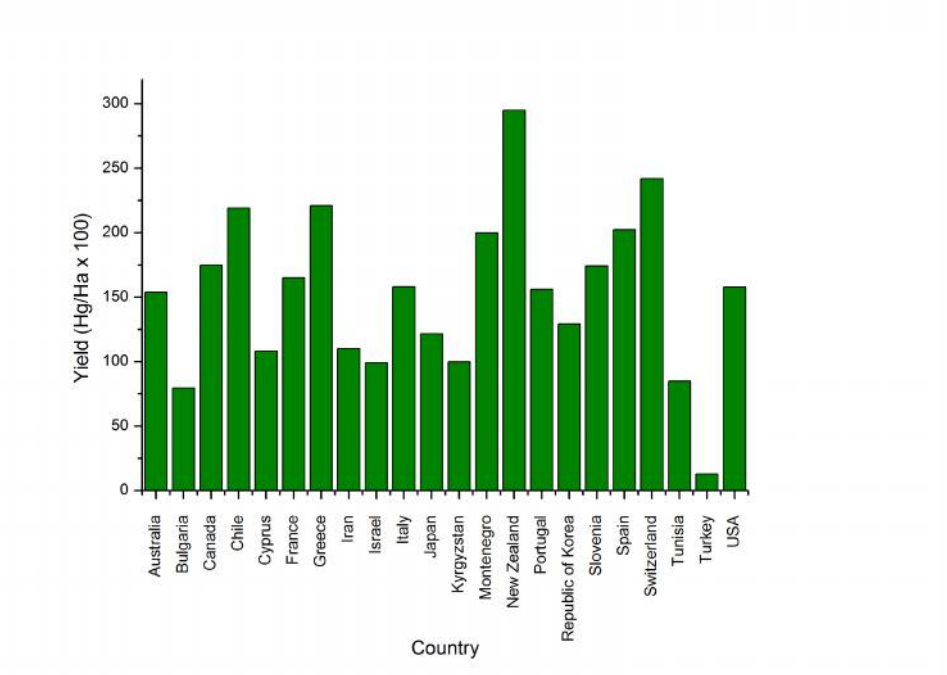

Figure 2: Global yields for kiwifruit harvests in units of hectograms per hectare (Hg/Ha) (FAOSTAT, 2012).

1.2.4 Economic importance to New Zealand

The kiwifruit export market contributes greatly to the New Zealand economy and this has been, in part, created by a global reputation of producing a high quality product. While Psa has been attributed to a recent loss in revenue, the export market of fresh fruit was still worth $817 million in the year ending March 2014 after 89 million trays were exported (MPI, 2014). As the industry recovers from Psa the economic returns are forecast to increase to over $1 billion by 2018. The marketing conducted by Zespri International Limited helps to increase the value of kiwifruit and this has consequently allowed New Zealand to be the world's largest seller of kiwifruit (Zespri, 2013-2014), despite only producing around a third of the world's total kiwifruit production (Figure 1). Advertising the nutritional content of kiwifruit is a key focus of the market campaigns used by companies in the kiwifruit industry and this has also promoted more scientific research to be conducted to understand the relationship between kiwifruit consumption and a healthy lifestyle.

1.3 Processed kiwifruit products

1.3.1 Actazin™ production

Up to one fifth of the harvested fruit is classified as 'process grade' and is not exported as a whole fruit (Warrington *et al.*, 1990). The process grade kiwifruit can be transformed into kiwifruit products that are sold in the health-food, beverage, and cosmetic industries. Actazin™ is a kiwifruit product that is produced by Anagenix Ltd from processed kiwifruit and utilises the bioactive components that are naturally present in kiwifruit to aid digestion. The production of Actazin™ involves pulping kiwifruit that is then freeze dried to produce a kiwifruit powder. The process is summarised in Figure 3 and several stages have been identified to be important for the production of Actazin™. These include: fruit harvesting, post-harvest ripening and storage, pulping, and freeze drying.

Fruit harvest

Kiwifruit used to produce Actazin™ is harvested between March and May in the Bay of Plenty. Commercial harvesting begins after the fruit has reached a certain stage of maturity. This stage is correlated with changes in the composition of the fruit, which makes the fruit desirable for consumption. Soluble solids concentration, flesh firmness, and sugar composition have all been measured as parameters that reflect the maturity of the fruit

(Bonvehi *et al.*, 1997) and are commonly measured to determine when the commercial harvest will commence.

Post-harvest ripening and storage

Harvested fruit is transported to a local pack house where the 'process grade' is separated from 'export grade' and 'reject grade' fruit. The fruit is then stored under cool storage before it is ready to be processed into a pulp. Fruit stored at a temperature of $0^{o}C \pm 0.5^{o}C$ with a relative humidity of at least 95% with no ethylene in the air has been found to be optimal for storing kiwifruit between 4-6 months (Warrington *et al.*, 1990). The fruit is ripened at ambient temperature (~12-15^{o}C) before it is pulped at the Kiwifruit Processing Company Ltd, which is also located in the Bay of Plenty. A qualitative firmness and sensory test of the ripened fruit confirms that the fruit is at a sufficient ripeness to be pulped. The fruit is also graded throughout the ripening to remove any fruit that is over ripe or spoiled as the result of microbial contamination.

Pulping

The pulping is an automated process that removes the skin, seeds, and central core from the kiwifruit. Part of the pulping process involves pressing of the kiwifruit skin so that any residual pulp is removed off the skin. The process from whole kiwifruit to a pulp takes approximately 3-5 minutes and is conducted under temperature control. Periodically the batches of pulp are tested to assess qualities, such as viscosity, sugar composition, and pH before the batches are blast frozen and stored at -20^{o}C.

Freeze drying

Freeze drying is conducted at Genesis Bio-Laboratory Ltd in Christchurch. Frozen blocks of the kiwifruit pulp are transported from the Bay of Plenty, under refrigeration upon the demand for Actazin™. The blocks are cut into ~1 cm thick slices and placed onto trays before being stored at -20^{o}C until the freeze drying commences. Freeze drying involves drying the frozen product by increasing the temperature inside a sealed freeze dryer that has low pressure. This removes the moisture without damaging the structural integrity of the product over a period between 24-48 hours. After the pulp has been sufficiently dried the resulting block of powder is milled to a powder in the presence of anti-caking agents before the powder is packaged for exporting.

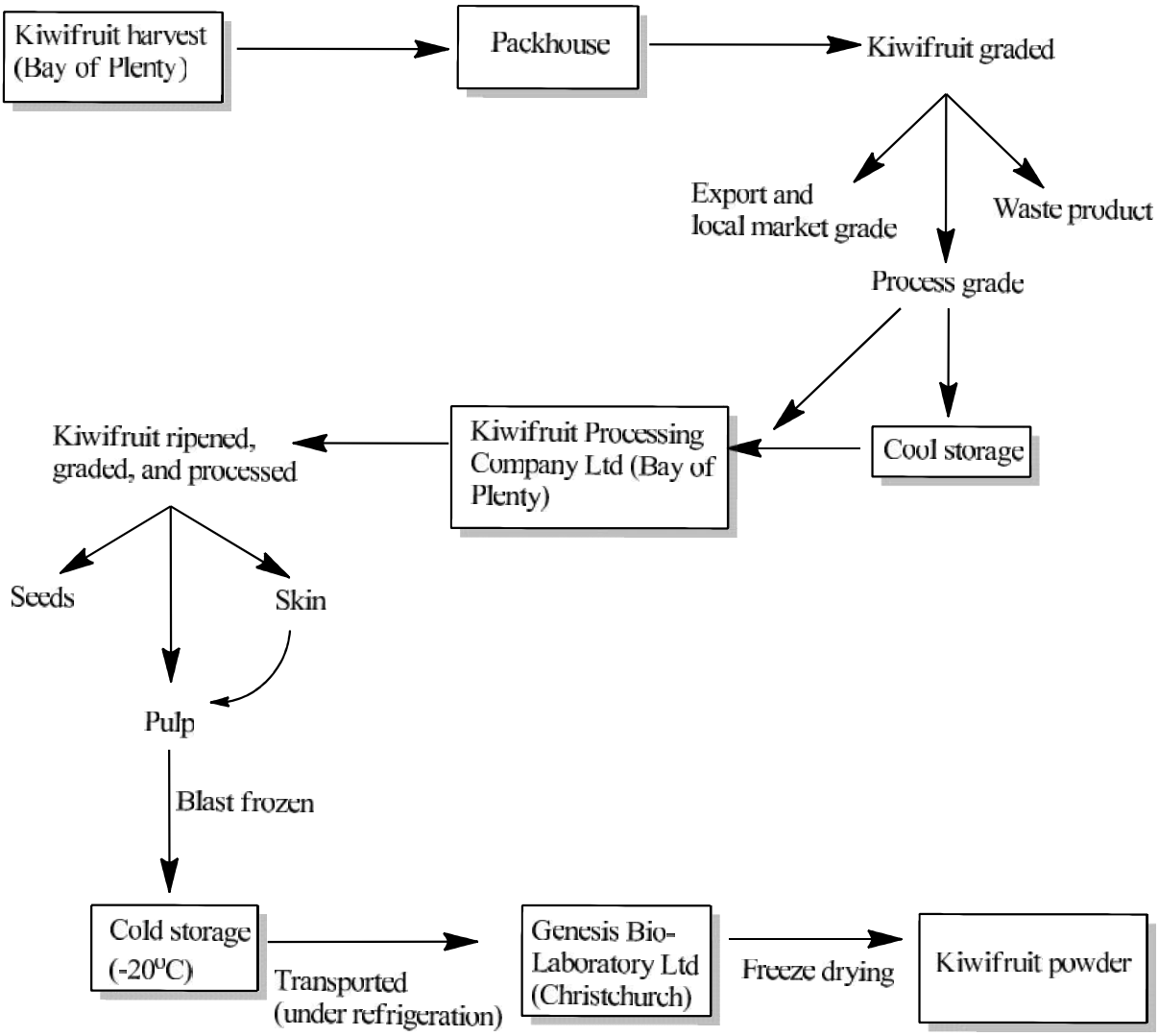

Figure 3: Process flow diagram of Actazin™ production.

1.4 Health benefits from kiwifruit consumption

1.4.1 Nutrients important for health

Regular consumption of fresh fruit and vegetables are well known to provide personal health benefits. Many of the health benefits are attributed to the presence of bioactive compounds in these natural products. For example antioxidant compounds, such as vitamin C have shown that they can have a protective effect for a variety of disease states, including several types of cancer (Steinmetz *et al.*, 1996) and also functional bowel disorders, which often incurs high oxidative stress (Russo *et al.*, 2012). A wide selection of plant proteins have also been shown to have bioactive properties and exhibits a wide diversity of implied health benefits such as

showing immunomodularoty, anti-hypertensive, anti-carcinogenic, anti-microbial and anti-inflammatory properties (Kitts *et al.*, 2003).

Kiwifruit is a rich source of nutrients, including bioactive compounds. In particular kiwifruit is a good source of several nutrients, such as dietary fibre, potassium, vitamin C, vitamin E, and folate. These nutrients heavily contribute to kiwifruit being regarded as 'nutrient dense' and a comparison with other common fruits shows that kiwifruit rates highly among them (Table 1). Other bioactive compounds that are found in kiwifruit include: polyphenols (Du *et al.*, 2009), flavonoids (Fiorentino *et al.*, 2009), and bioactive proteins (Maddumage *et al.*, 2013). Although the level of these compounds is not exceptionally higher than other fruits (USDA, 2011) they still provide important health benefits. For example the array of phytochemicals in *A. deliciosa* have shown high antioxidant and radical scavenging capabilites (Fiorentino *et al.*, 2009), and the bioactive protein, actinidin, that is unique to kiwifruit, is an important contributor to the digestive health benefits that kiwifruit have shown to provide (Chang *et al.*, 2010).

Table 1: Amount of selected nutrients (folate, vitamin E, vitamin C, potassium, dietary fibre) measured in common fruits (USDA, 2011)

Fruit	**Folate (µg) Per 100 g**	**Vitamin E (mg) Per 100 g**	**Vitamin C (mg) Per 100 g**	**Potassium (mg) Per 100 g**	**Fibre, total dietary (g) Per 100 g**
Apples, raw, fuji, with skin	3	0.2	--	109	2.1
Bananas, raw	20	0.1	8.7	358	2.6
Blueberries, raw	6	0.6	9.7	77	2.4
Grapes, muscadine, raw	2	0.2	6.5	203	3.9
Kiwifruit, gold, raw	**34**	**1.5**	**105.4**	**316**	**2.1**
Kiwifruit, green, raw	**25**	**1.5**	**92.7**	**312**	**3.0**
Oranges, raw,	30	0.2	53.2	181	2.4
Pears, raw	7	0.1	4.3	116	3.1
Pineapple, raw, all varieties	18	0.0	47.8	109	1.4
Strawberries, raw	24	0.3	58.8	153	2

1.4.2 An overview of health benefits from kiwifruit consumption

A wide range of health benefits have been attributed to kiwifruit consumption and this has had a major impact on marketing kiwifruit in increasingly health conscious societies. The strength of the health claims differs and this is correlated with the type and amount of research that has been conducted. Kiwifruit extracts have shown anti-microbial (Eshamah *et al.,* 2014), anti-cancer (Motohashi *et al.,* 2002), and anti-inflammatory (Edmunds *et al.,* 2011) properties using *in vitro* assays. This, however has been shown to not always be reliable when the assay is extrapolated to an *in vivo* system (Edmunds *et al.,* 2012). A number of clinical trials have been conducted which measured the effects that regular kiwifruit consumption have on disease-states, and this has provided more applicable data to the

benefits of kiwifruits on personal health. For example the anti-oxidant capacity (Ko *et al.*, 2005), risk of cardiovascular disease (Karlsen *et al.*, 2013), and DNA repair capacity (Brevik *et al.*, 2011) of patients all responded favorably during the trials. Digestive health can also be improved and there has been substantial evidence that consuming kiwifruit can relieve constipation in a number of populations (Chan *et al.*, 2007; Chang *et al.*, 2010; Rush *et al.*, 2002).

1.4.3 Improved digestive health

Digestive health problems

Functional bowel diseases are wide spread and can have severe implications on quality of life. Irritable bowel syndrome (IBS), one of the most common gastrointestinal disorders shows high prevalence in developed countrities and in 1998 there was upwards of 15 million cases in the United States, which directly and indirectly cost more than $1.5 billion to treat (Sandler *et al.*, 2002). According to the Rome III criteria IBS is diagnosed by symptoms, such as recurrent abdominal pain or discomfort and changes in stool form and frequency (Drossman, 2006). However a lack of a definitive diagnosis for IBS patients has prompted the use of a number of different treatment options, including pharmacologic treatments and increasing the uptake of dietary substances that have been shown to reduce the symptoms of IBS (Yoon *et al.*, 2011). The complexity of the disease and associated risk factors encourages further research and treatments for the symptoms that this disease can be responsible for.

Effects of kiwifruit on digestive flow

Improving digestive health in patients who suffer from constipation is desirable and kiwifruit consumption supports this goal. With a group of 33 patients who suffered from constipation Chan, *et al* (Chan *et al.*, 2007) demonstrated that ingesting kiwifruit twice daily for 4 weeks significantly improved the transit time and satisfaction of excretion when compared to a control group. Another clinical trial that measured the frequency of defecation in elderly on a similar kiwifruit diet also measured an increase and it was proposed that kiwifruit had a laxative effect in elderly populations (Rush *et al.*, 2002). A third study observed the effects that kiwifruit had on 41 patients who suffered from IBS and had symptoms of constipation. The findings suggested that kiwifruit consumed daily, for 4 weeks shortens colon transit time, increases defecation frequency, and improves bowel function in adults who have been diagnosed with IBS (Chang *et al.*, 2010). All of the above studies used kiwifruit from the

Actinidia deliciosa Hayward cultivar and clearly showed that in-comparison to a control group regular consumption of kiwifruit had a positive effect on digestive health.

Mechanism of action

Several components of kiwifruit are attributed to the mechanisms that increase defecation and which thereby relieves patients that are suffering from constipation. Diets high in dietary fibre are well known for promoting digestive health (Buttriss *et al.*, 2008) and research has shown that the fibre in kiwifruit shares these properties. Kiwifruit, similar to other fruits, is a good source of dietary fibre (Table 1). An intake of 100 g of green kiwifruit will provide around 10% of the recommended daily intake of fibre (Ministry-of-Health, 2003). Using an *in vitro* assay the properties of kiwifruit fibre (both soluble and insoluble) were investigated and was shown to have a strong water retention and swelling capacities, which will have positive implications for digesta transiting through the gastrointestinal tract (Mishra *et al.*, 2012). The bioactive protein, actinidin is also an important contributor to improved digestive health (Montoya *et al.*, 2014). Actinidin is a cysteine protease and catalytically functions by cleaving proteins (Rawlings *et al.*, 2012). Kiwifruit extracts containing actinidin have enhanced the digestion of proteins, particularly those from milk, meat, and cereals in a small intestine and gastric digestion *in vitro* model (Kaur *et al.*, 2010a, 2010b). Similarly actinidin from *Actinidia deliciosia* cv. Hayward in a freeze dried powder increased the gastric protein digestion in growing rats (Montoya *et al.*, 2014). The gastric emptying rate for some of the dietary proteins assessed also increased by up to 43% and this is likely to be a mechanism for kiwifruit increasing defecation that has previously been observed (Rush *et al.*, 2002). Kissper, another bioactive protein and the cleavage product of the precursor protein, kiwellin is also postulated to increase digestion by its pore-forming voltage gated activity observed in an intestinal cell *in vitro* model (Ciardiello *et al.*, 2008), however further investigation of this bioactive function is needed for confirmation.

Chapter Two : Actinidin Purification and Characterisation

2.1 Actinidin isoforms in kiwifruit

Actinidin is classified as a cysteine protease and cleaves peptide chains by enzymatic cleavage. The physiological function of actindin is largely unknown, however it may have a regulatory role of processing of other proteins, including kiwellin (Tuppo *et al.*, 2008) and a class 4 chitinase (Nieuwenhuizen *et al.*, 2012). The protease has also shown anti-bacterial activity (Eshamah *et al.*, 2014) and has limited the development of larvae for the leafworm, *Spodoptera litura.* This could imply that actinidin has a role in plant defence. These functions are similar to those proposed for other cysteine protease (Konno *et al.*, 2004; van der Hoorn, 2008).

Actinidin exists as multiple isoforms in kiwifruit. In *A. deliciosa*, 2 isoforms and 6 other cysteine proteases were identified (Nieuwenhuizen *et al.*, 2007) after a cDNA sequence of actinidin (Podivinsky *et al.*, 1989) was BLAST searched against a kiwifruit EST database (Crowhurst *et al.*, 2008). A phylogenetic comparison of plant cysteine proteases showed that despite conservation of several catalytically and structural important residues (Figure 4), the isoforms grouped into different clades (Nieuwenhuizen *et al.*, 2007). The KFAct clade had both the ACT1A isoform and the ACT2A isoform. The six other kiwifruit cysteine proteases (KFCp1-6) were grouped in a variety of clades that also contained cysteine proteases from other plant species. The isoforms and other cysteine proteases are expressed as preproproteins and contains a signal peptide and extension sequences at the N- and/ or C-terminals regions (Nieuwenhuizen *et al.*, 2007). It is hypothesised that actinidin is expressed as a zymogen and requires post-translational processing of these extension sequences before becoming active in its mature form (Podivinsky *et al.*, 1989), however the mechanism for processing has not yet been elucidated.

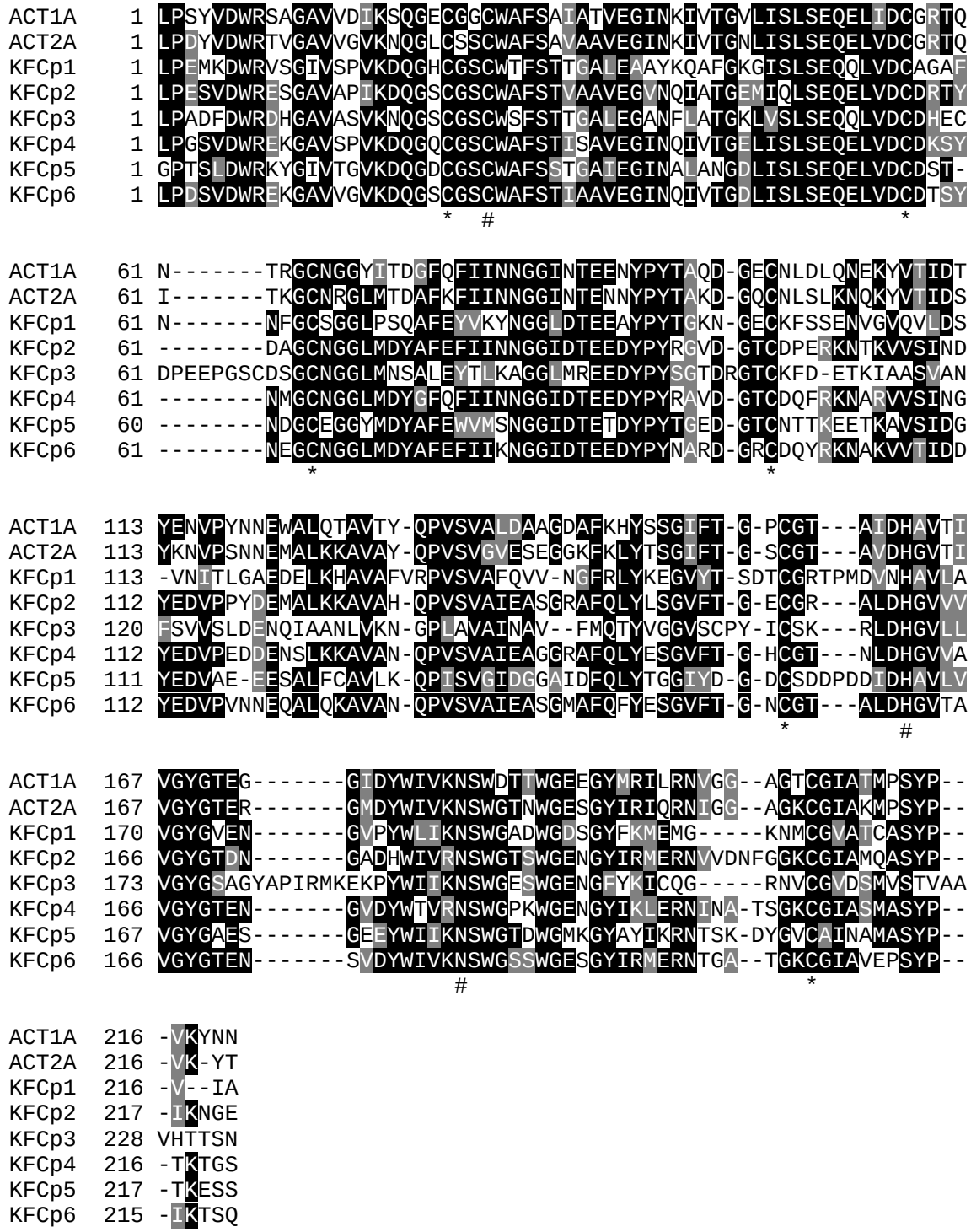

Figure 4: Alignment using T-Coffee (Notredame *et al.*, 2000; Tommaso *et al.*, 2011) of mature cysteine proteases found in *A. deliciosa* in their mature forms (Nieuwenhuizen *et al.*, 2007). Catalytically important residues (#) and cysteine residues that are involved in disulfide bonds (*) are conserved among the different isoforms.

2.2 Protocols used to purify actinidin

Actinidin has been well characterised and there are well established methods for protein purification that are used to obtain a purified sample. Actinidin is typically purified by extracting the enzyme from the fruit of the Hayward cultivar from the *A. deliciosa* species (GrK). The Hayward cultivar is a popular choice to extract actinidin for several different reason: the cultivar constituents 85% of the kiwifruit vines that are commercially grown (Datson *et al.,* 2011), the fruit has a high actinidin content when compared to other cultivars (Maddumage *et al.,* 2013), and the relative abundance of actinidin in the total soluble protein in GrK is approximately 40% (Ciardiello *et al.,* 2009). Actinidin has also been purified using Ni-affinity chromatography after it was recombinantly expressed in *Escherichia coli* cells (Nieuwenhuizen *et al.,* 2007).

Anion exchange chromatography is a common technique that is used to purify actinidin from GrK (Boland *et al.,* 1972). The ACT1A actinidin isoform has a isoelectric point (pI) of 4.1 (Nieuwenhuizen *et al.,* 2012), which enables actinidin to be separated from other kiwifruit proteins that have different pI values (Maddumage *et al.,* 2013). The ACT1A isoform is the major acidic isoform in *A. deliciosa*, however there are 6 other isoforms that are expressed in the kiwifruit that also have an acidic pI between the values of 3.7-4.7 (Table 2) and anion exchange chromatography has previously shown that it can be used to purify the different cysteine proteases in kiwifruit (Tello-Solis *et al.,* 1995). The different isoforms showed similarities between each other in their secondary structures (Tello-Solis *et al.,* 1995), however they have shown to have differences during enzymatic catalysis (Morimoto, 2002).

Table 2: Isoelectric point (pI) of actinidin, isoforms, and other cysteine proteases in *A. deliciosa* (Nieuwenhuizen *et al.,* 2007).

Isoform:	ACT1A	ACT2A	KFCp1	KFCp2	KFCp3	KFCp4	KFCp5	KFCp6
pI:	4.1	8.6	4.7	4.1	4.6	4.3	3.7	4.0

2.3 Results and Discussion

2.3.1 Purification of actinidin

Actinidin was purified from GrK kiwifruit to assess the structural and kinetic parameters of actinidin. The protocol from Boland, *et al* (Boland *et al.*, 1972) was modified to give better consistency in the yields. For example, the ammonium sulphate concentration was increased from 60% saturation to 80%. This amount was found to be the minimum to ensure that actinidin was precipitating out of the solution every time, which was an important step to reduce the volume and remove any impurities that did not precipitate before anion exchange chromatography was used.

The outer pericarp tissue of GrK was homogenised with phosphate buffer (100 mM, pH 6) containing DTT and EDTA to produce a crude sample. This was centrifuged and the resulting supernatant was decanted before solid ammonium sulphate was added to precipitate out the soluble proteins. The precipitant was resuspended in a minimal amount of extraction buffer (10-20 mL/ 100g of starting kiwifruit flesh) and injected onto a HiLoad™ Q HP anion exchange column (GE Healthcare) after the column was exchanged into phosphate buffer (50 mM, pH 6). Actinidin was eluted from the column using a NaCl gradient of high salt buffer and resulted with one peak (peak 1) eluting after approximately 206 mM (35 mS/cm) of the salt had been added (Figure 5). A purified sample of actinidin was pooled from the fractions containing the highest amount of protein (> 1000 mAU), as determined by the absorbance at 280 nm. The elution fractions under peak 1 had a considerably lower volume than what had been injected onto the column, making the chromatography step a useful method for concentrating the purified sample.

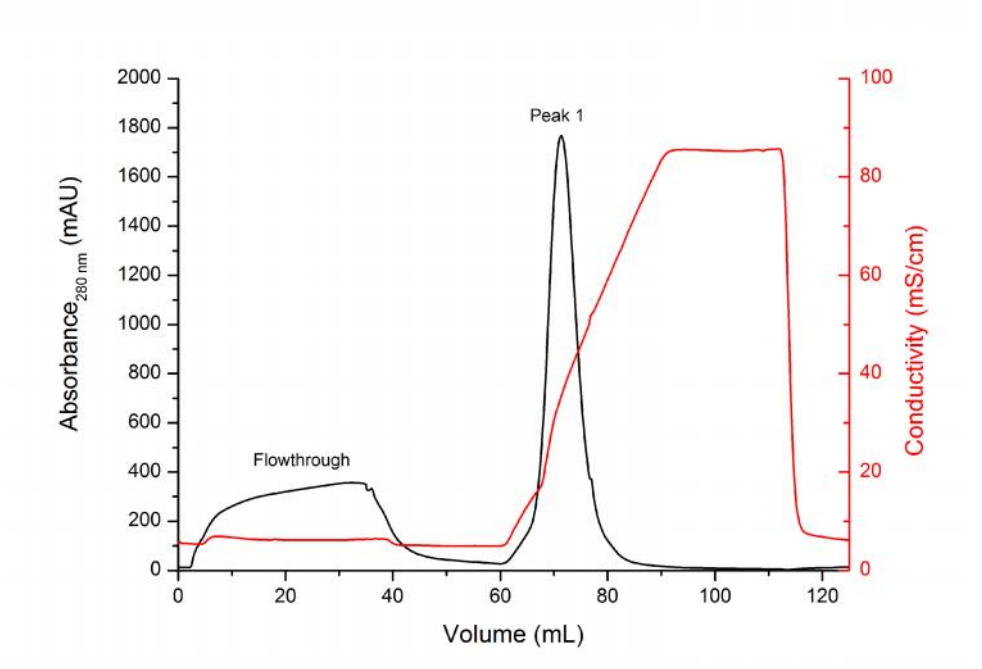

Figure 5: Elution chromatogram of actinidin, injected onto a 5 mL HiLoad™ Q HP anion exchange column. Elution was conducted by increasing the salt concentration (conductivity) with 0.5 M NaCl. The protein was measured by its absorbance at 280 nm.

Actinidin purified using anion exchange chromatography was exchanged into a low salt phosphate buffer by eluting the sample down a 120 mL HiLoad™ 16/600 Superdex™ 200 pg size exclusion column (GE Healthcare) before the sample was analysed using analytical ultracentrifugation (Figure 11). The protein eluted from the column as one peak (peak 1) at approximately 95 mL, as monitored by the UV absorbance at 280 nm (Figure 6). There was no aggregate present in the elutant and indicates that actinidin is stable in solution throughout the purification.

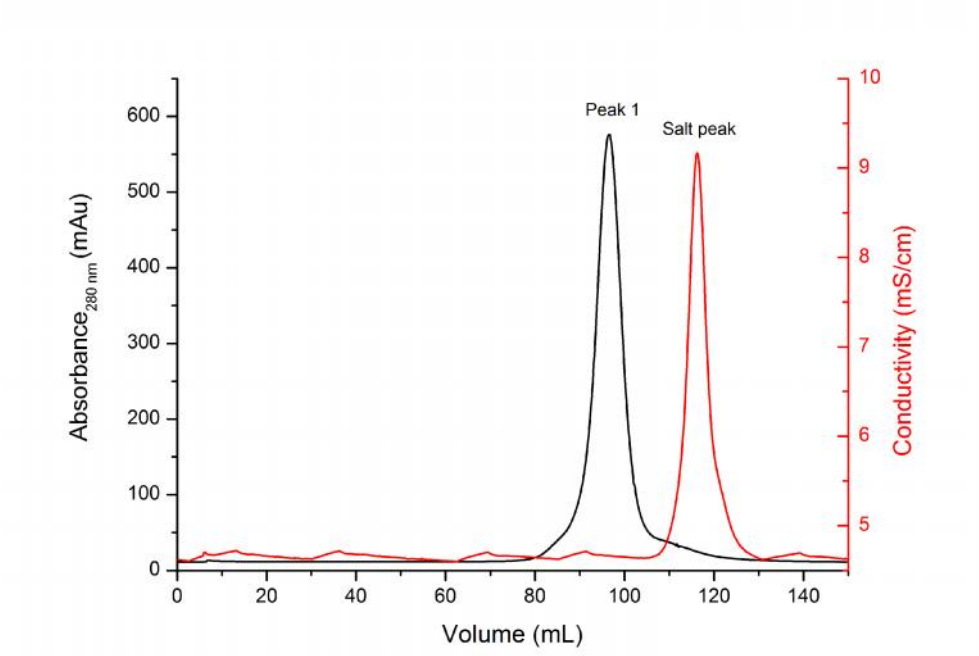

Figure 6: Elution chromatogram of actinidin eluting down a 120 mL HiLoad™ 16/600 Superdex™ pg 200 size exclusion column. Protein was detected by its absorbance at 280 nm.

SDS-PAGE analysis was used to assess the purity of actinidin. Between 5-10 µg of protein was taken from the different purification stages and the samples were loaded onto the gels under reducing conditions. Actinidin migrated as a 26 kDa protein under reducing conditions, in contrast under non-reducing conditions (data not shown). This is higher than its theoretical molecular weight of 24 kDa (Nieuwenhuizen *et al.*, 2007), however previous PAGE analysis of actinidin has shown that reducing agents change how the protein migrates and that it is common that actinidin runs as a higher molecular weight (Ciardiello *et al.*, 2009). Actinidin has three disulfide bonds (Baker, 1980) and the reducing agent is likely disrupting these, which is affecting how the protein migrates during electrophoresis.

Multiple protein bands were present in the crude (lane 2), supernatant (lane 3), precipitant (lane 4), and dialysis (lane 5) samples. Along with actinidin (26 kDa) there were bands that corresponded to a 22, 18, and 16 kDa protein. These were hypothesised to be from the Thaumatin-like protein (TLP) (Gavrovic-Jankulovic *et al.*, 2002), kirola (D'Avino *et al.*, 2011), and KiTH, which is a peptide that is cleaved from kiwellin (Tuppo *et al.*, 2008), respectively. From these, the band representing TLP had the strongest intensity and this is consistent with the abundance of TLP in kiwifruit compared to the other proteins (Ciardiello

et al., 2009). Lane 6, that consisted of the fractions pooled from peak 1 (Figure 5) showed that anion exchange chromatography can remove the 22 and 16 kDa proteins and reduce the amount of the 18 kDa protein, which is important for increasing the purity of the actinidin sample.

Actinidin, purified by anion exchange chromatography (lane 6) was the most prominant, however there were also the presence of lower molecular weight species that was eluted from the anion exchange column. These bands were also present in lanes 4 and 5 but not present in lanes 2 and 3 which was the crude and supernatant samples, respectively. It is hypothesised that these bands represented the product of proteolytic digestion occurring throughout the purification and that their low concentrations were responsible for the absence of absorbance at 280 nm (Figure 5) and during mass spectroscopy analysis (Figure 8).

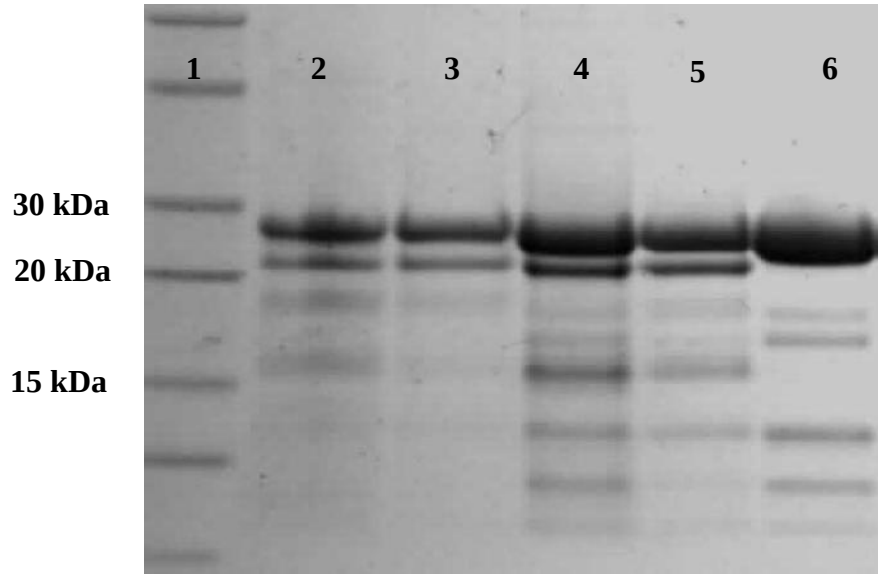

Figure 7: SDS-PAGE during the purification stages to isolate actinidin from GrK. The samples were run under reducing conditions and contained between 5-10 µg of protein in each lane. lane 1: molecular marker, 2: crude sample, 3: supernatant, 4: ammonium sulfate precipitation, 5: after dialysis, 6: pooled fractions from peak 1 after anion exchange chromatography (Figure 5).

Actinidin retention at each step during the purification was quantified by measuring the actinidin activity and protein concentration. The yield of actinidin dropped by 69% after the anion exchange chromatography step, which can either be due to protein loss during the purification steps or actinidin becoming inactivated (Table 3). Centrifuging the crude sample

resulted in a 16% loss of yield between the crude and supernatant samples. Proteins in kiwifruit have been shown to associate with the insoluble kiwifruit material (Ciardiello *et al.*, 2009) and this could have affected the amount of actinidin retained in this sample. The largest loss of yield (43%) occurred after the protein had been precipitated using ammonium sulphate. It is hypothesised that this is the result of the protein not re-suspending properly or becoming denatured. To increase the concentration of the purified sample not all of the fractions were pooled from peak 1 (Figure 5) and this would have contributed to the 10% loss in yield that occurred during anion exchange chromatography.

Overall there was a reduction in total protein and this was correlated with an increase in the specific activity. From 146 g of starting kiwifruit flesh 25 mg of actinidin was purified, which is equivalent to 17 mg/ 100g. This is similar to other published values of 13.3 mg/ 100 g (M. Grozdanovic *et al.*, 2012) and 20 mg/ 100 g (Cavic *et al.*, 2012). The specific activity of 39.5 µmol/min/mg is lower than the published values of 60 µmol/min/mg (K. Brocklehurst *et al.*, 1981) and 64 µmol/min/mg (Carotti *et al.*, 1984), which also used CBZ-Lys-ONP as a substrate. Actinidin can become inactivated during purification (M. Grozdanovic *et al.*, 2012) and this may have been occurring throughout the purification and resulting in a decrease in specific activity.

Table 3: Purification table for the steps used to purify actinidin from 146 g of GrK flesh. The actinidin activity and protein concentration were measured as described in Chapter 2 during the purification.

Sample	**Volume (mL)**	**Total protein (mg)**	**Specific activity (µmol/min/mg)**	**Total activity**	**Yield (%)**
Crude:	409	586	5.4	3164	100
Supernatant:	400	460	5.8	2669	84
Protein Ppt:	20	79	16.6	1308	41
IEX:	6	25	39.5	995	31

2.3.2 Mass spectrometry

Electro-spray ionisation mass spectrometry (ESI-MS) was conducted to confirm the presence of actinidin after it had been purified from GrK using anion exchange chromatography. The mass spectrum shows a cluster of peaks between the mass values of 23,765.47 to 24,202.53 Da (Figure 8). This shows that the data has come from a heterogeneous sample, and indicates that there are multiple proteins present in the purified sample. The masses also do not correlate with the molecular weight of 26 kDa after SDS-PAGE analysis (Figure 7, (lane 6)) and suggests that actinidin, under reducing conditions migrates differently during electrophoresis.

The major peak at 23,802.22 Da (Figure 8) is predicted to represent the ACT1A isoform (23809.3 Da) with an error of 7.08 Da (297 ppm). The mass of the other peaks, however did not correlate to the theoretical mass of any of the other six identified cysteine proteases in *A. deliciosa* (Table 4) with a similar, or lower error value and the masses are also different from previous studies that purified actinidin from GrK that gave a mass of 23,883.1 Da using MALDI-TOF mass spectrometry (M. M. Grozdanovic *et al.*, 2014). It is hypothesised that amino acid substitutions, extensions, or deletions are occurring in one or several of the different isoforms. The mass differences in Table 4 were analysed to determine whether truncations, incorrect processing of C- and N-terminal extensions (Nieuwenhuizen *et al.*, 2007), or amino acid substitutions were occurring, however the masses did not correlate. The high heterogeneity of the sample may be responsible for the masses not aligning accurately and therefore greater separation of the isoforms during anion exchange chromatography and amino acid sequencing is required to confirm what sequence modifications are present.

Table 4: Theoretical mass of the actinidin isoforms expressed in *A. deliciosa* (Nieuwenhuizen *et al.*, 2007) and the difference between the theoretical masses and the experimental masses (Figure 8).

.

Isoform:			**ACT1A**	**KFCp1**	**KFCp2**	**KFCp3**	**KFCp4**	**KFCp5**	**KFCp6**
Theoretical mass (Da):			23,809.3	23,457.3	23,957.4	24,869.8	23,695.1	23,738.8	23,671.0
Experimental mass (Da):	23,765.47	**Mass difference (Da):**	43.83	-308.17	191.93	1104.33	-70.37	-26.67	-94.47
	23,779.91		29.39	-322.61	177.49	1089.89	-84.81	-41.11	-108.91
	23,802.22		7.08	-344.92	155.18	1067.58	-107.12	-63.42	-131.22
	23,835.03		-25.73	-377.73	122.37	1034.77	-139.93	-96.23	-164.03
	23,900.66		-91.36	-443.36	56.74	969.14	-205.56	-161.86	-229.66
	24,002.38		-193.08	-545.08	-44.95	867.42	-307.28	-263.58	-331.38
	24,069.31		-260.01	-612.01	-111.91	800.49	-374.21	-330.51	-398.31
	24,104.75		-295.45	-647.45	-147.35	765.05	-409.65	-365.95	-433.75
	24,202.53		-393.23	-745.23	-245.13	667.27	-507.43	-463.73	-531.53

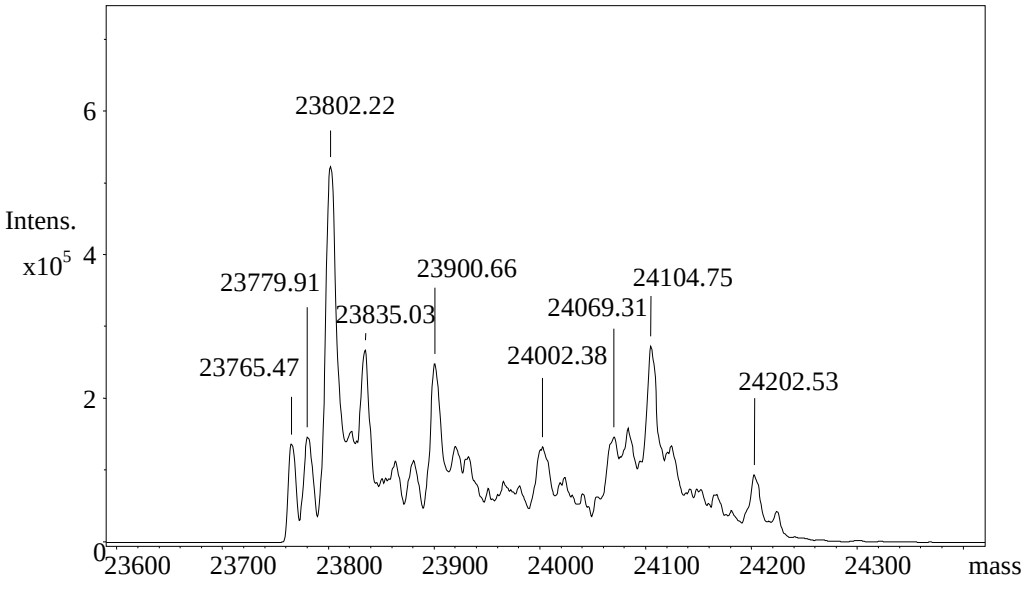

Figure 8: Deconvoluted mass spectrum of the purified actinidin obtained after the anion exchange chromatography purification step (Figure 5) at 1 mg/mL using ESI-MS. The masses of the major peaks are shown as Daltons (Da).

2.3.3 Thermal stability

To understand how different pH environments affect the stability of actinidin, a thermal shift assay was used over the pH range 3.7-9.3. The fluorescence of SYPRO® Orange increased as the actinidin samples were exposed to an increase in temperature from 20 to 100°C, which is indicative of the protein becoming unfolded (Figure 9). There was a thermal shift in the maximum fluorescence between the different conditions and this shows that pH is having an effect on the thermal stability of actinidin.

The intensity of the fluorescence differed for each condition that was tested. At low pH (3.7, 4.7), the fluorescence intensity was larger than the fluorescence that occurred at high pH (8.7, 9.3), and implies that deprotonation is affecting the interaction(s) between the dye and the protein. SYPRO® Orange interacts strongly with amino acids that have positively charged side chains, such as lysine and arginine (Yue *et al.*, 2003), and deprotonating these side chains at high pH may be responsible for the decrease in fluorescence that is seen in Figure 9.

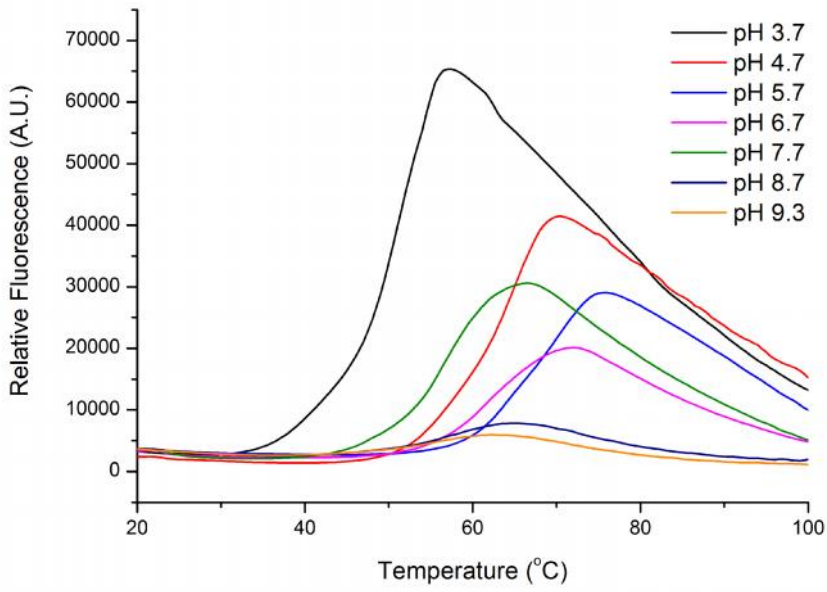

Figure 9: Thermal shift assay of the relationship between the thermal stability of actinidin to pH as measured by differential scanning fluorimetry (DSF). Increase in fluorescence shows that actinidin is becoming unfolded as the temperature is increased. The different pH environments (pH 3.7-9.3) are represented by the different colours.

A melting temperature (T_m) was obtained by calculating the midpoint of the fluorescence transition from the data in Figure 9. The highest melting temperature was 71^{o}C at pH 5.7 (Figure 10) and indicates that the phosphate buffer at pH 6 used in the purification protocol is at an appropriate pH to stabilise actinidin in solution. At pH 6.7, the melting temperature was lower (62^{o}C) than that of a previous study, which measured a melting temperature of active actinidin at pH 6.5 to be 73.9^{o}C, using differential scanning calorimetry (M. M. Grozdanovic *et al.*, 2014). The study compared the thermal stability between active actinidin and actinidin that had been inactivated by the E-64 inhibitor and showed that the inactive actinidin had a lower melting temperature of 61^{o}C when compared to the active form. This suggests that the actinidin tested in Figure 9 could have been inactivated and this change is having a negative impact on the thermal stability.

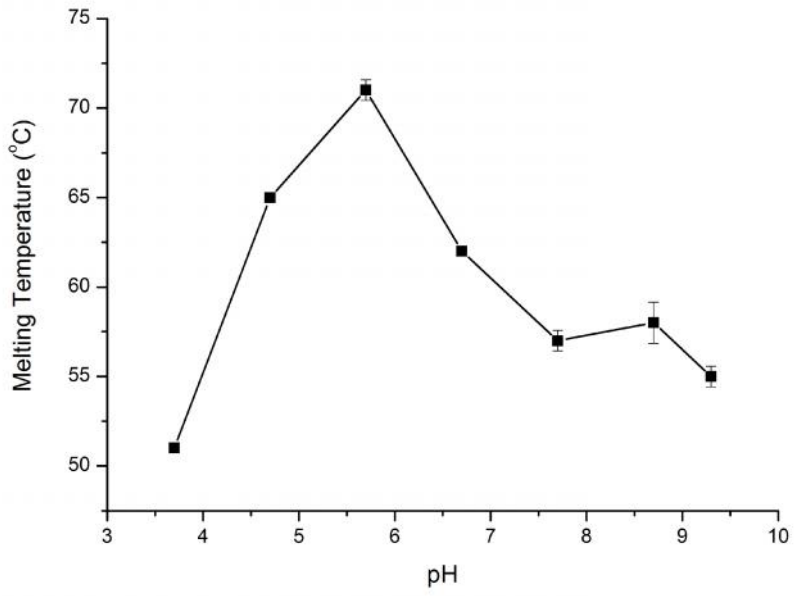

Figure 10: Melting temperature of actinidin, present in different buffers. Measurements were conducted in triplicates and the standard deviation of the mean is represented by error bars.

2.3.4 Analytical ultracentrifugation

The crystal structure of actinidin is monomeric (Baker, 1980) and to determine whether actinidin was also a monomer in solution, the quaternary structure was assessed by measuring the rate at which the protein sediments when a gravitational field is applied, during an analytical ultracentrifugation (AUC) sedimentation velocity experiment (Figure 11). The absorbance at 285 nm was used to measure the sedimentation of actinidin throughout the AUC experiment (Figure 11 (a)) and the uniformity of the residuals (Figure 11 (b)) show that the sigmoids, which are fitted to the data, represent the experimental data well. A $c(M)$ distribution was modelled using SEDFIT (Schuck, 2000), with the calculated frictional coefficient of 1.14 and showed that there was a single peak present that had an integrated mass of 23,862 Da (Figure 11 (c)). This indicates that at 0.3 mg/mL actinidin sediments as a monodisperse species, which has a molecular weight similar to the theoretical molecular weight of a monomer at 23,809 Da (Nieuwenhuizen *et al.*, 2007) and this confirms that actinidin is a monomer.

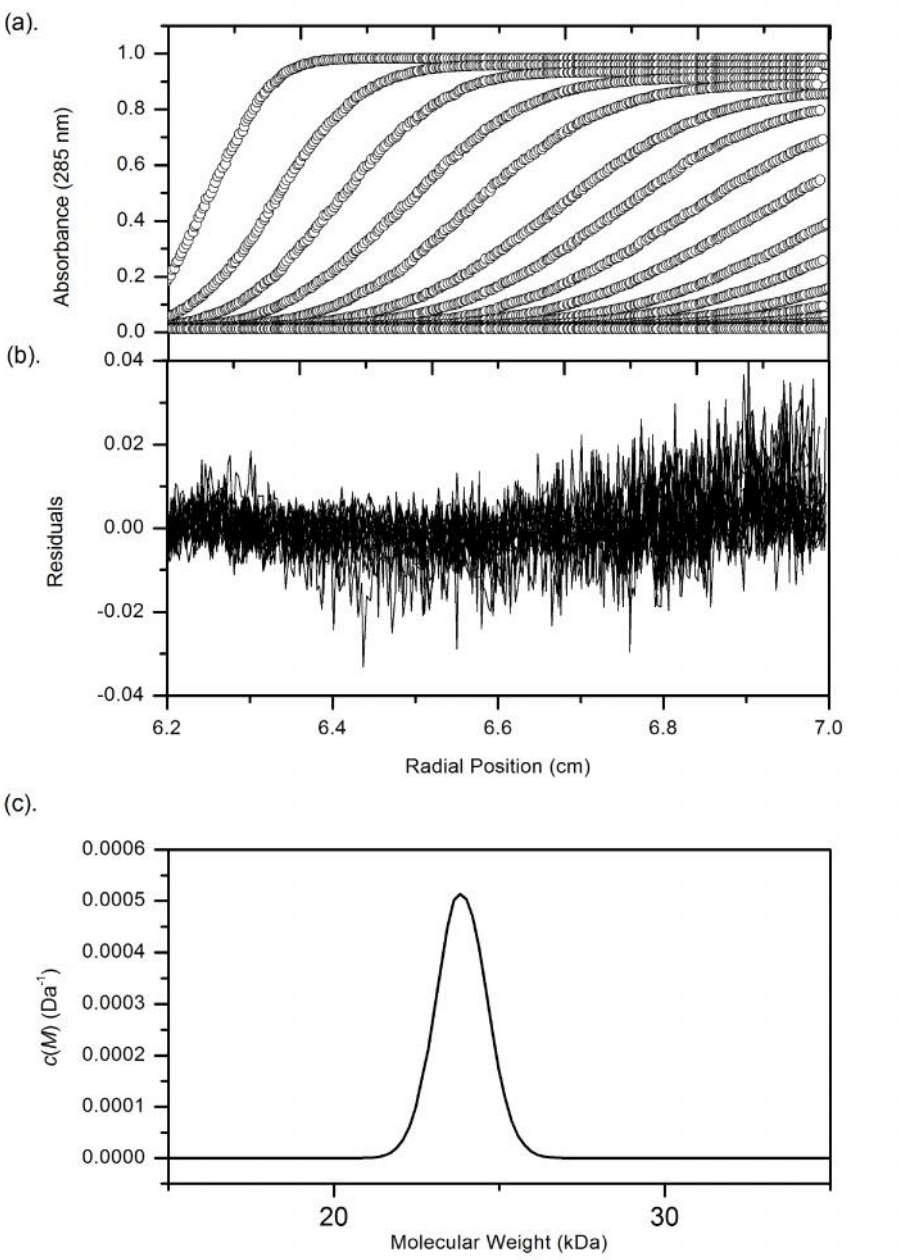

Figure 11: Sedimentation velocity experiment of purified actinidin at 0.3 mg/ml in 50 mM phosphate buffer. A sigmoid was fitted to the sedmentation data of actinidin (a) with the quality of the fit shown by the residuals (b). A *c*(*M*) distribution of the data was modelled using SEDFIT (Schuck, 2000) and shows that the molecular weight of actinidin in solution is 23,830 Da.

2.3.5 Kinetics of actinidin

To determine the kinetic parameters of actinidin towards N-α-carbobenzoxy-L-lysine-*p*-nitrophenyl ester (CBZ-Lys-ONP), the activity at increasing substrate concentration was measured. The activity rate was plotted as a function of substrate concentration and was shown to fit the Michaelis-Menten equation (Figure 12). From the fit of a hyperbola a K_m value of 37 µM and a V_{max} value of 0.081 µmol/min was determined and a k_{cat} value was calculated to be 18.9 sec^{-1}. The values for the kinetic parameters between actinidin and CBZ-Lys-ONP have previously been calculated and are shown to differ from the values that were obtained using the data from Figure 12 (Table 5: Comparison of the kinetic parameters, Km and kcat for the catalysis of actinidin with CBZ-Lys-ONP between (Table 5). Inactivated actinidin that might have occurred during protein purification and the presence of multiple actinidin isoforms that can have different kinetic parameters (Morimoto, 2002) may be factors which are contributing to the difference in values, however further investigation is required.

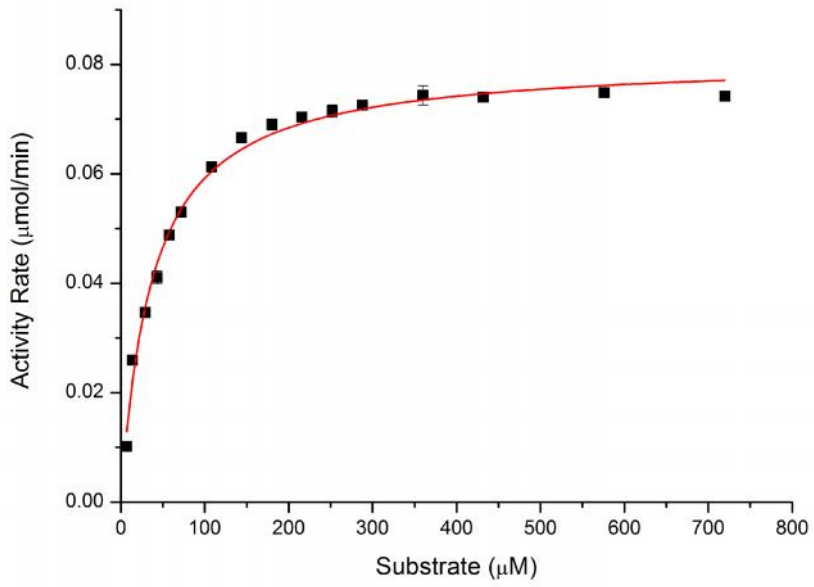

Figure 12: Measurements of actinidin activity with varying concentrations of CBZ-Lys-ONP at pH 6. A Michaelis-Menten hyperbola curve was fitted to the data to identify the kinetic parameters K_m and V_{max}. Assays were conducted in duplicates and the standard deviation of the mean is represented as error bars.

Table 5: Comparison of the kinetic parameters, K_m and k_{cat} for the catalysis of actinidin with CBZ-Lys-ONP between Figure 12 and previous studies.

K_m (µM)	**k_{cat} (sec^{-1})**	**Reference**
37	18.9	Figure 12
22	29	(Boland *et al.*, 1972)
91	101	(Lewis *et al.*, 1988)
AC-1: 33.6 AC-2: 52.8	AC-1: 61.4 AC-2: 53.6	(Morimoto, 2002)

The relationship between actinidin activity towards CBZ-Lys-ONP and pH was investigated over a pH range of 1.9-8.6. Activity was seen to decrease in more acidic and basic environments and the data resembled a bell-shaped curve with the highest activity occurring between pH 5-7 (Figure 13). The activity-pH profile is consistent with previous studies (S. Boyes *et al.*, 1997; Sugiyama *et al.*, 1997), which measured the activity of CBZ-Lys-ONP to be at its highest between pH 5-7.

The loss of actinidin activity that occurred in acidic environments (pH 1.9-4), was considered to be detrimental to the bioactive properties of actinidin, which increased gastric protein digestion in a rat model (Montoya *et al.*, 2014). However, actinidin has shown to increase the digestion of some food proteins in an *in vitro* digestion assay, which is conducted at pH 1.9 (Kaur *et al.*, 2010b) and therefore the loss of activity is more likely to be isolated to the assay using the synthetic peptide derivative.

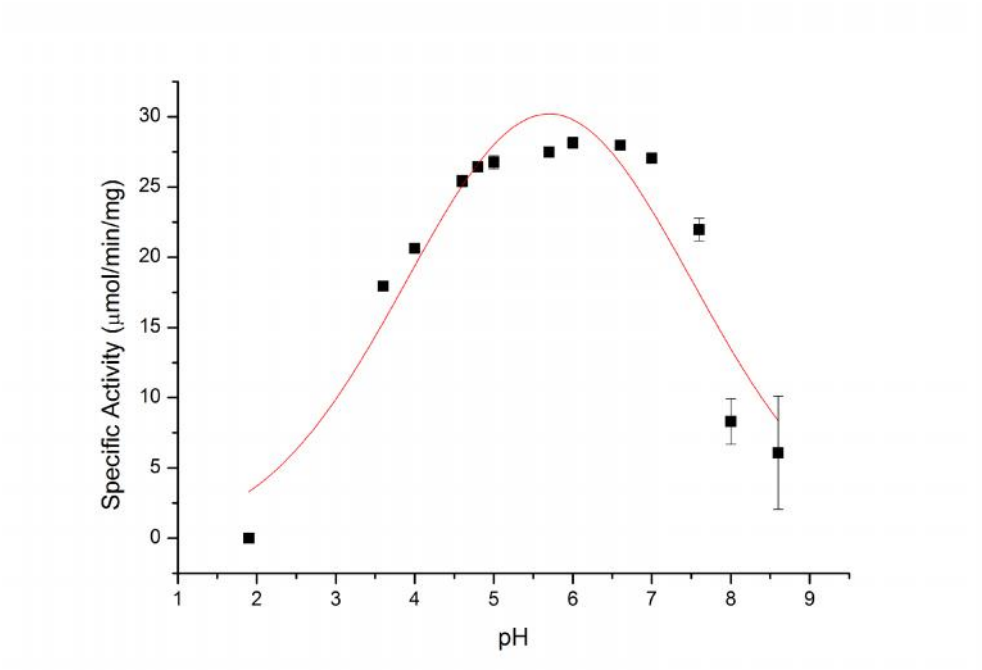

Figure 13: Relationship between actinidin activity and pH using CBZ-Lys-ONP as a substrate. A pH range of 1.9-9 was formulated using citric (pH 1.9), citric-phosphate (pH 3.6-7.6), and tris-base (pH 8-8.6) buffers. The data was modelled using a Gaussian distribution that was fitted to the data. Assays were conducted in duplicates and the standard deviation of the mean is represented as error bars.

The background rate of CBZ-Lys-ONP hydrolysis in buffer, that was subtracted from the activity rate, showed a pH dependence. As the pH increased above pH 6.6 there was an exponential increase in the reaction rate of CBZ-Lys-ONP becoming hydrolysed (Figure 14). The alkaline dependent hydrolysis shows that measuring the actinidin activity at pH 6 does not induce competition for hydrolysing the substrate between actinidin and the buffer.

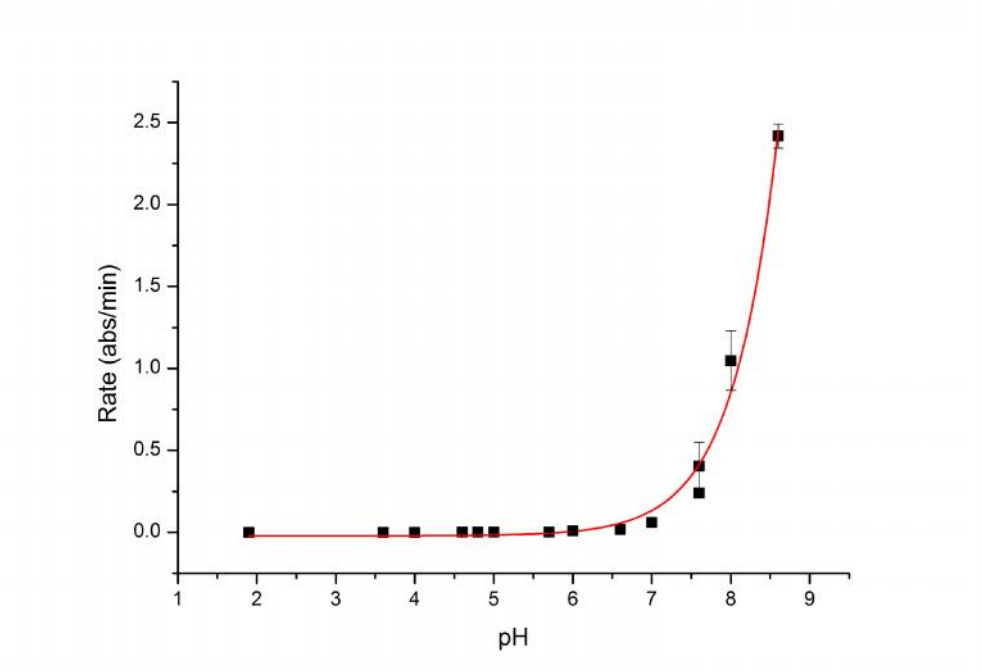

Figure 14: Reaction rate between CBZ-Lys-ONP and buffers (pH 1.9-8.6) showing an exponential rate increase at high pH. The assays were conducted with the buffers used in Figure 14 and did not contain any presence of actinidin. Assays were conducted in duplicates and the standard deviation of the mean is shown as error bars.

2.4 Conclusions

2.4.1 Purification

Actinidin from GrK (*Actinidia deliciosa* cv. Hayward) was purified from other kiwifruit proteins using anion exchange chromatography. The purified sample did not show any aggregation, however it may have been partially inactivated. From 100 g of starting kiwifruit flesh, 17 mg of protein was obtained, which is similar to previous studies (Cavic *et al.*, 2012; M. Grozdanovic *et al.*, 2012).

The deconvoluted mass spectrum showed a cluster of peaks between 23,765.47 to 24,202.53 Da and it was hypothesised that, as well as the major acidic isoform, ACT1A other acidic isoforms of actinidin (Nieuwenhuizen *et al.*, 2007) had been purified. Further investigation, including sequencing of the different peaks, is required to confirm this hypothesis.

2.4.2 Characterisation

Actinidin, consistent to previous studies was a monomer in solution and both the thermal stability and activity of actinidin towards the CBZ-Lys-ONP substrate was shown to be influenced by pH. The melting temperature of 62^{o}C at pH 6.7 was similar to the melting temperature of inactivated actinidin at a similar pH, which has been described previously (M. M. Grozdanovic *et al.*, 2014). This indicates that the purified actinidin may be partially inactivated. Inactivated actinidin could also explain why the k_{cat} value of 18.9 sec^{-1} was lower than previous studies, (Boland *et al.*, 1972; Lewis *et al.*, 1988; Morimoto, 2002), however, the different actinidin isoforms in the actinidin sample may also have contributed to this value.

Chapter Three : Catalytic Inactivation of Actinidin

3.1 Actinidin

3.1.1 Protein structure

Actinidin, as part of the CA clan, shares close structural similarities to papain (Rawlings *et al.*, 2012). The primary structure between actindin (PDB: 2ACT) (Baker, 1980) and papain (PDB: 9PAP) (Kamphuis *et al.*, 1984) aligns well and shows conservations of 103 residues, including residues that are important for forming disulfide bonds and catalytically important residues (Figure 15). The secondary structure folds also align well (rmsd= 0.484) between the two cysteine proteases (Figure 16). Both structures are folded into two domains, termed L and R. The L domain is dominated by α-helices while the R domain is characterised by an anti-parallel β-sheet, which is centred between two surface α-helices. The active site of papain and actinidin is located in the cleft between the two domains. Aligning 86 residues, which constitute the active site including, Cys-25, His-162, and Asn-182 residues (Figure 16 (b)) aligned very well (rmsd= 0.294) (Kamphuis *et al.*, 1985). This indicates that the mechanism of catalysis is conserved between actinidin and papain.

```
Actinidin     1 LPSYVDWRSAGAVVDIKSQGECGGCWAFSAIATVEGINKITSGSLISLSEQELIDCGRTQ
Papain        1 IPEYVDWRQKGAVTPVKNQGSCGSCWAFSAVVTIEGIIKIRTGNLNQYSEQELLDCDRR-
                                          *   #                          *

Actinidin    61 NTRGCDGGYITDGFQFIINDGGINTEENYPYTAQDGDCDVALQDQKYVTIDTYENVPYNN
Papain       60 -SYGCNGGYPWSALQLVA-QYGIHYRNTYPYEGVQRYCRSREKGPYAAKTDGVRQVQPYN
                    *                                  *

Actinidin   121 EWALQTAVTYQPVSVALDAAGDAFKQYASGIFTGPCGTAVDHAIVIVGYGTEGGVDYWIV
Papain      118 QGALLYSIANQPVSVVLQAAGKDFQLYRGGIFVGPCGNKVDHAVAAVGYGP----NYILI
                                                    *      #

Actinidin   181 KNSWDTTWGEEGYMRILRNVGGA-GTCGIATMPSYPVKYNN
Papain      174 KNSWGTGWGENGYIRIKRGTGNSYGVCGLYTSSFYPVK--N
                 #                    *
```

Figure 15: Sequence alignment of actinidin (PDB: 2ACT) (Baker, 1980), and papain (PDB: 9PAP) (Kamphuis *et al.*, 1984) by T-Coffee (Notredame *et al.*, 2000; Tommaso *et al.*, 2011). Conserved residues are highlighted in black and residues involved in disulfide bonds (*) and residues important for catalysis (#) are indicated.

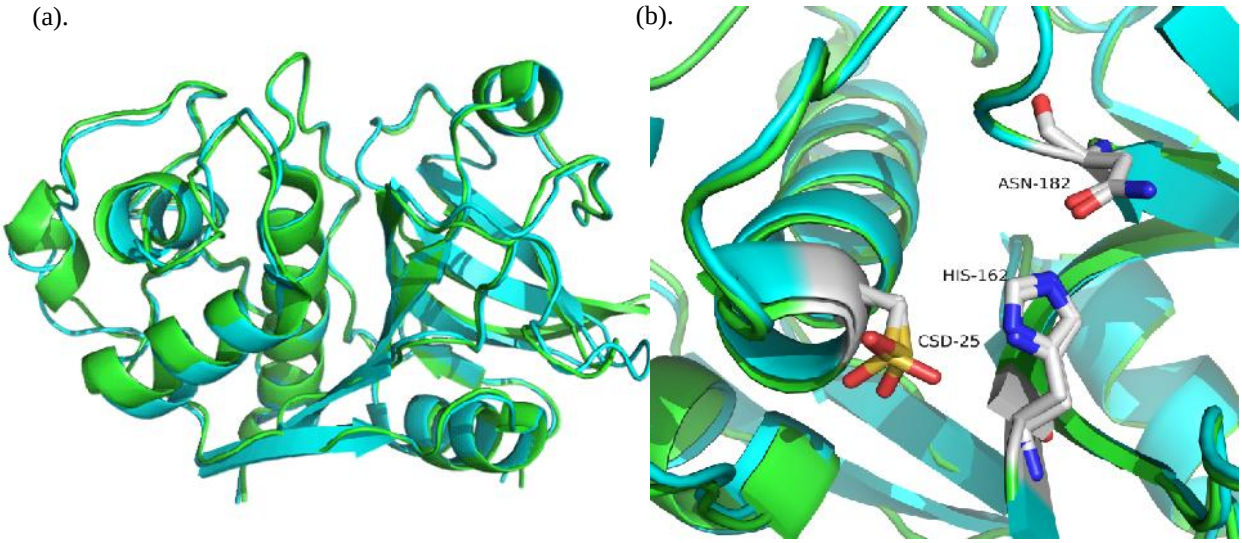

Figure 16: Structural alignment of actinidin (2ACT) (Baker, 1980) and papain (9PAP) (Kamphuis *et al.*, 1984), shown in green and blue, respectively, depicting both the L and R domains (a) and catalytically important residues, such as (actinidin numbering): CSD-25 (Cys-25 present in oxidised form), His-162 and Asn-182 in the active site cleft (b).

3.1.2 Catalytic function

The catalytic reaction of cysteine protease enzymes is a multi-step process that results in peptide bond cleavage, and the formation of two products as shown in Equation 1. An

enzyme substrate complex (ES) initially forms by a catalytically active cysteine residue (Cys-25 in actinidin) (Baker, 1980) binding to the peptide substrate. The ES complex is known as an acylenzyme intermediate and at this stage the first product (P_1) is released. A hydrolysis reaction subsequently allows the second product (P_2) to be released and this step also regenerates the enzyme for further peptide cleavage (Keith Brocklehurst *et al.*, 1987).

In actinidin, the catalytic mechanism has been investigated and been found to differ slightly from papain. A higher catalytic efficiency has been shown in actinidin for synthetic peptide derivatives that have aliphatic moieties when compared to substrates with aromatic moieties, in contrast to papain (Baker, 1980). Subsequent molecular dynamic simulations have suggested that the binding affinities for peptides and the constraint for product diffusion, due to a salt bridge that is unique to actinidin, are responsible for the lower catalytic efficiency for the substrates that have aromatic moieties in actindin (Reid *et al.*, 2001). These same differences in the composition of amino acids in the active site may be the reason why actinidin has shown a higher caseinolytic activity at lower pH, when compared to papain (M. Ha *et al.*, 2013), which has important implications for the bioactive properties (Kaur *et al.*, 2010a, 2010b) and biotechnological applications (Katsaros *et al.*, 2010) that actinidin is involved in.

$$E + S \underset{K_{-1}}{\overset{K_1}{\rightleftharpoons}} ES \xrightarrow{K_2} P_1 + ES' \xrightarrow{K_3} P_2 + E$$

Equation 1: Reaction schematic of cysteine proteases involving peptide bond cleavage and the formation of two products (Keith Brocklehurst *et al.*, 1987).

3.2 Catalytic inactivation of cysteine proteases

The catalytic activity of a cysteine protease can inactivate and this has been correlated with the susceptibility of a catalytically important cysteine residue towards oxidative reactions. In papain and actinidin, a cysteine residue important for catalysis (Cys-25) is positioned in the active site cleft between the two domains (Baker, 1980; Kamphuis *et al.*, 1984). This residue sticks out away from the enzyme and exposes the thiol functional group of the amino acid to the surrounding solution (Figure 17).

(a) (b)

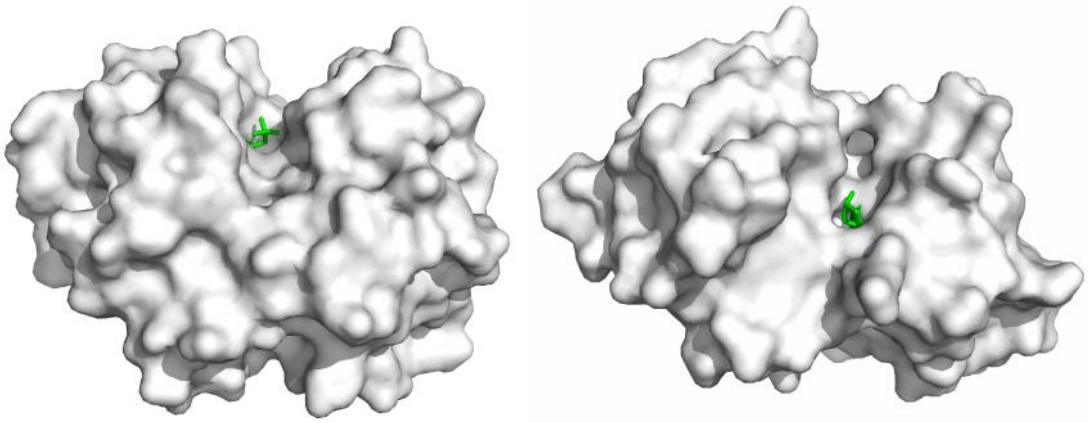

Figure 17: Surface structure of (a) papain (PDB: 9PAP) (Kamphuis *et al.*, 1984) and (b) actinidin (2ACT) (Baker, 1980) . The catalytically important cysteine residue (Cys-25), in which the thiol group has been modified to a sulfinic acid is depicted as a green residue in the active site cleft of each protease.

Exposed thiol groups can react readily with oxygen-containing compounds, especially when the sulfur atom is deprotonated, and will form oxygen derivatives, such as sulfenic (RSOH), sulfinic (RSO_2H), and sulfonic (RSO_3H) acid (Reddie, 2008). These modifications of the thiol groups can have important implications in biology, for example a 67% activity loss was measured when papain was incubated with hydrogen peroxide (Lin, Armstrong, *et al.*, 1975). Similarly the addition of the reactive oxygen species, such as superoxide (Offer *et al.*, 1998) and hydroxyl radicals (Lin, Clement, *et al.*, 1975) as well as vitamin C (Ozawa *et al.*, 1962), oxygen (Nagaoka *et al.*, 2005), and nitric oxide (Xian *et al.*, 2000) have all been measured to inactivate papain. The reaction between hydrogen peroxide and papain was correlated with a loss of sulfhydryl groups and the inactivation was found to be reversible when a reducing agent was added (Lin, Armstrong, *et al.*, 1975). Because the cysteine residue at position 25 represents the only free cysteine sulfhydryl group in papain (Kamphuis *et al.*, 1984) thiol oxidation of this cysteine residue is probable and likely to be responsible for the observed inactivation. A reaction schematic showing the reversible oxidation reaction with papain has been proposed (Armstrong *et al.*, 1978) and shows that hydrogen peroxide reacts with the thiol group to form a sulfenic acid, which can be reduced when another thiol-containing compound (reducing agent) is added, as shown in Equation 2. The susceptibility of cysteine proteases to oxidation reactions has made it necessary for researchers to purify these enzymes under reducing conditions, in order to prevent any unwanted catalytic inactivation (Boland *et al.*, 1972).

Inactivation:

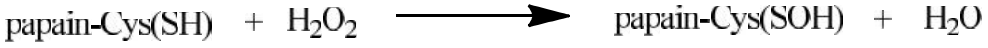

Reactivation:

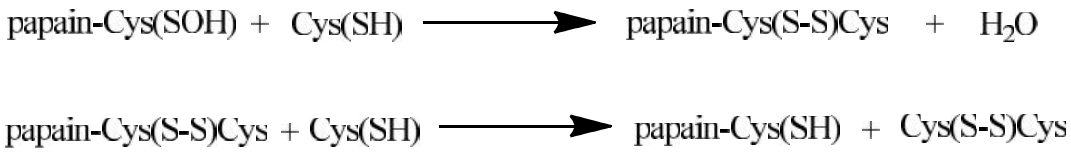

Equation 2: Reaction schematic of reversible inactivation of papain with hydrogen peroxide and a thiol-containing species (Armstrong *et al.*, 1978).

3.3 Results and discussion

3.3.1 Time-based activity loss

Kinetic analysis of the specific activity of actinidin in Actazin™ revealed that the activity decreased over time. Activity measurements were conducted immediately after the kiwifruit powder was solubilised in phosphate buffer (100 mM, pH 6) at a concentration of 100 mg/mL and centrifuged to separate the solution from the insoluble kiwifruit material. The rate of activity loss over 120 minutes was fitted to an exponential curve (R^2= 0.92), which better represented the data than a linear fit (R^2= 0.87) and showed an activity loss of 63% between time 0 and 120 minutes of incubating the sample at room temperature (Figure 18).

During the first 10 minutes there was a 23% decrease in activity and this indicates that the inactivation occurs rapidly. It is hypothesised that a chemical species in the kiwifruit powder is inactivating actinidin. The rapid nature of the inactivation suggests that this inactivator is present at high concentrations in the solution or that there is a collection of molecules that inhibit actinidin activity and collectively is present in a high concentration. Because the inactivation occurs rapidly the activity at time 0 may not accurately reflect the initial actinidin activity before it is inactivated. This could have implications for the quality control tests for actinidin activity in the different kiwifruit powder batches that are conducted by Anagenix Ltd, and therefore warranted further investigation.

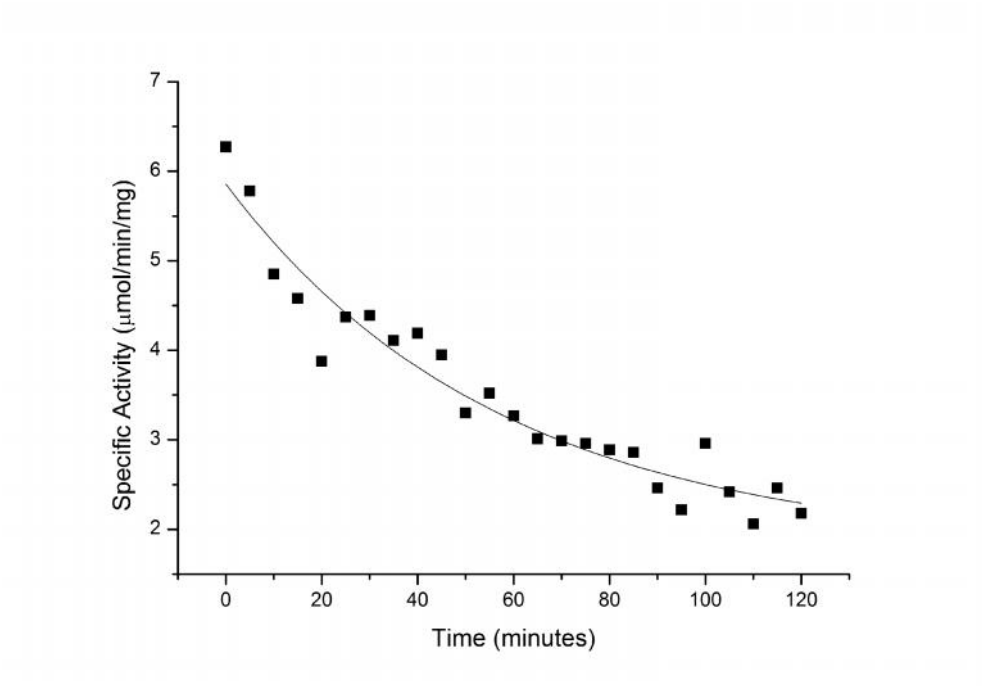

Figure 18: Exponential loss (R^2= 0.92) of actinidin activity after the kiwifruit powder was solubilised in phosphate buffer, centrifuged and assayed with CBZ-Lys-ONP every 5 minutes. The sample used to test for actinidin activity was stored at room temperature throughout the experiment.

The time-based inactivation of actinidin in kiwifruit powder (Figure 18) is not observed in the purified actinidin samples. Actinidin purified from GrK was assayed over a time span of 120 minutes while the sample was similarly incubated at room temperature. The linear regression fit showed that there was little decrease between time 0 and after 120 minutes of incubation (Figure 19). This suggests that there are compounds in the kiwifruit powder that are responsible for the inactivation. One difference between the purified actinidin and kiwifruit powder was that the purification protocol purified actinidin under reducing conditions, analogous to previously published protocols (K. Brocklehurst *et al.*, 1981). It was therefore hypothesised that an oxidant in the kiwifruit powder when it is solubilised in buffer is having an effect on the activity of actinidin.

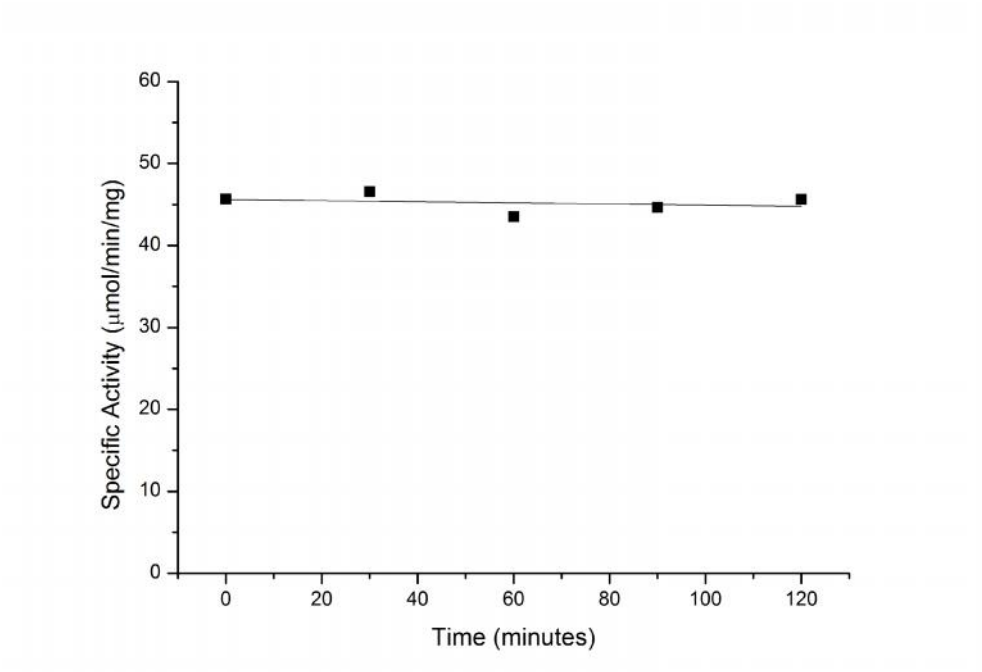

Figure 19: Linear fit of the change in actinidin activity from a purified sample when incubated at room temperature.

3.3.2 Reversible inactivation with reducing agents

The activity loss that is occurring when actinidin is inactivated can be reversed in the presence of a reducing agent. Kiwifruit powder was solubilised at a concentration of 100 mg/mL in phosphate buffer (100 mM, pH 6) and centrifuged. The supernatant was immediately assayed and then assayed every 30 minutes thereafter for 120 minutes. This represented the control and was replicated for the three samples. After the control had been measured for each sample a reducing agent (cysteine, DTT, or β-mercaptoethanol) was added to the cuvette at a concentration of 5 mM. The enzyme was incubated with the reducing agent, in buffer, for 2 minutes before the assay commenced. The actinidin activity for all control samples inactivated at an exponential rate (Figure 20 (a-c)). The decay is similar to what was observed previously (Figure 18), however the inactivation rates were different among the different samples and this could be the result of insufficient solubilisation of the kiwifruit powder in buffer.

Inactivated actinidin activity was reactivated over the 120 minutes in all three samples after the respective reducing agent was added indicating that oxidation is likely to be the cause of inactivation (Figure 20 (a-c)). The most effective reducing agent at protecting actinidin from

becoming inactivated over 120 minutes was cysteine. This was followed by samples containing DTT and β-mercaptoethanol (Figure 20 (d)). The reducing agents, however, did not completely restore the activity across the 120 minutes as shown by the negative gradient of the data (Figure 20 (a-c)). This indicates that either the reduction reaction needed a longer incubation period than 2 minutes in order to reactivate actinidin or that the inactivation is partially irreversible.

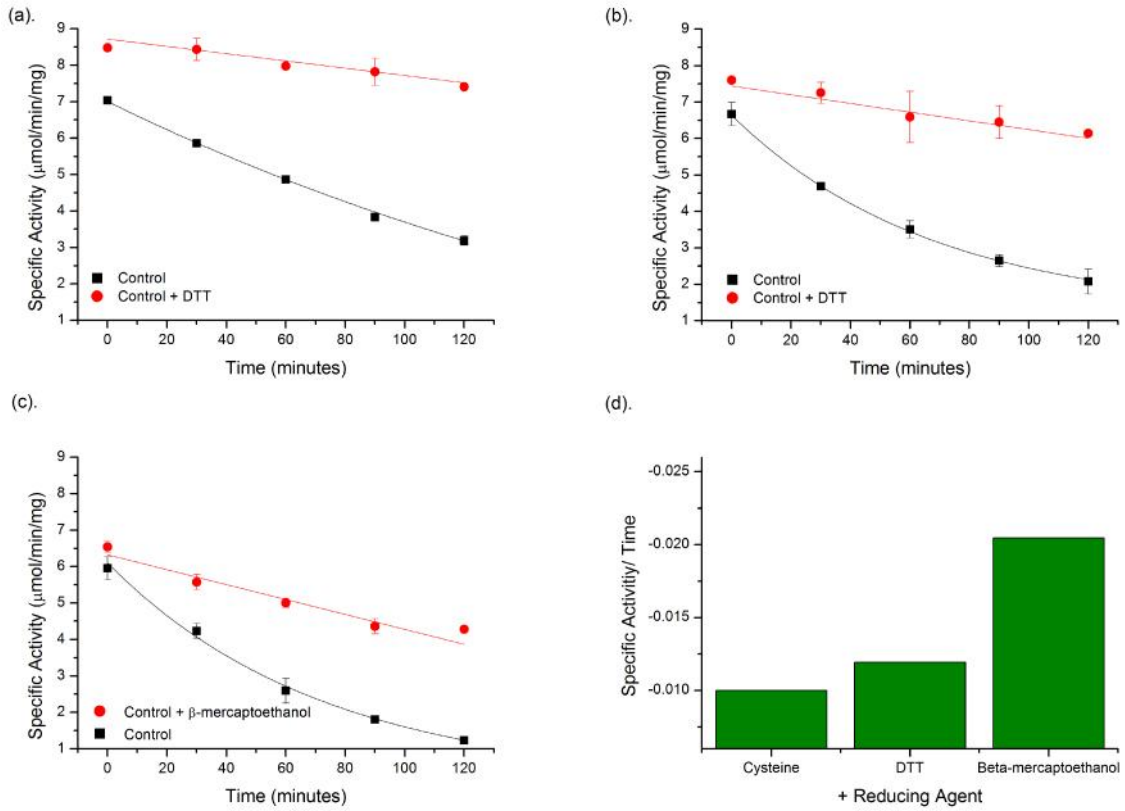

Figure 20: Reversible inactivation of actinidin in kiwifruit powder upon the addition of 5 mM cysteine (a), DTT (b), or β-mercaptoethanol (c). The slope of the linear decrease the reducing agent was added to the cuvette (d) shows the effectiveness of the reducing agent at maintaining activity over 120 minutes.

Inactivation of papain by oxidation has been well characterised and it is hypothesised that actinidin similarly becomes oxidised when the kiwifruit powder is solubilised in phosphate buffer. Papain has been shown to be reversibly inactivated with hydrogen peroxide (Lin, Armstrong, *et al.*, 1975) and the catalytically active cysteine residue was shown to be affected by the inactivation, by measuring the free sulfhydryl groups. As illustrated above (Figure 16), actinidin has a homologous catalytically active cysteine residue in the active site (Figure 16)

and this residue is also exposed to solution in the active site cleft (Figure 17). In support of this, the crystal structure of actinidin shows a partially oxidised Cys-25 residue (Figure 16). The vulnerability of Cys-25 and generally known sensitivity of thiol groups to oxidation (Luo *et al.*, 2005) makes Cys-25 a plausible target for biological oxidation. Whilst hydrogen peroxide-induced oxidation is used as a model system to explore oxidation processes *in vitro* on purified enzymes the exact mechanism of oxidation with the kiwifruit powder has not been determined. A proposed mechanism for this reaction given in Equation 2, which produces a catalytically inactive sulfenic group that can be reversed back to a catalytically active thiol group upon addition of a reducing agent such as cysteine. An alternative mechanism could, however involve non-oxidative reactions, such as conjugate addition and disulfide bond formation of Cys-25 that is similarly reversible by the addition of cysteine.

Either of these reactions would explain the results shown in Figure 20, of reversible inactivation after a reducing agent is added. The inability to completely restore the activity with the reducing agents also suggests that a fraction of the actinidin is becoming irreversibly inactivated or is not reactivating after the 2 minute incubation period. This may mean that the oxidative inactivation reaction is more complex and leads on to other oxidation reactions, which has been shown previously by reacting hydrogen peroxide with thiol-containing compounds (Luo *et al.*, 2005). Hydroxyl and superoxide radicals may also be present in the solution and these have similarly been shown to react with sulfhydryl containing enzymes to induce irreversible inactivation (Armstrong *et al.*, 1978). A model for the possible pathways that lead to actinidin becoming denatured or inactivated through oxidation reactions is summarised in Figure 21.

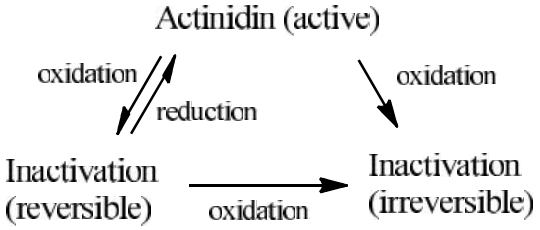

Figure 21: Model for the loss of actinidin activity measured over 120 minutes after kiwifruit powder is solubilised in phosphate buffer showing how the different oxidation states can determine whether the inactivation is reversible or irreversible.

3.3.3 Concentration dependent activation

Various concentrations of cysteine were trialled to understand whether the protective effect that reducing agents had would last for an extended period of time. Samples were incubated at room temperature with the presence of cysteine at a concentration of 1-40 mM for 30 hours. The activity measured approximately every 5 hours showed that a concentration of cysteine below 5 mM did not protect actinidin within the maximal range of 14-15 µmol/min/mg while above 5 mM cysteine did protect actinidin, however over time the effectiveness was reduced (Figure 22). This indicates that at a kiwifruit powder concentration of 100 mg/mL a cysteine concentration of at least 5 mM is needed to prevent any unwanted inactivation. The inactivation over time also indicates that the chemical species that inactivates actinidin may only be partially blocked with the reducing agents or that incubating the samples over time, at room temperature, is sufficient to form more inactivating species. This is consistent with the model of inactivation proposed where inactivation can move between reversible and irreversible states (Figure 22). The difference in the initial rates for the samples that contained a high cysteine concentration is hypothesised to be due to a mixing error or errors in subtracting the background rate, however it may simply be due to a more complex reaction system that is occurring with the addition of high cysteine concentrations to the sample.

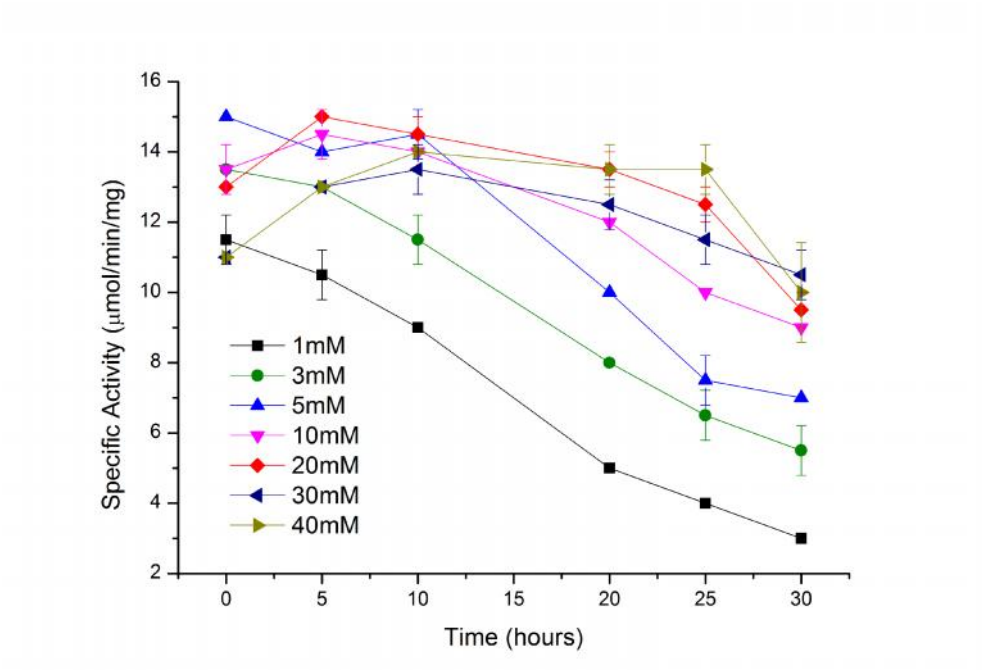

Figure 22: Actinidin activity change over 30 hours in the presence of cysteine at varying concentrations (1-40 mM). Standard deviation between replicates is shown as error bars.

The substrate, CBZ-Lys-ONP was shown to react with reducing agents in a concentration dependent manner. Upon addition of a reducing agent CBZ-Lys-ONP is hydrolysed, resulting in an increase in absorbance at 348 nm. This reaction is linear with respect to the concentration of the reducing agent (Figure 23). Cysteine appears to be the most effective at hydrolysing the substrate, and is followed by DTT and β-mercaptoethanol, and this also correlates with the effectiveness of reducing agents at reactivating actinidin after it had become oxidised (Figure 20). This reducing agent-promoted reaction that is occurring in the absence of actinidin was subtracted from activity measured in samples that contained reducing agents and actinidin to prevent any inaccuracies.

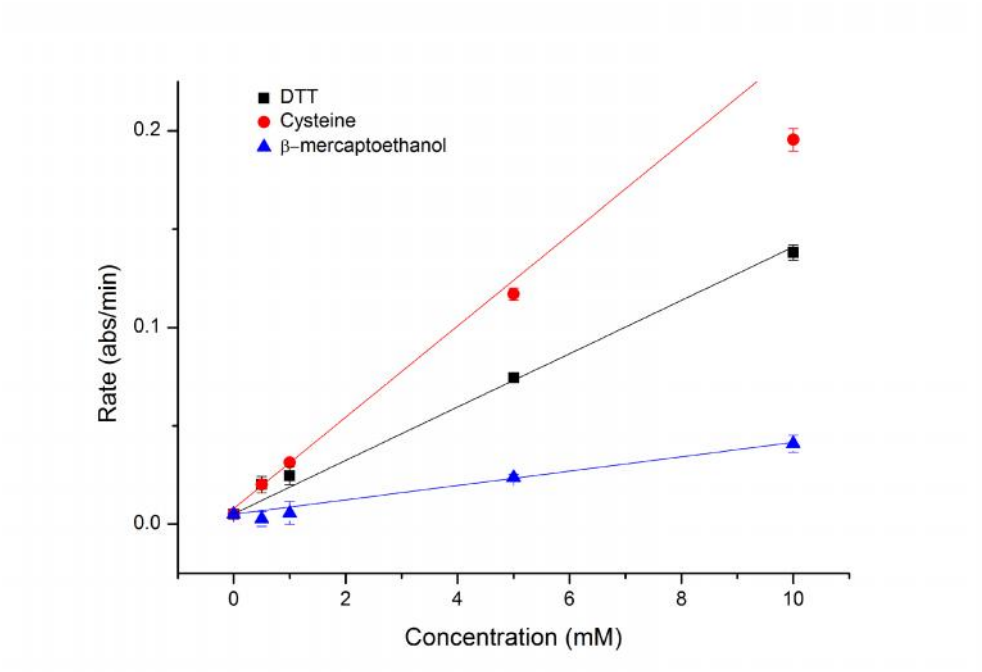

Figure 23: Linear fit for the reaction rate of CBZ-Lys-ONP with increasing concentrations of reducing agent (cysteine, DTT, or β-mercaptoethanol). Standard deviation between replicates are shown as error bars.

3.3.4 Effect of vitamin C on actinidin activity

The absence of inactivation in the purified actinidin sample (Figure 19) suggests that the oxidant responsible for inactivation is specific to the kiwifruit powder. Two components in kiwifruit were investigated to determine whether they were able to inactivate purified actinidin and therefore responsible for the inactivation occurring in the kiwifruit powder. The components investigated were vitamin C and dissolved oxygen. Kiwifruit have high levels of vitamin C (USDA, 2011) and vitamin C can be readily oxidised to dehydroascorbic acid and hydrogen peroxide. Dissolved oxygen in the phosphate buffer may also provide the catalyst for oxidation reactions, such as vitamin C oxidation that produce reactive oxygen species which can inactivate actinidin.

To investigate the effects of vitamin C on actinidin activity vitamin C, at a concentration between 1-100 mM, was added to a cuvette that contained active actinidin. No reducing agents were present in the reaction to protect actinidin from oxidation. With an increase in vitamin C concentration the specific activity of actinidin exponentially decreased (R^2= 0.99) (Figure 24). This decrease was accentuated when the cuvette, containing vitamin C and actinidin, was incubated in an aerobic environment for 5 minutes, prior to being assayed.

Vitamin C-induced inactivation upon incubation has been previously reported for papain (Fukal *et al.*, 1984; Ozawa *et al.*, 1962), and the inactivation of papain by vitamin C was further shown to be dependent on aerobic conditions. The mechanism of inactivation was hypothesised to be due to the formation of reactive oxygen species, such as hydrogen peroxide and hydroxyl radicals during vitamin C oxidation. This hypothesis was supported by showing that catalase, which neutralises hydrogen peroxide, partially prevented the vitamin C-induced inactivation (Kanazawa *et al.*, 1994). While vitamin C has been shown to inactivate papain, it is unclear whether it has the same effects on actinidin. A previous study has shown that vitamin C at concentrations of 0.8-3.2 mM actually increased the activity of actinidin (Minh Ha *et al.*, 2014), which is in contrast to the results in Figure 24. The concentration of vitamin C used in this experiment is substantially higher ($> 10^4$) than the physiological ratio of vitamin C and actinidin in GrK. This indicates that vitamin C, regardless of whether or not it inactivates actinidin, is most likely not responsible for the exponential loss of actinidin activity seen (Figure 18). The oxidation reaction that inactivates actinidin, however, could be a collective sum of reactions caused from a number of different species, which may include vitamin C.

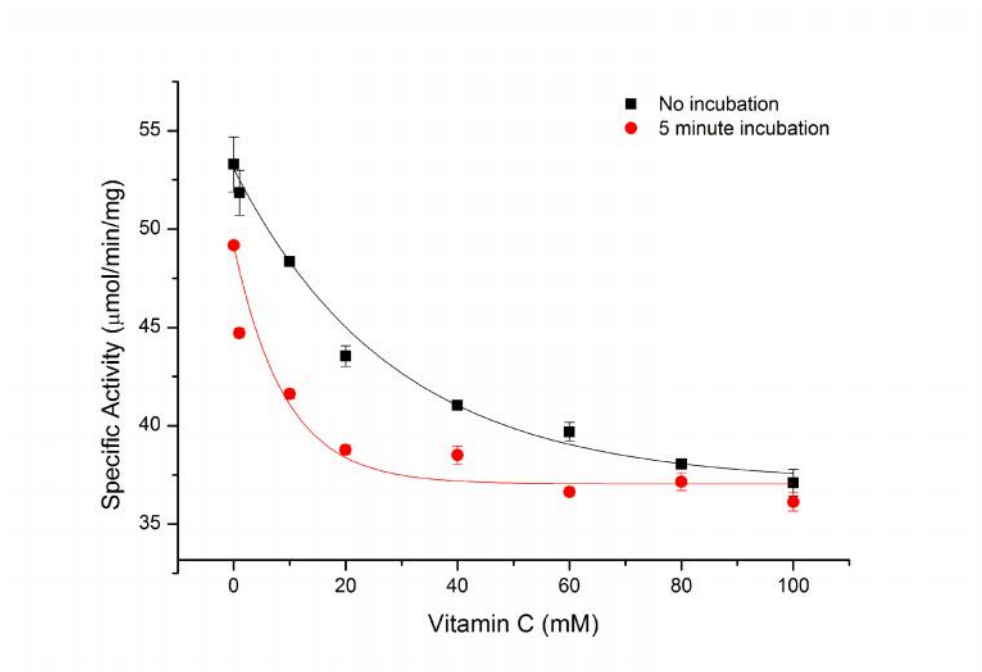

Figure 24: Exponential loss of actinidin activity after 1-100 mM of vitamin C was added. Sample containing vitamin C and actinidin were either assayed immediately, or incubated at room temperature for 5 minutes before the assay commenced. Standard deviation between the replicates is shown as error bars.

3.3.5 Effect of oxygen on activity

Oxygen that was produced from endoperoxidases has been shown to affect the activity of cysteine proteases in previous studies (Nagaoka *et al.*, 2005) and it was hypothesised that the phosphate buffer, which contains oxygen, may be responsible for inactivating actinidin in the kiwifruit powder. The experiment conducted to test this hypothesis measured the activity of a purified actinidin sample in phosphate buffer (50 mM, pH 6) that had or had not been degassed. The measure of dissolved oxygen before and after degassing was 106% and 56%, respectively, after the probe was calibrated against tap water, which provided contrasting assay conditions. The activity measurement for actinidin did not show a significant change ($p > 0.05$) in the two different buffers, which disagreed with the predicted hypothesis. The difference between the initial activity and after the enzyme was incubated in phosphate buffer for one hour, was also non-significant ($p > 0.05$) for either the oxygen saturated and moderately saturated buffers (Figure 25 (a)). Water, saturated with oxygen, has been reported to form reactive oxygen species such as hydrogen peroxide and hydroxyl radicals under the influence of visible and infrared radiation (Gudkov *et al.*, 2012), however these conditions are more forcing than those used in the current study, or the conditions that the actinidin

powder would reasonably be exposed to during processing. The current study indicates that these radicals are not forming by showing that oxygen mediated inactivation is not significant.

The addition of vitamin C resulted in inactivation, which increased after incubation (Figure 25 (b)), consistent with previous results (Figure 24). The increase in dissolved oxygen did not have a large impact on the inactivation that was occurring in the presence of vitamin C. This indicates that the inactivation seen with vitamin C is not correlated with the concentration of dissolved oxygen. The results in Figure 25 imply that the dissolved oxygen in the phosphate buffer is not causing an effect on the inactivation of actinidin in buffer.

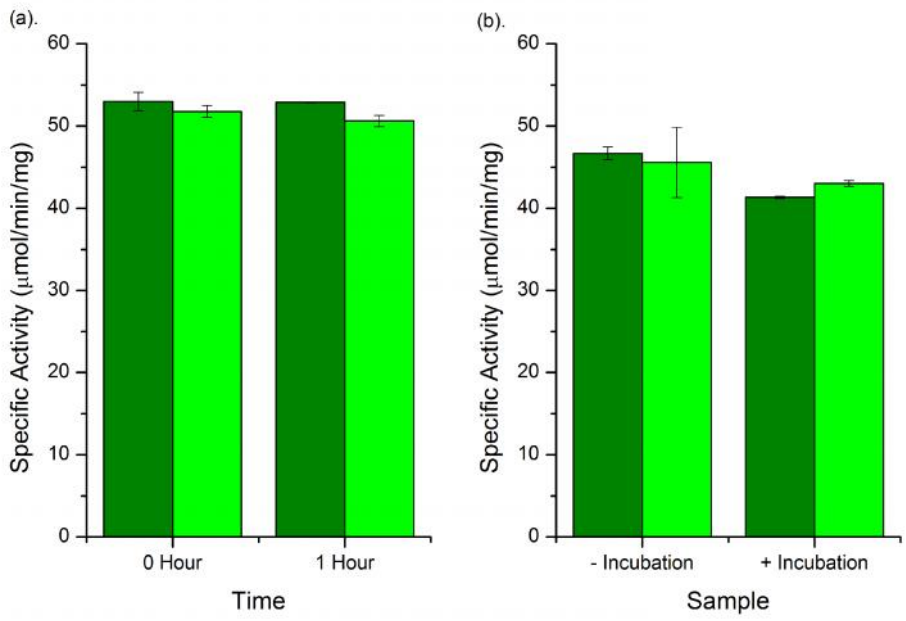

Figure 25: Effect of dissolved oxygen on actinidin activity. The super saturated oxygen buffer (106%) sample is shown in dark green. The moderately saturated oxygen (56%) buffer is shown in light green. Samples were assayed at time 0 and after one hour (a). 20 mM of vitamin C was added to the sample after incubation for one hour and assayed immediately or after the vitamin C was incubated with actinidin for 5 minutes (b). Standard deviation between the replicates is shown as error bars.

3.4 Conclusion

3.4.1 Inactivation of actinidin

Upon solubilising the kiwifruit powder, actinidin activity is lost over time. The inactivation is most prominent at the start of the time measurement with 23% of activity lost within the first 10 minutes, and continues thereafter to a 63% drop after 120 minutes. Actinidin, purified under reducing conditions does not show the activity loss and this leads to the hypothesis that the oxidation state of actinidin is important for the retention of activity in solution and that components of the pulp are involved in the inactivation. The inactivation is reversible when a reducing agent, such as cysteine, DTT, or β-mercaptoethanol was added, and this supports the hypothesis.

3.4.2 Mechanism of inactivation

The inactivation of actinidin was characteristic of the inactivation of cysteine protease homolog, papain and this supports the hypothesis that inactivation is caused by the formation of reactive oxygen species in the solution. The mechanism for generating the oxygen species, such as hydrogen peroxide, superoxide, and hydroxyl radicals is, however unclear. The magnitude of inactivation that is occurring in Figure 18 was anticipated to be driven by a chemical that is either highly reactive and specific or is present in high concentration in the sample. Vitamin C occurs in kiwifruit at high concentration and has previously been shown to inactivate papain (Fukal *et al.*, 1984; Ozawa *et al.*, 1962). This may be due to the formation of reactive oxygen species after vitamin C becomes oxidised. The results from Figure 24 showed that actinidin is inactivated by vitamin C, which is similar to papain. The inactivation from vitamin C is concentration dependent, however the concentrations are much higher than the physiological level found in kiwifruit. This makes it improbable that vitamin C is solely responsible for the inactivation. Vitamin C could still be contributing to a combined effect. Dissolved oxygen in the buffer was also determined not to inactivate actinidin, despite previous studies showing that cysteine proteases can be inactivated by oxygen (Nagaoka *et al.*, 2005). A number of oxidising agents present in kiwifruit powder may be oxidising or reacting with the active site Cys-25 residue when the powder is solubilised, which results in the inactivation, and this would also explain why the inactivation does not occur in purified actinidin.

3.4.3 Implications

The inactivation of actinidin may have implications for the quality control of different batches of the kiwifruit powder. The protocol for the quality control tests does not use a reducing agent and therefore could be affected by inactivation occurring with the onset of powder solubilisation. It is recommended that a reducing agent, such as cysteine, be included in the routine quality control assays and that the concentration of the reducing agent be 5 mM or more, with appropriate subtraction of the background rate, in order to provide sufficient protection from actinidin inactivation.

Chapter Four : Actinidin Retention during Kiwifruit Processing

4.1 Introduction

4.1.1 Processed fruit products

Harvested fruit, that are not consumed as fresh fruit, can be processed to form fruit-derived products which are sold in the health-food, beverage, and cosmetics industries. The processed fruit have qualities that make them suitable for an intended product. For example processing technologies can prevent the fruit from perishing from microbial, enzymatic activities, and oxidation reactions (Rodrigues *et al.*, 2012), which result in increased shelf life of the product, flavour and colour retention, and reduced food safety risk. Processing technologies are also used to change the aesthetics of the fruit and allows the processed product to be readily accessible and easy to use or consume.

There is a wide selection of technologies that exist to process fruits, which have varying affects on the nutritional, organoleptic, and textural properties of the fruits in different ways. Choosing one technology over another requires balancing the effects that the processing has on the quality of the product with the cost, safety, and through-put capacity of the operation. Spray-drying and freeze-drying are commonly used for dehydration, with spray-drying being the more cost effective practice. Both technologies reduce the moisture content of the fruit; however the impacts on the nutritional value, structural integrity, and biological function makes freeze drying a more sensitive technology that results in a final product that is regarded as higher quality (Sagar *et al.*, 2010). Currently, Actazin™ powder is produced by the dehydration of fresh kiwifruit pulp using a minimal freeze-drying processing practice.

4.1.2 Loss of bioactive molecules during processing

Processing of fruit offers significant benefits by increasing product storage life but can also have a negative impact on the bioactive molecules in fruits that are important for health. The

act of fruit processing exposes the bioactive molecules to both internal factors from within the fruit and external factors from the surrounding environment of the fruit. These internal factors that affect the retention of bioactive molecules involve chemical reactions that affect retention of bioactive molecules. Processing fruit, such as by pulping, disrupts the fruit structure to release its cellular components. The biomolecules become exposed to interactions that were not normally encountered whilst the cell was intact and this may increase the chance of detrimental reactions to the bioactive compounds. The bioactive molecules can be damaged by physical external factors, such as heat, light, pressure, and oxygen. For example, vitamin C, an important antioxidant molecule is susceptible to both heat and oxidation reactions (Riaz *et al.*, 2009) and this reduces the protection the molecule can provide against reactive oxygen species. Proteins are also affected by processing with freezing, thawing, and drying stresses affecting the protein hydration shell that is important for its structural stability (Arakawa *et al.*, 2001). These have direct consequences on the retention of enzymatic activity after processes, such as freeze drying, that expose enzymes to these stresses (Carpenter *et al.*, 1987; Matsubara *et al.*, 2006).

The enzymatic activity of the bioactive protein, actinidin, which is an important component in Actazin™ could be affected by the processing of kiwifruit. Actinidin activity has been found to increase the digestion of food proteins in a digestive tract environment *in vitro* (Kaur *et al.*, 2010a, 2010b) and therefore a maximal amount of active actinidin is desired in the Actazin™ product, that is sold as a digestive aid. Routine quality control checks performed by Anagenix, Ltd, however found that the actinidin activity varies 48% between the highest and lowest actinidin containing batches of kiwifruit powder (Figure 26). Kiwifruit, as a biological material, is expected to display some variability as a result of the initial harvest and ripening process, and the processing of kiwifruit to produce Actazin™, which involves several transformation stages such as ripening, pulping, and freeze drying. As Anagenix Ltd desires a maximal amount of actinidin in Actazin™, variations introduced during processing warrants further investigation.

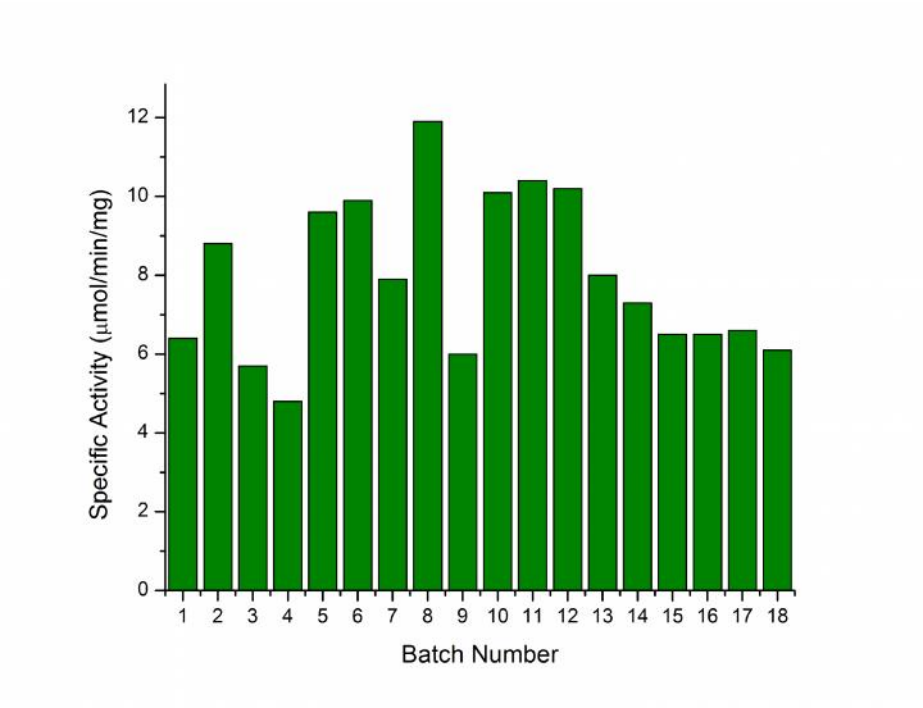

Figure 26: Activity rates of actinidin in different batches of kiwifruit powder measured as routine quality control checks by Anagenix Ltd.

4.1.3 Pre- and post-harvest factors that affect the composition of fruits

Pre-harvest factors

Pre-harvest factors influence the growth of plants and can have important contributions to the quality of the fruit. Pruning, which is conducted throughout the growing season has been associated with an increase in soluble solids content (Gerasopoulos *et al.*, 2005), as well as fruit yield in kiwifruit orchards (Miller *et al.*, 2001). Other growing practices, such as spraying, also impacts the composition of kiwifruit. Treating the fruit with a 1% solution of calcium chloride four times during fruit development resulted in the fruit increasing its firmness and calcium content, which had a positive effect on fruit storability (Gerasopoulos *et al.*, 2005). Similarly, a synthetic plant hormone that was sprayed at a low dosage (4 µL/L) before flowering increased the fruit weight, soluble solids content, vitamin C, and other key indicators of nutritional quality (Cruz-Castillo *et al.*, 2014). Water, temperature, and light stresses have all been shown to have an effect on the composition of grapes, including the accumulation of secondary metabolites in berry pulps, seeds, and skins as the plant responds to the stress (Ferrandino *et al.*, 2014). These examples show that pre-harvest factors can influence the development of fruit leading to changes in the composition of the fruit.

Fruit growth

Fruit growth is also important and has been shown to play an essential role for protein development in kiwifruit. From a point 100 days before the commercial harvest start date until harvest the protein content increases approximately 200 fold in GrK fruits (Ciardiello *et al.*, 2009). The protein concentration, reaches the highest amount when harvested, and appears to plateau for at least 40 days. The ratio of the individual soluble proteins present was measured by densitometry of the protein bands that migrated during SDS-PAGE analysis. Actinidin, from GrK kiwifruit had a high relative abundance compared to the other soluble proteins and remains consistently high during the harvest season (Ciardiello *et al.*, 2009). Actinidin activity continually increased during fruit growth until the date that harvest typically commences (S. Boyes *et al.*, 1997). These results indicate that, over the harvest period, the protein content is high and this also correlates with high actinidin activity.

Post-harvest ripening

Post-harvest ripening allows fruit to develop to more desirable composition and this may also have an effect on the actinidin content. Northern analysis reported actinidin expression levels decreased after the *A. deliciosia* fruit was ripened with ethylene (Nieuwenhuizen *et al.*, 2007). Contrary to this result, the same study measured the protein levels using western analysis and showed there was no significant change in actinidin levels. In support of the latter, the actinidin activity increased when the fruit was ripened with ethylene, however the activity did sharply decline if the fruit was over ripened (S. Boyes *et al.*, 1997).

Fruit storage

Fruit storage is an important practice that is used to control the ripening of fruits. Kiwifruit stored for 182 days at 0-0.5^{o}C, with a relative humidity of 90-95%, showed a steady increase in sugar content, soluble solids, and vitamin C as well as a decrease in fruit firmness and total acidity (Bonvehi *et al.*, 1997). The respiration rates of harvested fruits affects the rate at which a fruit ripens by breaking down carbohydrates, and kiwifruit in cool storage have reduced respiration rates, which would delay ripening (Ritenour *et al.*, 1999). Storage at 4^{o}C had no substantial effect on actinidin activity during a 2 month period, in fact, the activity slightly increased, which may have been from the fruit ripening (S. Boyes *et al.*, 1997).

4.1.4 Aims

This chapter aims to identify any factors during Actazin™ production that has an effect on the actinidin activity which may contribute variations observed in kiwifruit powder batches (Figure 26). The factors that affect actinidin retention throughout the production could occur both pre- and post-harvest. Pre-harvest factors affect the growth and maturity of fruits ultimately picked. Post-harvest factors can affect the ripeness of the fruit, with the development and retention of protein levels influenced by processes involved in transformation of the kiwifruit from a fruit to a powder. Actinidin activity was measured at different stages of the processing line in order to optimise Actazin™ production so that maximal content of actinidin is present in the final product.

4.2 Results and discussion

4.2.1 Activity variation between individual kiwifruits

To explore the variation in actinidin activity between individual kiwifruit that is caused by pre-harvest factors the specific activity of six kiwifruit, which were representative fruit that would be pulped at Kiwifruit Processing Company Ltd, was measured. The flesh of each kiwifruit was homogenised, centrifuged, and the resulting supernatant was assayed as described in Chapter 2. The specific activities of the kiwifruit fell around the median value of 8.2 µmol/min/mg, however there were outliers that had a specific activity above and below this value (Figure 27 (a)). The data was assessed to understand whether the specific activity variations represented the expected variation in a normal distribution using a Q-Q plot. The data using six kiwifruit fits a normal distribution (Figure 27 (b)) and indicates that while pre-harvest factors introduces variation, that this is normal. Therefore we can assume that the actinidin activity between pulped kiwifruit batches should all be similar, although further testing between pulped kiwifruit batches at the Kiwifruit Processing Company Ltd is recommended.

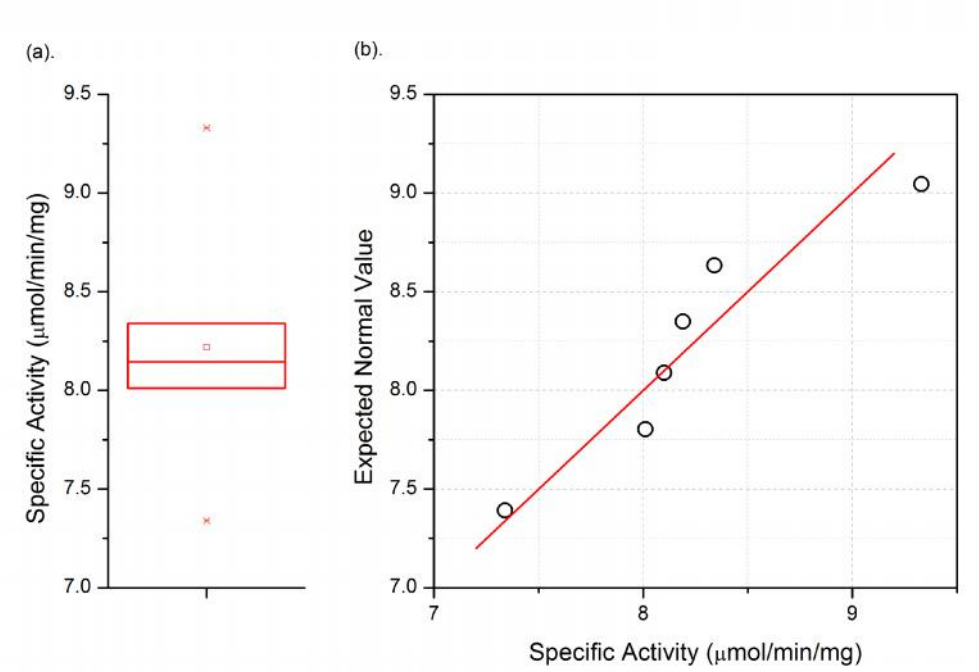

Figure 27: Activity variation between six individual kiwifruit represented by a (a) box and whisker plot (a) and (b) Q-Q plot.

4.2.2 Post-harvest storage effects on activity

Kiwifruit is commonly kept in cool storage to prevent the fruit from degrading. The effects cold storage had on actinidin activity was assessed by comparing the specific activity of recently harvested fruit and fruit after an additional 4-5 months of cool storage. Both samples were taken from bins of kiwifruit that had been ripened and were about to be pulped, however the samples sent down from Tauranga after the extended cool storage period were heavily bruised. The comparison (Figure 28) showed on average 73% of activity was retained after the extended cool storage. The standard deviation of the fruit sample "after storage" was considerably higher than that of the sample "before storage" (Figure 28). An explanation for this variance is that the fruit was individually assayed unlike the fruit that was assayed for the "before storage" sample, which was homogenised. The variance, however could have also been caused by the condition of the fruit as they were considerably bruised. More fruit samples will be needed to understand whether the bruising was having an effect or not. Overall, however the cool storage did not substantially reduce the actinidin activity which is consistent with previous studies (S. Boyes *et al.*, 1997).

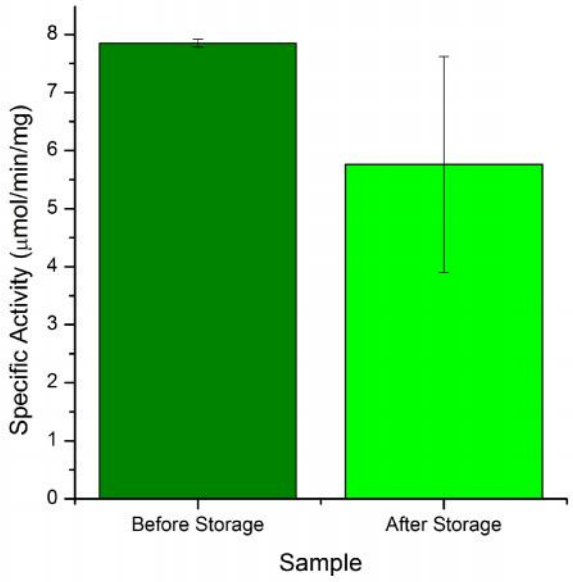

Figure 28: Actinidin activity before and after 4-5 months in cool storage. Four kiwifruit were homogenised together for the "before storage" sample and standard deviation between the reps is shown as error bars. Nine individual fruit was assayed for the "after storage" samples and the standard deviation between these samples is shown as error bars.

4.2.3 Post-harvest ripening effects on activity

Post-harvest ripening of kiwifruit has previously been shown to be important for the actinidin activity (S. Boyes *et al.*, 1997). Kiwifruit that arrives at the Kiwifruit Processing Company Ltd is stored in different facilities that manage how the fruit ripens. Initially the fruit is stored at 0^{o}C to retard ripening and this storage stage is utilised to control the amount of kiwifruit that is ready to be processed into pulp ("pre-process"). The fruit is moved to ambient temperature (~12-15^{o}C), which allows the fruit to ripen before being refrigerated (4^{o}C) until they are ready to be processed into a pulp ("process-ready"). Throughout the ripening, the fruit is graded to remove any fruit that appears to be over-ripe or has become spoiled from microbial contamination ("past-process").

Fruit samples at each of these stages were assessed for specific activity and showed that the ripening process, conducted at Kiwifruit Processing Company Ltd is important to achieve a high activity of actinidin. Between "pre-process" and "process-ready" samples there was a highly significant increase in average specific activity of 45% ($p < 0.01$), and between the

"process-ready" and "past-process" samples there was a 8% decrease ($p < 0.05$) (Figure 29). The result indicates that post-harvest ripening has an impact on the actinidin activity and that "process-ready" fruit is at an appropriate ripeness to pulp for a high actinidin content. However the 45% increase between "pre-process" and "process-ready" samples was much higher than reported values after kiwifruits were ripened, post-harvest with ethylene (Stewart Boyes *et al.*, 1997). This may mean that ethylene ripening does not increase the actinidin activity as much as natural ripening that is conducted at the Kiwifruit Processing Company Ltd.

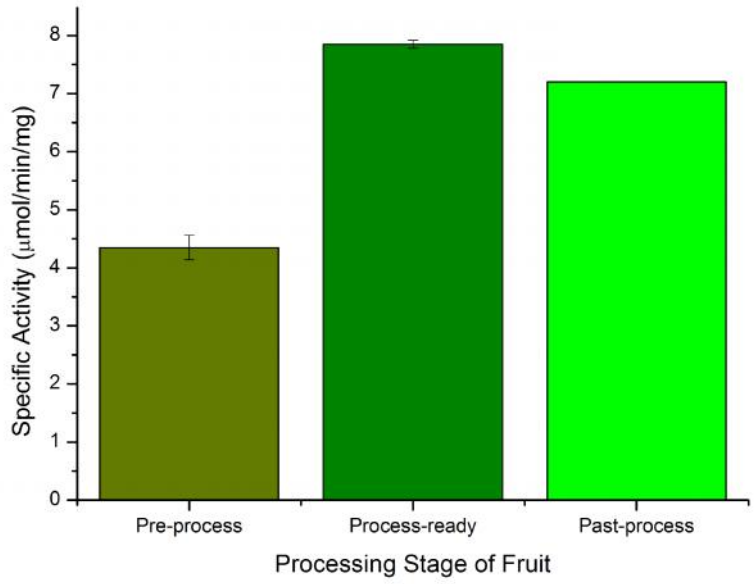

Figure 29: Actinidin activity in fruit at the different processing stages at the processing plant. Four fruit at each stage were homogenised together and assays were conducted in duplicates. Standard deviation of the mean is shown as error bars.

4.2.4 Freeze drying

Pulp freezing

Kiwifruit pulp is blast frozen and stored at -20^{o}C before it is transported to Christchurch and freeze dried at Genesis Bio-Labs. Kiwifruit pulp from fresh fruit and pulp that had been frozen and frozen pulp ready to be freeze dried was measured for actinidin activity to measure the difference between the samples. A significant 46% loss ($p < 0.01$) of average total activity for 100 mg of dry kiwifruit weight between the kiwifruit pulp and frozen pulp

was determined (Figure 30 (a)). This shows that kiwifruit pulping, freezing, and/or transportation to Christchurch is having a negative impact on the retention of actinidin during the production of Actazin™.

The activity drop appeared to correlate well with a highly significant drop ($p < 0.01$) in total soluble protein content, also in 100 mg of kiwifruit dry weight (Figure 30 (b)). This indicates that actinidin is becoming structurally denatured rather than catalytically inactivated. Proteins are known to be sensitive to being frozen and thawed (Arakawa *et al.*, 2001) and actinidin has shown to lose 22% of its activity after it was purified from GrK, frozen and stored at -80^{o}C for 2 months before being thawed and assayed, as described in Chapter 2. It is therefore recommended that the pulp is assayed for actinidin activity before and after it is frozen to determine if the freezing, storage, or transportation is responsible for the loss of activity.

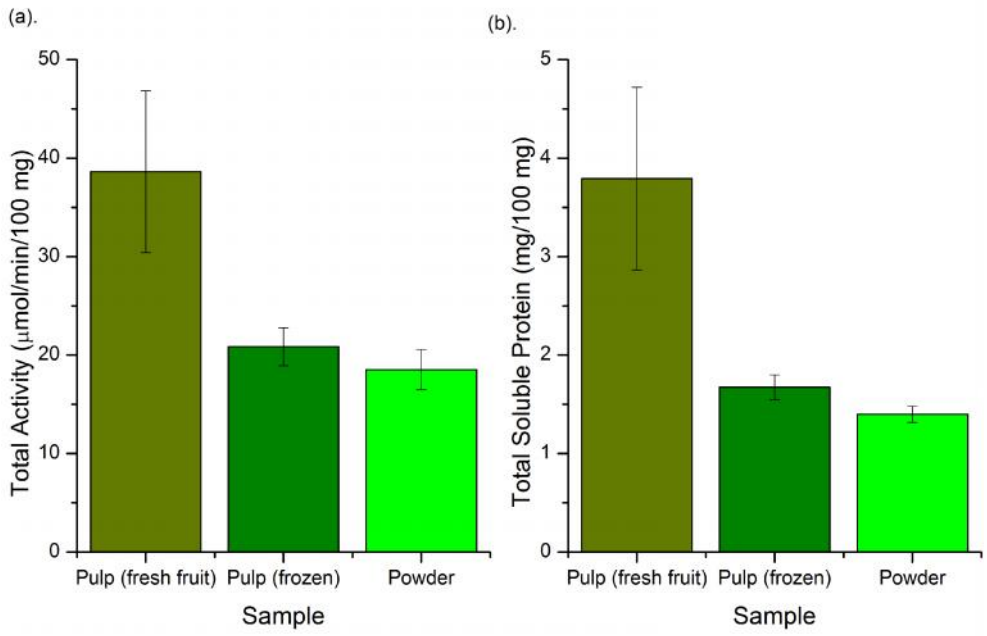

Figure 30: Process loss summary of actinidin in 100 mg of kiwifruit dry weight depicting the (a) total activity and (b) total soluble protein content. Measurements were conducted from various samples including six fresh fruit ("fresh fruit") and at four locations on the frozen pulp ("frozen") and resulting freeze dried powder ("powder"). Standard deviation between these samples is shown as error bars.

Pulp drying

Freeze drying is a major transformation step during the processing of kiwifruit to Actazin™ powder. Frozen pulp is dried by applying a thermal gradient from below and around the trays

that contain the pulp. The moisture is removed by sublimation, under vacuum as the temperature is raised until the pulp becomes a powder. The temperature increase was measured to understand whether the drying stage could affect the stability of actinidin. Temperature data loggers were placed in the frozen pulp, which was then dried with the temperature recorded at 5 minute intervals (Figure 31). From an initial starting temperature of the frozen pulp at [redacted] the temperature increased during the drying stages to a maximal temperature of [redacted] before reducing to an ambient temperature of approximately [redacted], after the sample had been removed from the freeze drier. The temperature profiles for the individual data loggers, that were spaced across the tray (Figure 31) were similar and shows that the heat is evenly distributed throughout the freeze drier.

Protein structure and function relies on the intricate folding of the protein, which can be disrupted by temperature. The stability of actinidin's structure with increasing temperature was measured previously using differential scanning fluorimetry (DSF) and was shown to be affected by pH (Figure 10). The melting temperature of actinidin was 51^{o}C at pH 3.7, which is a similar pH as what was measured for the kiwifruit pulp. This could imply that the thermal stability of actinidin at pH 3.7 is lower than the maximal temperature of [redacted] reached during freeze drying. The activity of actinidin, as determined using a casein-based assay has also been found to be temperature dependent with the activity decreasing when temperatures were raised above 45^{o}C (M. Ha *et al.*, 2012).This indicates that the stability and activity of actinidin may be affected by the increases in temperature such as experienced during the drying stages of freeze drying.

Figure 31: Temperature change during freeze drying, as measured by iButton temperature data loggers every 5 minutes. The different lines represent individual data loggers that were positioned across the tray of frozen kiwifruit pulp.

The retention of actinidin activity after the freeze drying stage was measured to assess if this process had an effect on the activity. Both the frozen pulp (after defrosting) and the powder were weighed out to a calculated kiwifruit dry weight in 50 mM phosphate buffer, pH 6 at a concentration of 100 mg/mL dry weight. The measurements showed that there was a small drop in average total activity for 100 mg of kiwifruit dry weight (Figure 30 (a)) before and after the freeze drying. The changes, however were not significant and this indicates that despite the fact that some actinidin can be lost during freeze drying (Figure 30 (b)) the majority of actinidin is not negatively affected by the increase in temperature that occurs (Figure 31) or the transformation from a liquid to an anhydrous state.

The retention of activity results are surprising given that the thermal stability of actinidin was previously determined to be 51^{o}C at pH 3.7 as assessed by DSF (Figure 10) whereas the freeze drying process exposed the dried pulp to temperatures of [redacted] for approximately [redacted] (Figure 31). It was anticipated that there would be a significant drop of enzymatic activity during drying. These results indicate that either differential scanning fluorimetry does not appropriately simulate the thermal stability of actinidin in an anhydrous state or that other

components in the pulp can protect actinidin as the pulp becomes dehydrated. There have been previous studies that have shown the importance of lyoprotectants, such as sucrose for the retention of enzymatic activity, (Carpenter *et al.*, 1987) and structure (Prestrelski *et al.*, 1993) during freeze drying. Sugars can stabilise proteins when their hydration shell is lost during freeze drying by forming a hydrogen bond network which prevents conformational changes from occurring when the protein is dried (Carpenter *et al.*, 1989; Hedoux *et al.*, 2013). Green kiwifruit contains 9 g of total sugars per 100 g of fruit (USDA, 2011) and this may provide similar stabilising capacity to the proteins as the frozen pulp is exposed to an increase in temperature. Thermal stability studies that investigate how saccharides affect the stability of actinidin will help to determine the mechanism of actinidin stabilisation during the drying. Studies on the thermal denaturation and inactivation of actinidin in an anhydrous environment would also be desirable as these have direct implications on shelf life of stored proteins in a variety of contexts. However within the current studies the absence of a significant drop in actinidin activity after drying eliminates the possibility that freeze drying is having a detrimental effect on actinidin activity retention.

4.3 Conclusion

4.3.1 Pre-harvest factors on actinidin activity

Pre-harvest factors are diverse and make it difficult to assess individual factors that affect the actinidin content in kiwifruit. Instead the accumulative effect of the factors was assessed by assaying a selection of fruit that was a representative sample of the kiwifruit used in the pulping process. The results presented in Figure 27 showed that pre-harvest factors do affect actinidin activity, however the variance follows a normal distribution and the pulping will average the activity to a median value, which makes it unlikely that pre-harvest factors are influential factors on the actinidin activity between batches of kiwifruit pulp.

4.3.2 Post-harvest factors on actinidin activity

The retention of actinidin activity after a 4-5 month cool storage period was high at 73% and most likely not a significant contributor to losses of actinidin. The large variance in the samples that had been stored for the extended period was hypothesised to be from the condition of the fruit after it had been transported from the Bay of Plenty to Christchurch for the activity to be analysed and therefore further testing is recommended for a more accurate

idea as to the effects that cool storage has on actinidin.

Kiwifruit ripening has previously been found to increase actinidin activity (S. Boyes *et al.*, 1997). This literature precedent was supported by the results in Figure 29 that showed 'unripe' kiwifruit had a lower specific activity to 'ripe' kiwifruit. This encourages the use of ripening that is already conducted at the Kiwifruit Processing Company Ltd before the kiwifruit is pulped.

Between pulping and freeze drying the frozen pulp at Genesis Bio-Labs there was a significant loss of actinidin. Actinidin has shown to be sensitive to freezing and thawing over a period of 2 months and this might be the major contributor to the retention of actinidin during the production of Actazin™, however further testing is required to understand whether the freezing, thawing, or storage at low temperatures is having the biggest impact on the protein structure of actinidin.

The freeze drying process did not significantly affect the actinidin activity or content. This was a surprising result as the temperature reached during the drying exceeded the thermal stability of actinidin measured at pH 3.7. This implies that actinidin is stable during the transformation of the kiwifruit pulp to the powder even if the temperature is raised up to [redacted].

Chapter Five : Kiwellin Purification and Characterisation

5.1 Introduction

5.1.1 Isolating kiwellin from kiwifruit

Kiwellin, constitutes a major portion of the soluble proteins that are found in kiwifruit (Ciardiello *et al.*, 2009) and can be isolated successfully from *Actinidia chinesis* kiwifruit cultivars. The protein was first isolated using a high salt extraction method, that involved separating kiwellin from the insoluble kiwifruit tissue with a salt solution. This was followed with both anion- and cation-exchange chromatography steps, which isolated kiwellin from the other soluble proteins present in the fruit (Tamburrini *et al.*, 2005). An amino acid sequence analysis of the purified kiwellin from (*Actinidia chinensis*) revealed that the protein contained 189 residues in its sequence and had a theoretical molecular weight of 19,968 Da (Tamburrini *et al.*, 2005). The experimental molecular weight of kiwellin, shown by SDS-PAGE analysis results in protein migration of a 28 kDa or 20 kDa species depending on whether the analysis is conducted in reducing or non-reducing conditions, respectively (Tamburrini *et al.*, 2005) . The discrepancy in the experimental molecular weight is likely to be from the reducing agent disrupting disulfide bonds that may be occurring between the 14 cysteine residues found in kiwellin's primary sequence.

Several isoforms of kiwellin exist amongst the most widely grown kiwifruit species. A published sequence of kiwellin (Tamburrini *et al.*, 2005) was BLAST searched on an *Actinidia* expressed sequence tag database (Crowhurst *et al.*, 2008) and revealed the different isoforms (Maddumage *et al.*, 2013). The sequences each contained 189 amino acids, as well as a predicted signal peptide at the N-terminus of 23 amino acids. The sequences of the different isoforms of kiwellin showed close homology with > 95% sequence identity when the sequences were aligned (Maddumage *et al.*, 2013).

The level of kiwellin in *Actinidia* species varies considerably and this variation may be

connected to the interactions kiwellin has with actinidin. Cultivars, such as Zespri® Hort16a (*Actinidia chinensis*) shows high levels of kiwellin and low levels of actinidin (Maddumage *et al.*, 2013). Other cultivars also show this inverse relationship. The popular green kiwifruit Hayward cultivars (*Actinidia delicosia*) has a high abundance of actinidin and a low abundance of kiwellin (Maddumage *et al.*, 2013). This relationship is postulated to be a result of the proteolytic activity that actinidin has been shown to have for kiwellin. Kiwellin can be cleaved into two domains, termed KiTH and kissper, which are 16 and 4 kDa respectively (Tuppo *et al.*, 2008). It is unclear why kiwellin is cleaved into KiTH and kissper, however the cleavage may be connected to the physiological function of kiwellin.

5.1.2 Structure and function

Despite kiwellin contributing a major portion of the soluble proteins found in kiwifruit (Ciardiello *et al.*, 2009) there is no known physiological function for kiwellin. A sequence alignment between kiwellin (Tamburrini *et al.*, 2005) and homologs from a diverse range of plant species, that were identified from BLAST searching NCBI databases, indicates that kiwellin shows close homology with other plant proteins (between 74-79%) and conservation of a number of amino acids (Figure 32). The plant homologs also did not have a known biological function and were the product of annotated genome sequencing. This could imply that these proteins share a physiological function, however further investigation is required.

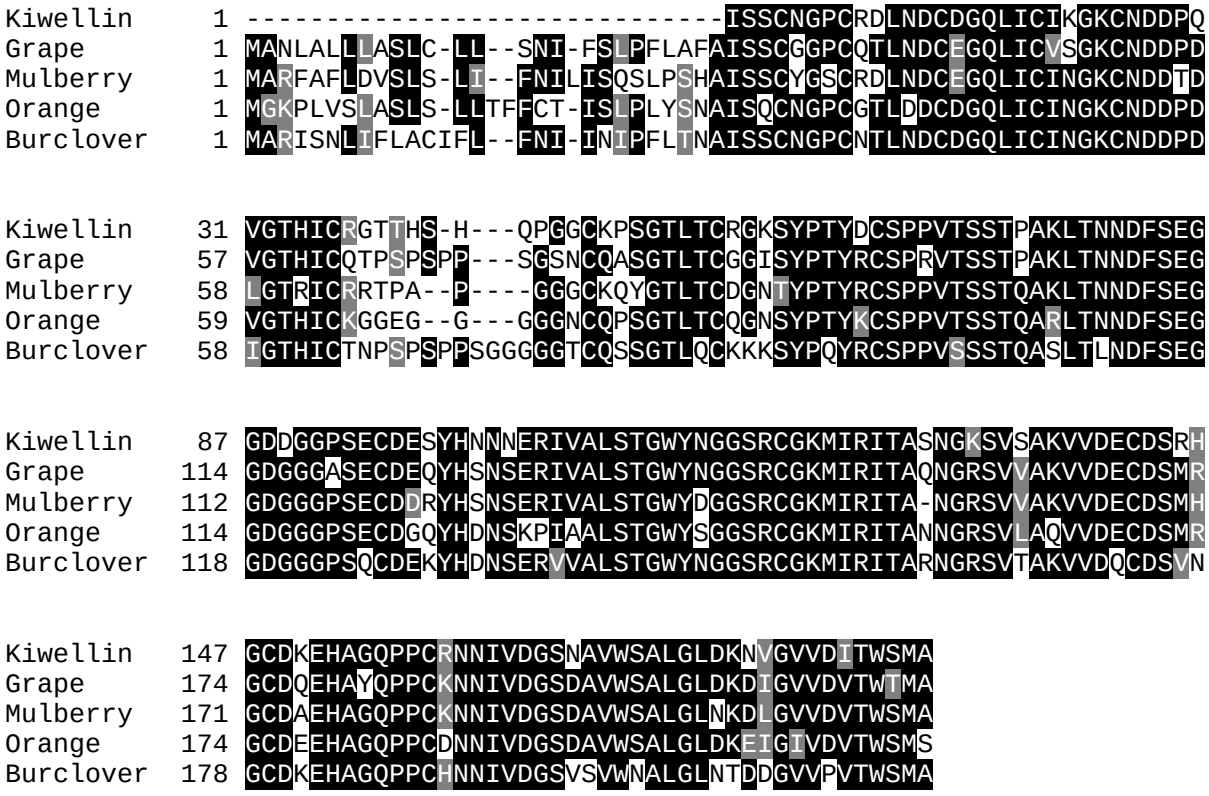

Figure 32: Sequence alignment of homologs for kiwellin from other plant species using T-Coffee alignment software (Notredame *et al.*, 2000; Tommaso *et al.*, 2011). The species, in order of appearance were, kiwellin (*Actinidia chinesis*), grape (*Vitis vinifera*), mulberry (*Morus, notabilis*), orange (*Citrus sinensis*), burclover (*Medicago truncatula*). GenBank accession numbers: P84527.1, XP_002285296.1, EXC22900.1, XP_006488056.1, XP_003638071.1, respectively.

The secondary structure of kiwellin, as determined by circular dichroism spectroscopy (CD) indicates that there are mainly helical structures, characterised by a CD trace with two minima around 222 and 206 nm (Bernardi *et al.*, 2010). The intensity of the two troughs was affected by pH and increases in acidic (pH 4.5) environments. While there is an absence of further structural information available for kiwellin the tertiary structure of the kissper domain has been solved by NMR spectroscopy (Ciardiello *et al.*, 2008). The resolved spectra identifies two short β-strands as well as a helical stretch for the 39 amino acid sequence. Three disulfide bonds connect different regions of the peptide together and contribute to the overall fold. The tight folding and secondary structures that kissper exhibits may also be present in the corresponding region of its precursor, kiwellin, however the peptide may become re-folded after cleavage from kiwellin. This provides uncertainties as to the structure that kiwellin holds in solution and encourages further investigation.

5.1.3 Bioactivity

There has been no evidence that kiwellin has bioactive properties, however there has been preliminary results indicating that the kissper domain would have a positive impact in the gastrointestinal (GI) tract. Despite also not knowing a physiological function of kissper, the structural and chemical properties of the peptide are hypothesised to influence ion flux in intestinal cells and combat inflammatory responses, such as neutralising reactive oxygen species.

Kissper has shown a pH-dependent and voltage-gated pore-forming activity in model synthetic planar lipid membranes (Ciardiello *et al.*, 2008). The pore size of the channel was calculated to have a diameter in the range of 1.9 to 7.6 Å for KCl and the ion selectivity can change from anion to neutral to cation depending on the nature of the salt solution (Meleleo *et al.*, 2012). It is hypothesised that multiple kissper subunits contribute to the channel and that the pore forming activity might promote the adsorption of substances in the GI tract (Meleleo *et al.*, 2012).

Inflammation can be a chronic symptom of functional bowel disorders, which creates a desire to find anti-inflammatory agents that can prevent this response (Lee *et al.*, 2014). The antioxidant and anti-inflammatory properties of kissper on *in vitro* models for intestinal cells from healthy and diseased patients was investigated and it was shown that kissper efficiently counteracted oxidative stress and inflammatory responses after the cell lines were induced to show an inflammatory response (Ciacci *et al.*, 2013). This could provide a possible mechanism to the anti-inflammatory responses that have been shown previously for aqueous kiwifruit extracts (Edmunds *et al.*, 2011). However further investigation is warranted in light of the inconsistencies of the anti-inflammatory effects that kiwifruit extracts show between *in vitro* and *in vivo* models (Edmunds *et al.*, 2012).

5.2 Results and discussion

5.2.1 Purification of kiwellin

Kiwellin was extracted from two cultivars of *Actinidia chinensis* (GoK), which were Zespri® Hort16a and Zespri® SunGold. The change between the Hort16a and SunGold cultivars

occurred because of the prevalence of the bacteria *Pseudomonas syringae* pv. *actinidiae* (Psa) that devastated the Hort16a orchards (Kiwifruit-Vine-Health, 2014). Kiwellin was purified using a high salt extraction method, as previously described (Tamburrini *et al.*, 2005). The soluble proteins were extracted from the cell wall of the kiwifruit tissue upon addition of a high salt solution in an alkaline environment. Kiwellin was separated from the other proteins in this extract by using ion exchange chromatography. The kiwellin isoforms separated from the Hort16a cultivar was used for the static light scattering and small angle X-ray scattering experiments while kiwellin from the SunGold cultivar was used for the remaining experiments outlined in this thesis.

The kiwifruit extract solution containing kiwellin was loaded onto a HiLoad™ Q HP anion exchange chromatography column (GE Healthcare) after it had been dialysed into 10 mM Tris-HCl, pH 7.5 buffer. Proteins that did not bind to the positively charged resin passed out of the column as the flowthrough. Bound proteins were displaced using a 0 to 0.5 M NaCl gradient (Figure 33). Five protein peaks eluted during the salt gradient (Figure 33), showing that there are multiple proteins from GoK that bind to an anion exchange chromatography column. The two major peaks (peak 3 and 4) that both appeared to show the presence of kiwellin upon SDS-PAGE analysis was pooled in order to characterise both isoforms of kiwellin. Further work characterising the two isoforms of kiwellin, separated using anion exchange chromatography was proposed, however time restraints did not allow for the additional characterisation experiments and is recommended in future studies that aim to characterise kiwellin from *A. chinensis* cultivars.

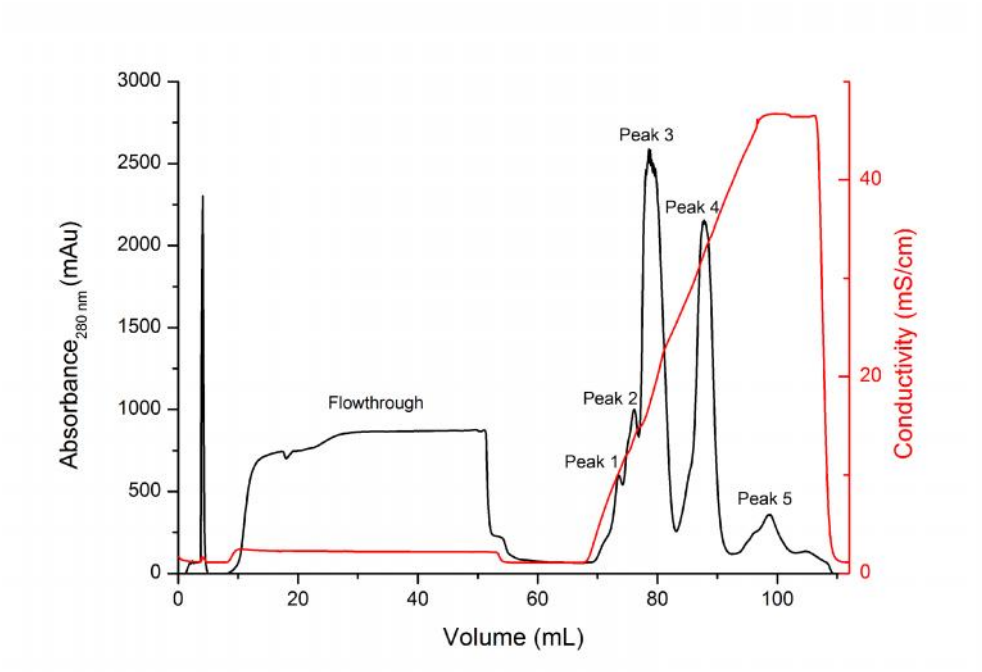

Figure 33: Anion exchange chromatography using a 5 mL HiLoad™ Q HP anion exchange column (GE Healthcare). Protein that bound to the column was eluted by increasing the salt concentration to 0.5 M NaCl over six column volumes.

A cation exchange chromatography was used to further separate the kiwellin isoforms from the other kiwifruit proteins. The pooled fractions from the anion exchange step were exchanged into 10 mM Na acetate buffer at pH 5 by using a desalting column. The solution was then injected onto a HiLoad™ SP HP cation exchange column (GE Healthcare), which had been pre-equilibrated into the same buffer. Elution was carried out using a salt gradient from 0 to 0.5 M NaCl over 6 column volumes. At a NaCl concentration of around 310 mM kiwellin eluted as a single peak (peak 1) (Figure 34). A small shoulder was present at the start of peak 1, however the protein species was unable to be identified by SDS-PAGE analysis (data not shown). From a starting mass of 100 g of kiwifruit flesh 2.5 mg of kiwellin was purified using anion and cation exchange chromatography. This is lower than previous studies that reported 4 mg of kiwellin was purified from an equivalent starting mass (Tamburrini *et al.*, 2005).

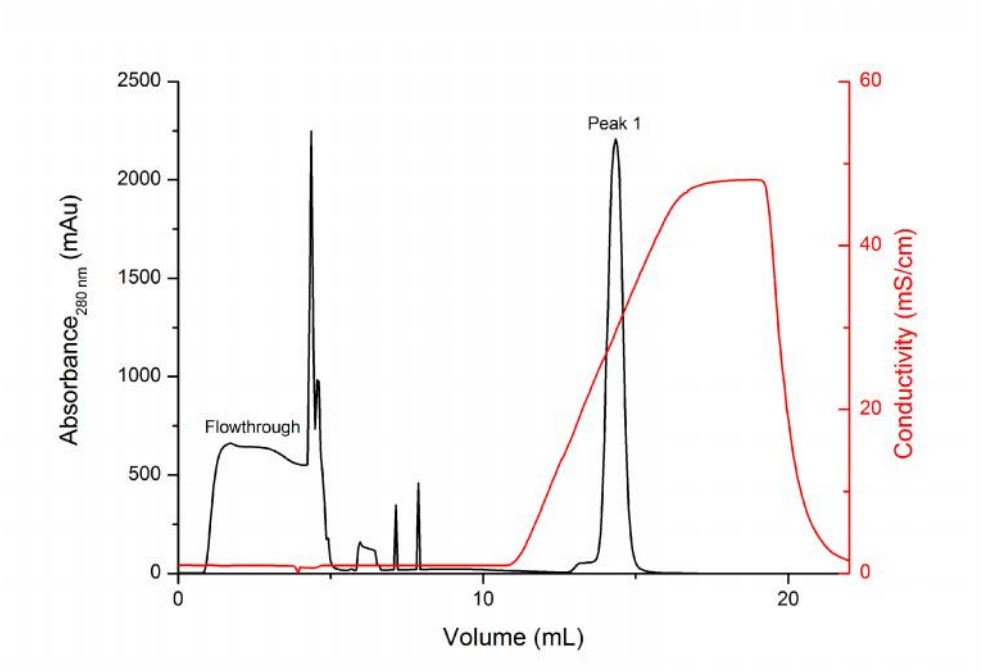

Figure 34: Cation exchange chromatography step using a 5 mL HiLoad™ Q SP cation exchange chromatography column (GE Healthcare). Protein that bound to the column was eluted by increasing the salt concentration to 0.5 M NaCl over six column volumes.

Size exclusion chromatography was used to assess if any aggregate was present in the purified kiwellin sample. It was also used to buffer exchange the sample into a low salt phosphate buffer in preparation of characterisation studies including: static light scattering, analytical ultracentrifugation, and crystallography screening. The protein eluted from the HiLoad™ 16/600 Superdex™ pg 200 size exclusion column (GE Healthcare) as a single peak (peak 1) after approximately 92 mL (Figure 35). The chromatography trace showed that there was no aggregate that eluted as a higher molecular weight species.

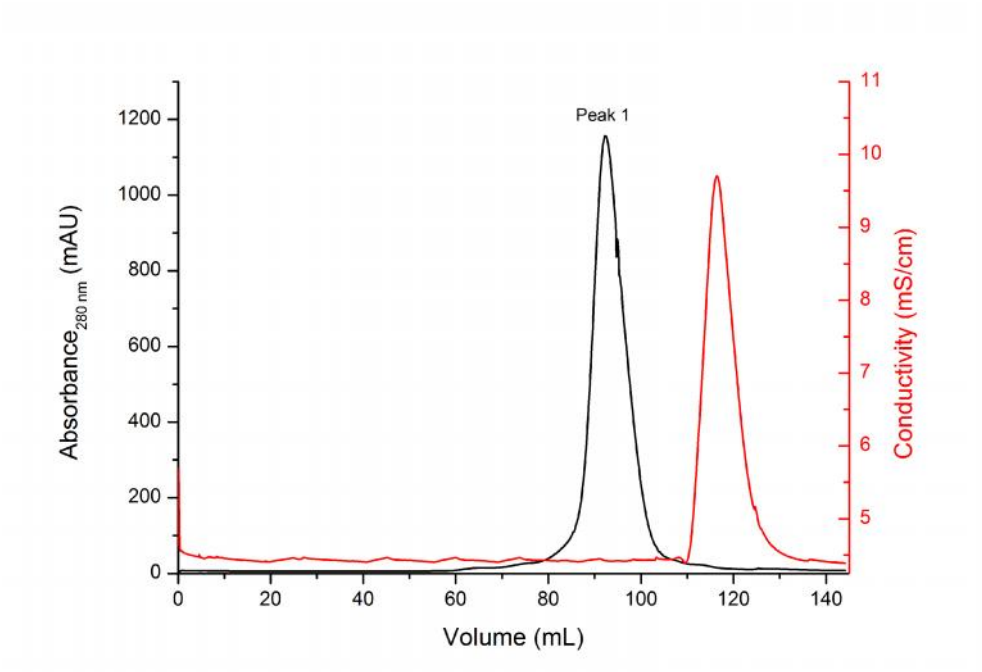

Figure 35: Size exclusion chromatography using a 120 mL HiLoad™ 16/600 Superdex™ pg 200 gel filtration column (GE Healthcare). Elution was performed at 0.5 mL/min using 50 mM sodium phosphate buffer, pH 6.

The purity of kiwellin was assessed throughout the purification by use of SDS-PAGE analysis, as there is no current assay to identify the presence of kiwellin in solution. A protein standard (Invitrogen) was added (lane 1) to correlate the protein migration during electrophoresis with a known molecular weight marker. Both the crude (lane 2) and supernatant (lane 3) samples showed prominent protein bands at 15, 16, and 26 kDa as well as minor bands below and between these bands. The 26 kDa protein band, which bound to both the anion (lane 5 and 6) and the cation (lane 8) exchange chromatography columns was hypothesised to be kiwellin. It has been previously shown that when kiwellin migrates during electrophoresis under reducing conditions the molecular weight is higher than its theoretical mass (Tamburrini *et al.*, 2005), which may be due to the presence of disulfide bonds. The flowthrough of the anion exchange step removed a 22 kDa protein (lane 4) and the flowthrough of the cation exchange removed the 15 and 16 kDa protein (lane 7) from the purified sample. The eluted kiwellin peak from (Figure 34) (lane 8) contained two protein bands that was the two kiwellin isoforms.

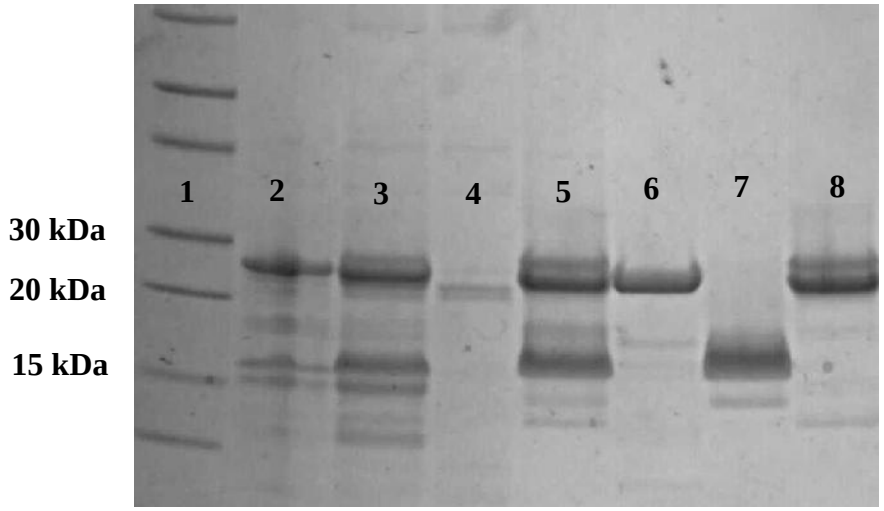

Figure 36: SDS-PAGE of the purification steps used to purify kiwellin. The proteins were in reducing conditions and between 5-10 µg of protein was present in each lane. From left to right 1: molecular marker, 2: crude, 3: supernatant, 4: anion exchange flow through, 5: anion exchange peak 3, 6: anion exchange peak 4, 7: cation exchange flow through, 8: cation exchange peak 1.

5.2.2 Mass spectrometry

Mass spectroscopy was used to measure the mass of kiwellin, purified using anion and cation exchange chromatography. The deconvoluted spectrum showed that there were two major peaks, representing the two kiwellin isoforms, which had molecular weights of 19,766.28 and 19,795.81 Da (Figure 37). The molecular weight values of these peaks differs from the theoretical molecular weight of 19,967.9 Da (Tamburrini *et al.*, 2005) by -201.62 and -172.09 Da, respectively. A mass difference of 202.08 Da is the mass of the two amino acids, methionine and alanine, which is present at the C-terminus of kiwellin (Figure 32). This may indicate that these residues are susceptible to becoming cleaved off in the kiwifruit. The difference between the two major peaks identified in Figure 37 is -29.53 Da. The difference is similar for substituting several amino acid with another (Table 6). The tryptophan to arginine substitution is proposed to be the most likely of these substitutions due to the binding differences observed during anion exchange chromatography (Figure 33). Sequencing the two kiwellin isoforms will identify what amino acid differences exist and the identity these isoforms share with other isoforms of kiwellin that are found in *Actinidia* species (Maddumage *et al.*, 2013).

Table 6: Potential amino acid substitutions that may occur in different isoforms of kiwellin.

Amino acid substitution	Average mass (Da)
Trp -> Arg	-30.02
Ser -> Gly	-30.03
Thr -> Ala	-30.03
Met -> Thr	-30.09

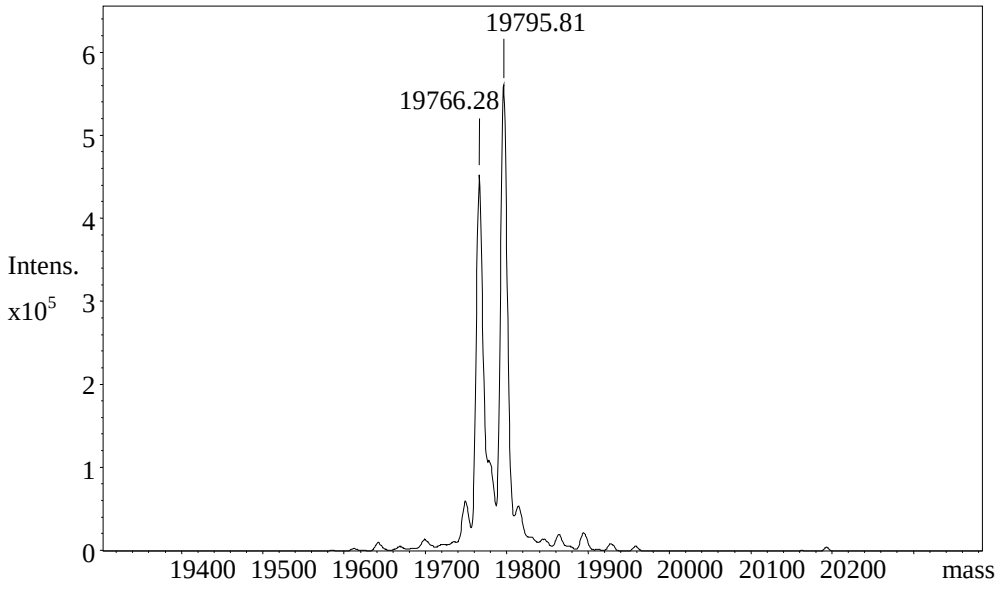

Figure 37: Deconvoluted ESI-MS spectrum of purified kiwellin at a concentration of 1 mg/mL. Two major peaks are present at 19766.28 and 19795.81 Da, respectively.

5.2.3 Thermal stability

The thermal stability of kiwellin over the pH range of 3.6-7.6 was measured using a thermal shift assay. The assay was conducted using differential scanning fluorimetry (DSF), which measures the fluorescence given from a dye (SYPRO® Orange) when it binds to residues that become exposed as the protein unfolds with increasing temperature (Niesen *et al.*, 2007). An increase in fluorescence of SYPRO® Orange was observed as the temperature was increased from 20 to 100°C in all of the conditions tested, which is indicative of the protein becoming

unfolded (Figure 38). Across the different conditions tested there was a shift in the melting curves indicating that pH is having an effect on the thermal stability of kiwellin. The intensity of the fluorescence was lower than the actinidin sample, which was tested over a similar pH range (Figure 9). This is likely to be due to actinidin (Podivinsky *et al.*, 1989) having a higher grand average of hydrophobicity score than kiwellin (Tamburrini *et al.*, 2005) of -0.206 and -0.656, respectively as computed by ProtParam (Gasteiger *et al.*, 2005).

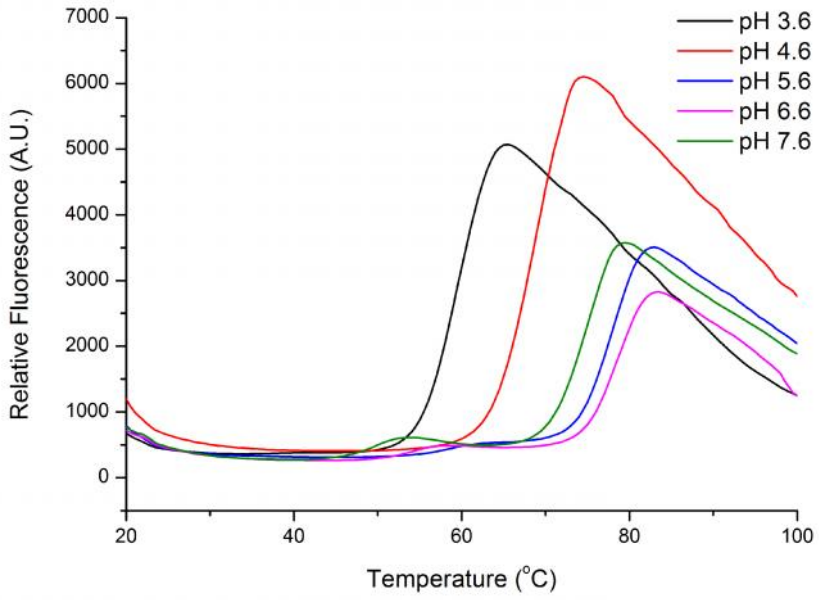

Figure 38: Melting curve of kiwellin, present in different buffers (pH 3.6-7.6), which are represented by different colours. An increase in the fluorescence of SYPRO® Orange as the samples were heated from 20°C to 100°C is indicative of kiwellin becoming unfolded.

The results show that pH does affect the thermal stability of kiwellin. A melting temperature was derived from the inflection point of the melting curve in each condition (Figure 38) and is plotted as a function of pH (Figure 39). From pH 3.6 (59.5°C) the temperature increases until it reaches pH 5.6 and 6.6 where it plateaus at 78°C and 78.5°C, respectively before decreasing thereafter in a more basic solution of pH 7.6 (75.7°C). Compared to other plant proteins (Gorinstein *et al.*, 1996), kiwellin has a high melting temperature and the influence that pH has on its melting temperature suggests that a network of hydrogen bonds and also salt bridges may be present in the tertiary structure.

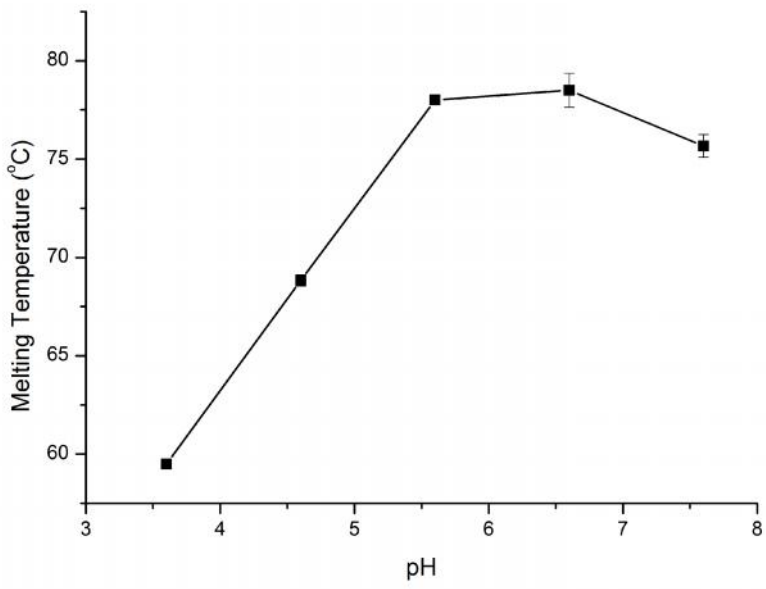

Figure 39: Melting temperature of kiwellin present in different buffers as determined from the inflection point of the DSF melting curve (Figure 38). Each condition was measured in triplicates and the standard deviation of the mean is shown as error bars.

5.2.4 Circular dichroism spectroscopy

The presence of secondary structures in purified kiwellin was assessed using circular dichroism (CD) spectroscopy. The sample was prepared for the analysis by diluting the sample in water to a concentration of 0.08 mg/mL to ensure that there was a sufficient amount of light that reached the detector. The spectra of kiwellin between 180 and 240 nm showed a peak at 200 nm that transitioned into a trough at 210 nm (Figure 40). The CD spectra for kiwellin appears to represent that of an unfolded protein rather than one with defined secondary structures, such as α-helices and β-strands (Greenfield, 2006), which would reduce the amount of hydrogen bonding between amino acids and have implications on the stability and flexibility of kiwellin. This result contrasts the CD spectra of kiwellin, which was purified using a similar protocol, that showed the presence of α-helices at pH 7.5 (Bernardi *et al.*, 2010). To confirm the reproducibility of the results the experiment was conducted again using another batch of purified kiwellin, however this also resulted in a similar measurement to the one shown in Figure 40 (data not shown). Bovine serum albumin (BSA) (Sigma), which has α-helical secondary structures (Bujacz, 2012) was tested as a positive control under analogous conditions to kiwellin to identify any experimental errors.

The BSA sample gave a trace that had a maxima at 195 nm and trough between 210 nm and 224 nm. This is more characteristic of a spectra from proteins containing α-helices, which typically show a minima at 206 nm and 222 nm (Greenfield, 2006) and this confirms that BSA has α-helical secondary structures.

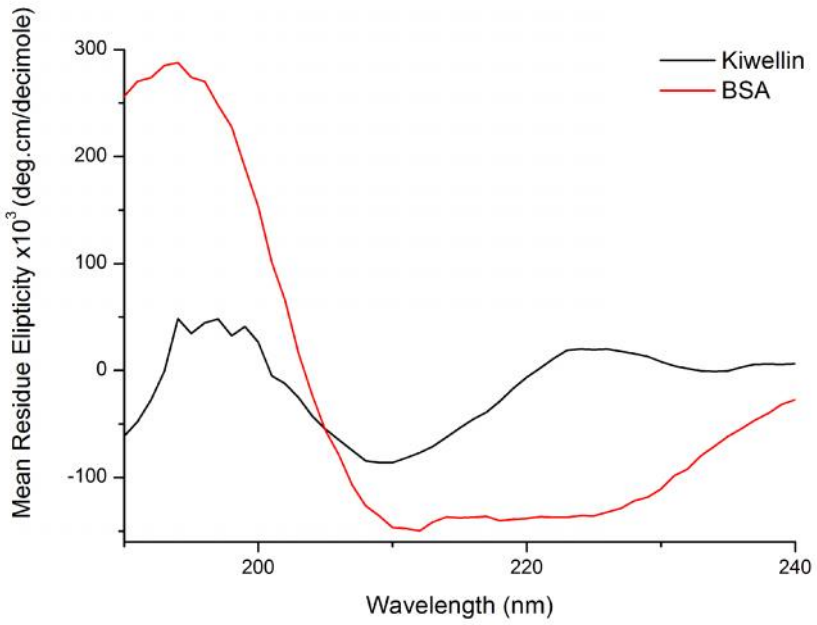

Figure 40: Circular dichroism spectra for kiwellin (black) and BSA (red). Each sample was measured three times before being averaged.

5.2.5 Static light scattering

The quaternary structure of kiwellin in solution was analysed using a system that couples static light scattering with size exclusion chromatography. Kiwellin eluted from the column as a single species, represented by a single peak in the RI trace at around 17.5 mL (Figure 41). The peak was calculated to have an average molecular weight of 24.7 kDa, which is higher than the theoretical molecular weight of 20.0 kDa (Tamburrini *et al.*, 2005), but is consistent with kiwellin existing as a monomer in solution. The range of molecular weight values varied from 27.0 to 23.4 kDa and this shows that the sample is reasonably monodisperse.

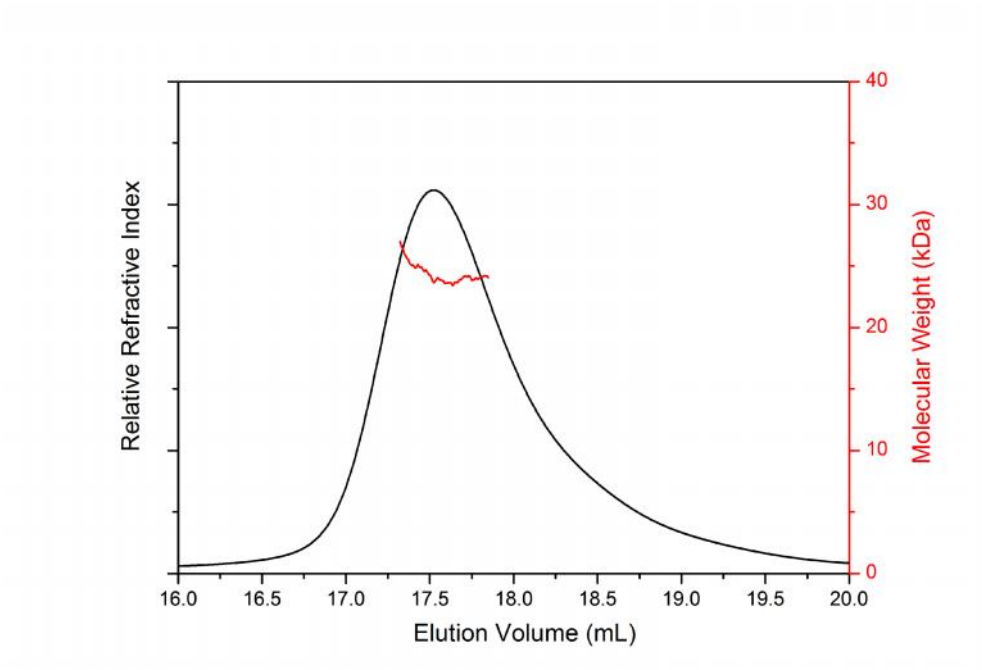

Figure 41: Light scattering of kiwellin after the purified protein was eluted from a size exclusion column (Superdex™ 200 10/300, GE Healthcare) with 100 mM sodium phosphate buffer, pH 7.

5.2.6 Analytical ultracentrifugation

Another technique that was used to measure the quaternary structure of kiwellin was analytical ultracentrifugation (AUC). The rate at which kiwellin moved through the solution after a gravitational field was applied was measured by the absorbance at 285 nm. The data was fitted to a sigmodial curve and this was used to calculate the standardised sedimentation coefficient of 2.4 S (Figure 42, (a)). The fitted data represented the experimental data well as shown by the residuals being evenly spaced (Figure 42, (b)).

A $c(M)$ distribution of molecular weights was modelled using the calculated frictional coefficient (f/f_0) of 1.2 and showed that at 0.5 mg/mL kiwellin sediments as a monodisperse species (Figure 42, (c)). The integrated peak gave an average molecular weight of 18.8 kDa, which is close to the theoretical molecular weight of the primary structure of 20.0 kDa (Tamburrini *et al.*, 2005). This indicates that kiwellin exists as a monomer in solution, consistent with the result obtained using static light scattering (Figure 41). The kissper domain of kiwellin can form voltage-gated channels in synthetic lipid membranes (Ciardiello *et al.*, 2008; Meleleo *et al.*, 2012), and this is hypothesised to be a bioactive property of the peptide. One theory as to how the 39 amino acid peptide is able to form the channels is by

multiple monomeric subunits bonding together to enable kissper to span the width of the membrane (Meleleo *et al.*, 2012). The interface used to form the higher oligomeric kissper structure may also be present in kiwellin, the precursor protein, however the data in Figure 41 and Figure 42 indicates that kiwellin does not form a higher oligomeric structure and exists as a monomer in solution.

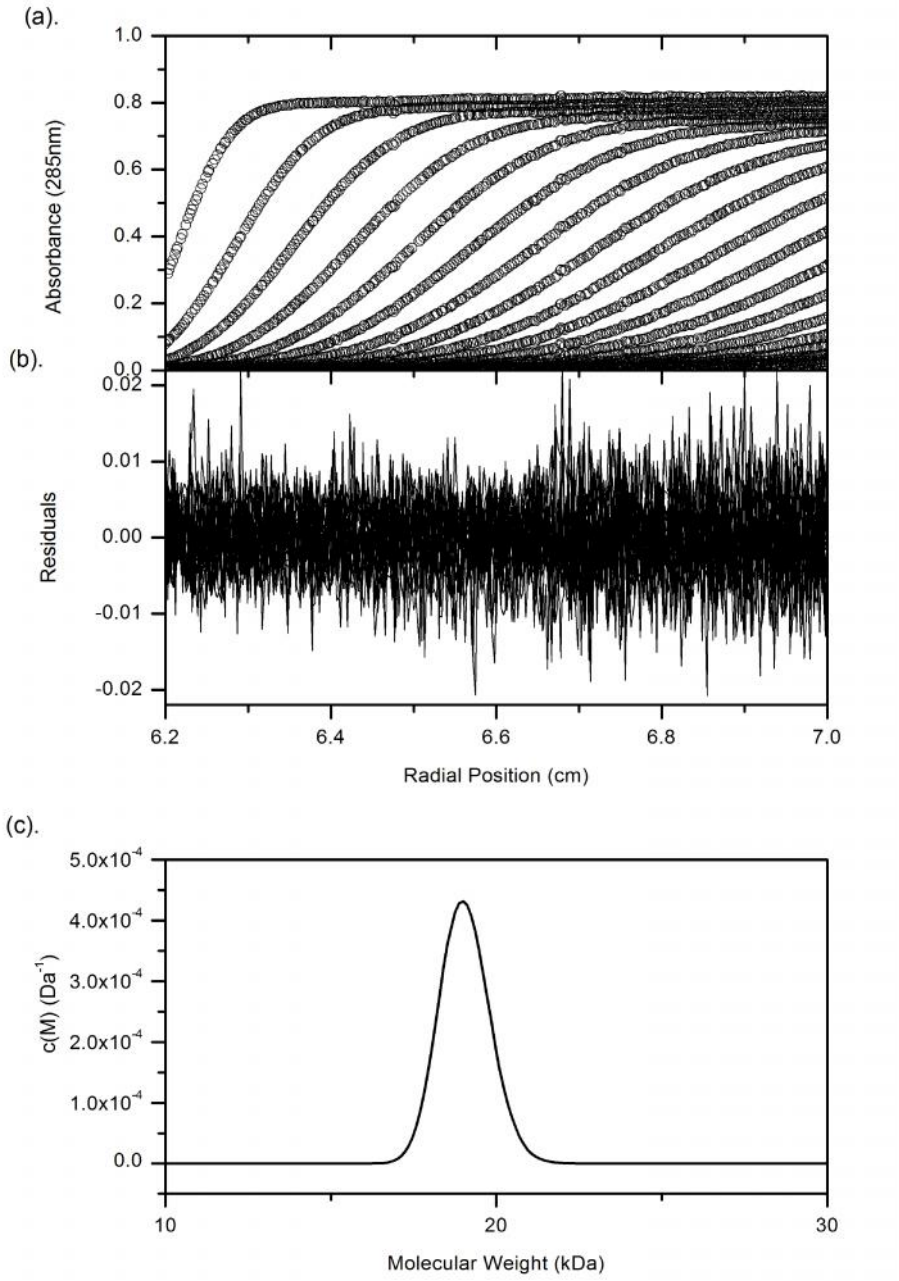

Figure 42: Analytical ultracentrifugation of kiwellin at 0.5 mg/ml. (a) absorbance at 285 nm measured the sedimentation of kiwellin along the radius of rotation. (b) residuals for the fitted data indicate that the noise is normally distributed. (c) A *c*(*M*) modelled size distribution shows a monodisperse species corresponding to a monomer.

5.2.7 Small angle X-ray scattering

Small angle X-ray scattering (SAXS) is a technique that can be used to describe the size and shape of a macromolecule and was used in order to further characterise kiwellin in solution. The intensity of the scattered X-rays is plotted as a function of the radial angle after the scatter pattern from the phosphate buffer had been subtracted (Figure 43 (a)). Using PRIMUS software (Konarev *et al.*, 2003) the scatter intensity plot was used to create a Guinier plot (Figure 43 (b)), which is an indication of data quality. The linearity of the Guinier plot shows that the sample does not contain aggregates and that the sample is homogenous. The size of kiwellin was calculated from the Guinier plot and resulted in a radius of gyration of 2.57 +/- 0.2 nm. The Porod volume, which estimates the maximum dimensions and molecular mass of the species (M. V. Petoukhov *et al.*, 2003) was also calculated using PRIMUS (Konarev *et al.*, 2003) to give a molecular weight of 17.2 kDa. This further confirms that kiwellin is a monomer in solution. A Kratky plot was also calculated using the scatter intensity data and is another indication of data quality (Figure 43 (d)). The incomplete bell-shaped curve, followed by a tail at increasing radial angles is characteristic of a partially unfolded, flexible protein (Putnam *et al.*, 2007). The lack of secondary structures in the purified kiwellin that was shown using CD spectroscopy (Figure 40) may be contributing to the flexible nature of the protein which is having detrimental effects to the efforts of crystallising kiwellin.

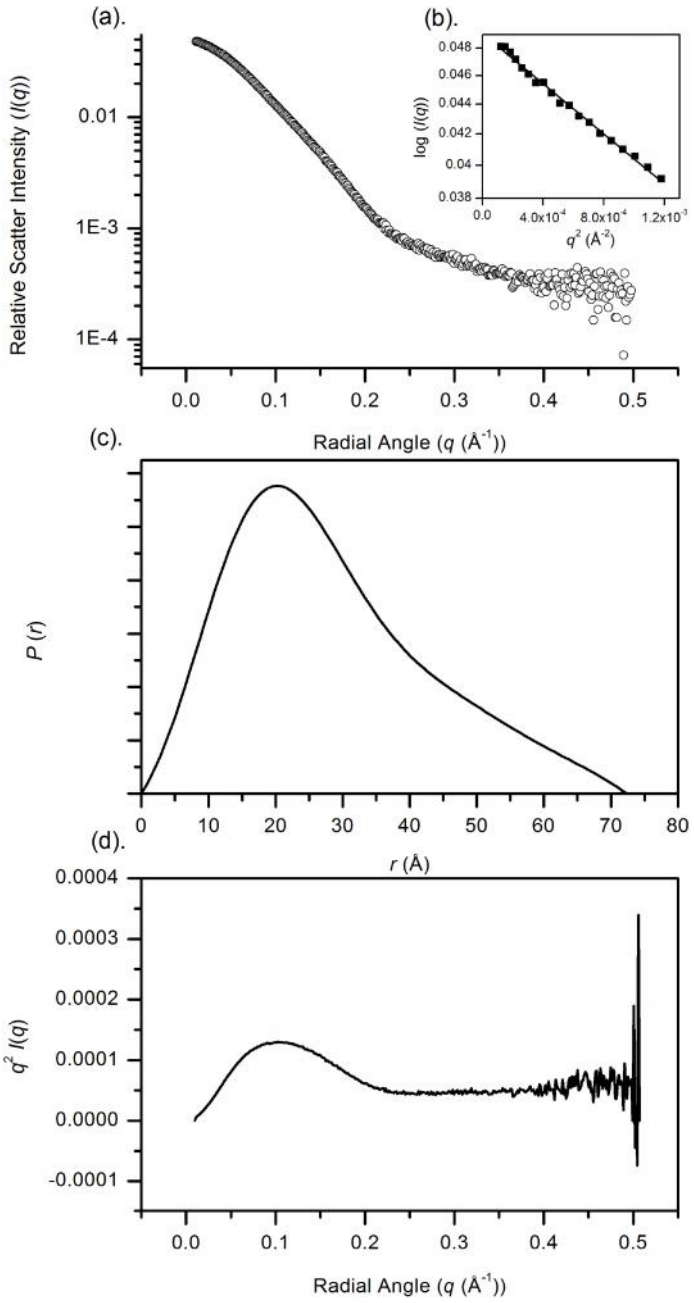

Figure 43: Small angle X-ray scattering of kiwellin at 5.11 mg/mL in 50 mM phosphate buffer, pH 7. (a). Scatter intensity plot at different angles. (b). Guinier plot calculated from the scatter intensity plot using PRIMUS software (Konarev, 2003). (c). *P*(*r*) distrbution. (d). Kratky plot calculated from the scatter intensity

The shape of a protein provides important structural information and can be obtained by creating a pair distribution function plot from the SAXS data. The *P*(*r*) plot (Figure 43 (c)) shows an asymmetrical curve that has a tail which trails down to a D_{max} at approximately 70 Å. This is indicative of an elongated structure and an *Ab initio* 3D envelope model of the SAXS data for kiwellin using GASBOR (Svergun, 1992) depicts this structure (Figure 44).

Kiwellin can be proteolytically cleaved by actinidin (Tuppo *et al.*, 2008) and it is hypothesised that the physiological function of kiwellin lies with the cleavage products, KiTH and kissper. The elongated structure and flexible nature that kiwellin has shown from the SAXS data may increase the chance that the cleavage site is exposed to actinidin and leads to kiwellin becoming cleaved, which supports this hypothesis.

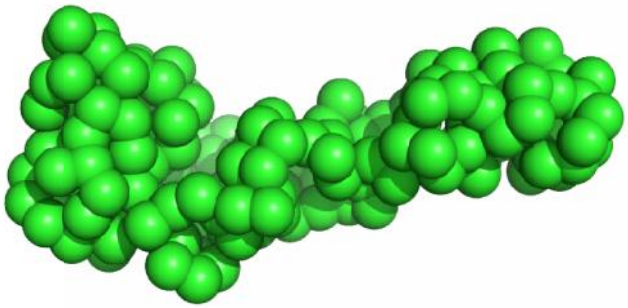

Figure 44: *Ab initio* model of kiwellin using the small angle X-ray scattering data and computed by GASBOR software (Svergun, 1992).

5.2.8 X-ray crystallography

Crystal trials were conducted to obtain a crystal structure of kiwellin to resolve the protein atomic structure. The crystal trays were prepared using the sitting drop method with a protein concentration of 9.4 mg/mL. Four crystal screens were selected, which were JSCG, Morpheus, PAC, and Clear Screen 1 (Molecular Dimensions) and the crystal trays were incubated at 20^{o}C to allow crystal formation. At time intervals of two weeks, one month, and two months the crystal trays were checked to identify any crystal formation by use of light microscopy, however no crystal formation was identified. The flexible nature of kiwellin, that was identified using small angle X-ray scattering (Figure 43) would hinder crystal formation and could explain why the protein is difficult to crystallise. Future crystal screens that cover an expanded range of conditions may help to identify more suitable conditions that encourages kiwellin to form crystals.

5.3 Conclusions

5.3.1 Purification

A purification protocol that was developed previously (Tamburrini *et al.*, 2005) which utilised anion and cation exchange chromatography was used to isolate kiwellin, present in *Actinidia chinensis* cultivars. Two kiwellin isoforms were purified and from 100 g of starting kiwifruit flesh 2.5 mg of protein was isolated. Mass spectroscopy analysis also showed that the two isoforms both had a molecular weight below that of the theoretical value of kiwellin (Tamburrini *et al.*, 2005). A truncated C-terminus was hypothesised to be the reason behind the difference between one isoform and the theoretical mass. An amino acid substitution of tryptophan to arginine was suggested to be the difference between the two isoforms, however more detailed investigation of their sequences is needed to elucidate whether this hypothesis is correct or not.

5.3.2 Biophysical characterisation

A biophysical characterisation of kiwellin was carried out using a number of analytical techniques in order to better characterise this physiologically novel kiwifruit protein. The thermal stability of kiwellin was measured using differential scanning fluorimetry and was found to be influenced by pH. The high melting point of kiwellin and susceptibility to pH indicates that a network of hydrogen bonds and salt bridges maintains its structure. Kiwellin, similar to kissper may also have disulfide bonds that increases the stability of the protein and the changes in electrophoresis migration during SDS-PAGE analysis under reducing conditions supports this. Its structure was, however not found to contain any defined secondary structure, as determined by CD spectroscopy. This is in contrast to previous studies that showed that kiwellin had α-helicies in both neutral and acidic conditions (Bernardi *et al.*, 2010). The lack of secondary structure would allow kiwellin to have a more dynamic structure in solution and this is consistent with the high flexibility that was observed from the Kratky plot after a small angle X-ray scattering (SAXS) experiment. Kiwellin was calculated to have a monomer in solution by using the three different techniques of: static light scattering (SLS), analytical ultracentrifugation (AUC), and small angle X-ray scattering (SAXS), as summarised in Table 6.

Table 7: Predicted molecular mass of kiwellin as calculated from different analytical techniques.

Technique:	Theoretical (Tamburrini *et al.*, 2005)	SLS	AUC	SAXS
Predicted mass (kDa):	20.0	24.7	18.8	17.2

SAXS was utilised to understand the shape of kiwellin in solution and was found to have an elongated structure that had high flexibility and a radius of gyration (R_g) of 2.57 nm. The shape was depicted using an *ab initio* model and it was hypothesised that these attributes could promote the proteolytic cleavage of kiwellin into KiTH and kissper, which may have a physiological relevance. The high flexibility was also hypothesised to have contributed to the reasons as to why kiwellin did not crystallise in the crystal trays, which prevented an atomic resolution of kiwellin from being obtained.

Chapter Six : Conclusions

6.1 Kiwifruit and digestive health benefits

Kiwifruit, a major horticultural export of New Zealand is associated with a number of health benefits (Singletary, 2012). The positive impacts that kiwifruit consumption have on digestive health has been particularly well researched. An increase in both the digestion of food proteins and the frequency of waste efflux are common results that have been measured during animal and human clinical trials, which assessed the health effects of kiwifruit consumption. (Chan *et al.*, 2007; Chang *et al.*, 2010; Rush *et al.*, 2002; Rutherfurd *et al.*, 2011). The components of kiwifruit that are implicated in improved digestive health include:, fibre, bulking (Mishra *et al.*, 2012), and the bioactive proteins: actinidin (Kaur *et al.*, 2010a, 2010b; Montoya *et al.*, 2014) and kissper (Ciacci *et al.*, 2013; Ciardiello *et al.*, 2008). The bioactive properties of these proteins are specific to kiwifruit and this has sparked interest from biotechnology companies that produce kiwifruit products, such as Actazin™ to investigate these proteins.

6.2 Project aims

The project has two aims. Firstly the processing that produces Actazin™ is potentially having a negative impact on the retention of actinidin. Routine quality control testing by Anagenix Ltd measured that the percentage of actinidin in individual production batches vary by up to 48%. The intention of this research is to determine what factors affect the actinidin activity and to provide direction for any optimisation of the production. The second aim of the project was to characterise both actinidin and kiwellin and enhance the scientific information that is known about these kiwifruit proteins. Kiwellin in particular has not been well characterised and the physiological function is not known despite having shown that it can be proteolytically cleaved into two domains (Tuppo *et al.*, 2008), one of which, kissper may have bioactive properties that increase digestive health (Ciardiello *et al.*, 2008).

6.3 Actinidin

6.3.1 Purification and characterisation of actinidin

Actinidin was purified from GrK kiwifruit (*Actinidia deliciosa* cv. Hayward) using anion exchange chromatography. From 100 g of starting kiwifruit flesh 17 mg of protein was isolated. The purified sample is hypothesised to contain multiple isoforms of actinidin as shown by the mass spectroscopy analysis, and actinidin may have become catalytically inactivated, which would explain why the specific activity was lower than previous studies (Boland *et al.*, 1972).

Purified actinidin was monomeric in solution and its melting temperature and catalytic activity was affected by pH. Actinidin was most thermostable at pH values between 5-7, and catalytically active at approximately pH 6. The melting point of actinidin at pH 6.7 was similar to the melting point of an inactive form of actinidin, which had been previously measured (M. M. Grozdanovic *et al.*, 2014). This is further evidence that the purified actinidin may be partially inactivated.

6.3.2 Pre- and post-harvest factors that affect actinidin activity

The specific activity of individual kiwifruit (GrK) demonstrated that the variation was normally distributed and would therefore not impact the actinidin activity in the batches of pulp after the kiwifruit had been pulped.

Cool storage, that slows kiwifruit ripening, had a limited impact on the actinidin activity. After an extended 4-5 months of cool storage 73% of the activity was retained, consistent with previous studies (S. Boyes *et al.*, 1997). The loss of activity could have also been affected by the condition of fruit, which was bruised and assaying a greater number of samples to confirm these results is suggested.

The fruit is ripened before it is pulped and this process was determined to be important for increasing actinidin activity. The ripening process that kiwifruit at the Kiwifruit Processing Company Ltd goes through was shown to appropriately ripen the fruit, resulting in high actinidin activity in comparison to fruit that had not been ripened.

Purified actinidin was found to be sensitive to freezing and thawing over a 2 month period of cold storage. Similarly, freezing the pulp before it was stored at -20^{o}C was a processing stage that had a detrimental impact on the retention of actinidin throughout the production of Actazin™. It is therefore suggested that further investigations are carried out as to whether the individual freezing, thawing, or storage stages at low temperatures are destabilising actinidin or whether it was a combination effect of these.

During freeze drying the frozen pulp recorded temperature of up to [redacted]. The rise in temperature, however, did not significantly affect the actinidin activity of Actazin™.

6.3.3 Inactivation of actinidin in Actazin™

Actinidin in the kiwifruit powder became inactivated after the powder was solubilised in phosphate buffer. The inactivation did not occur in the purified actinidin and it was hypothesised that an oxidant in the kiwifruit powder was oxidising the catalytically active cysteine residue. The hypothesis was supported by showing that in the presence of a reducing agent the inactivation can be largely reversible. To investigate the mechanism of this inactivation the effects that vitamin C and dissolved oxygen had on purified actinidin were measured. The testing showed that neither vitamin C or dissolved oxygen were responsible for actinidin becoming inactivated in the kiwifruit powder. Investigating the sensitivity of actinidin towards oxidative reaction would be of interest in future work. The understanding that actinidin is inactivated in the kiwifruit powder is, however more relevant to the project as this might affect the measurements obtained in the quality control tests that are performed regularly by Anagenix Ltd.

6.3.4 Recommendations to optimise Actazin™ production

Actazin™ is a kiwifruit product that is sold as a digestive aid. The production of Actazin™ involves pulping kiwifruit and freeze drying the pulp to produce a kiwifruit powder. To retain a high level of actinidin throughout production the following is recommended.

Select fruit at the start of the season to reduce time in cool storage

The extended cool storage resulted in a decrease of actinidin activity when compared to fruit that had not been stored for as long. The extended cool storage may have destabilised

actinidin and selecting fruit at the start of the season will minimise any detrimental effects.

Continue the post-harvest ripening at the Kiwifruit Processing Company Ltd

Actinidin activity has been shown to positively react to prior fruit ripening (S. Boyes *et al.*, 1997) and the results presented in section 5.2.3 supports this. The ripening that had been conducted was appropriate to increase the activity to a high value and this was supported by showing that an extended ripening period had a detrimental effect on the actinidin activity

Freeze dry kiwifruit pulp that had been stored for short periods

Actinidin was found to be sensitive to cold storage after freezing and thawing. While freezing is an essential part of production it is unclear whether storing the frozen pulp in cold storage is further destabilising actinidin. A minimal cold storage period is therefore recommended to prevent the potential for greater loss of actinidin activity.

Perform quality control tests under reducing conditions

Actinidin, in the kiwifruit powder become inactivated over time, but largely in the first 10 minutes of being solubilised in a buffer. To prevent the inactivation that may cause variations between quality control tests, the addition of a reducing agent to the assay, which has been shown to reverse the majority of the inactivation, is recommended.

6.4 Kiwellin

6.4.1 Purification and characterisation of kiwellin

Kiwellin was purified from two *Actinidia chinensis* cultivars using a protocol previously developed (Tamburrini *et al.*, 2005), which utilised both anion and cation exchange chromatography. From 100 g of starting kiwifruit flesh 2.5 mg of protein was obtained. The mass spectrum indicated that two truncated isoforms had been purified, however amino acid sequencing is required for any confirmation.

A number of analytical techniques were implemented to better understand the structure of kiwellin. The kiwifruit protein had a high melting temperature, which was also affected by pH. It was hypothesised that hydrogen bonds and salt bridges are contributing to the stability of kiwellin and are becoming destabilised in different pH environments. Disulfide bonds are also suspected to be occurring between the 14 cysteine residues that kiwellin has in its

primary structure. This conclusion was based upon the effects that reducing conditions had on the protein migration during SDS-PAGE analysis. These bonds are important to stabilise kiwellin in solution, which was found to be a dynamic species that did not have the presence of any defined secondary structure. Static light scattering, analytical ultracentrifugation, and small angle X-ray scattering (SAXS) determined that kiwellin was monomeric in solution. SAXS also showed that kiwellin was an elongated protein that had a radius of gyration (R_g) of 2.57 nm. The Kratky plot indicated that kiwellin was highly flexible and this may have contributed to the reason why kiwellin did not crystallise in the crystal trials that were set up. The flexiblity may also increase the chance that the cleavage site for actinidin that has previously been described (Tuppo *et al.*, 2008) had become exposed. This would promote proteolytic cleavage and increase the amount of kissper and KiTH in the cell which might be physiologically important.

Chapter Seven : Experimental

7.1 Materials

7.1.1 Chemicals

Unless otherwise stated, chemicals were purchased from: BDH, Thermo Fisher Scientific, Sigma-Aldrich, or Scharlau Chemie S.A. Milli-Q water was used for all buffers and was purified using an Advance A10 Water Purification System (Millipore).

7.1.2 Fruit selection

For protein extraction (actinidin and kiwellin) and for actinidin activity measurements, fruit was bought from a local supermarket. A qualitative firmness test determined whether the fruit was of sufficient ripeness. The green kiwifruit species used for studying actinidin was *Actinidia delicosia* cv. Hayward (GrK). Kiwellin was extracted from *Actinidia chinensis* species (GoK). Initially the *Actinidia chinensis* species used was the cultivar, Zespri® Hort16a, however with the increase of *Pseudomonas syringae* pv. *actinidiae* (Psa) prevalence (Mazzaglia *et al.*, 2012) this was replaced with the commercially new Gold3 cultivar, which is commonly known as Zespri® SunGold.

Fruit that was used to measure the influence of post-harvest factors on the retention of actinidin activity was kindly gifted by Grant Jeffrey from Kiwifruit Processing Company Ltd, which is based at Newnham Park in the Bay of Plenty. Harvested fruit was processed at this facility into a pulp, flash frozen and transported down to Christchurch to be freeze dried at Genesis Bio-Laboratory Ltd, New Zealand (Figure 3). Both the frozen pulp and kiwifruit powder was obtained from Genesis Bio-Lab with agreement from its Director, Stephen Parsons.

The section of the kiwifruit used to measure actinidin activity was the outer pericarp (flesh) without the presence of seeds. This has previously been shown to have the highest actinidin activity when compared to the flesh with seeds or the other sections of the fruit (Préstamo,

1995).

7.1.3 pH measurements

The pH of large volume buffers (> 250 mL) was confirmed using a UB-10 pH/mV meter from Denver Instrument after it was calibrated using pH 4, 7, and 10 pH standards (Thermo Fisher). For solutions with small volumes (100 µL to 50 mL) drops were pipetted onto a S2K712 pocket-sized pH meter (Ichiro Co) until a stable reading was given. The pH probe was initially calibrated with pH 4 and 7 standards, also from Ichiro Co. For fast confirmation of any major changes to the pH, Whatman® pH Indicator Paper, Type CF, pH 0-14 was used.

7.2 Protein purification

7.2.1 Actinidin

Protein extraction

Actinidin was extracted from the outer pericarp tissue (flesh) of GrK. The flesh was homogenised in a 2:1 ratio of extraction buffer (Table 8) (mL) to fruit weight (g) for 30-60 seconds, in a fruit blender. The crude mixture was centrifuged for 10 minutes at 17,600 rcf at 4^{o}C to remove insoluble material. The supernatant was then decanted through a miracloth filter and further centrifuged for 20 minutes at 52,600 rcf.

Ammonium sulfate was added to precipitate the soluble protein out of solution. Solid ammonium sulfate was ground down to a powder by using a mortar and pestle and added to the solution until the concentration reached 80% of the solution (53.3 g/100 mL). The solution was incubated on ice for approximately 1.5 hours to allow the precipitant to form. The precipitant was centrifuged for 15 minutes at 17,600 rcf before the solution, which was measured to have no actinidin activity was decanted out of the sample. The precipitant was usually found to float at the top of the solution and this was hypothesised to be due to the density of the solution.

The precipitate was resuspended in a minimal amount of extraction buffer (Table 8) (10-20 mL/ 100g of starting kiwifruit flesh). The resuspension was dialysed over night in 12,000-14,000 MWCO tubing (Medicell International Ltd) at 4^{o}C in dialysis buffer (Table 8) to remove any residual salt, after which the sample was centrifuged for 20 minutes at 52,600 rcf.

Finally the solution was pushed through a 0.45 µm, followed by, a 0.2 µm Minisart® filter (Sigma-Aldrich) with a syringe.

Table 8: Buffer composition used during protein extraction.

Solution	**Contents**
Actinidin extraction buffer	50 mM $NaPO_4$ 1 mM EDTA 1mM DTT pH 6.0
Actinidin dialysis buffer	50 mM $NaPO_4$ 1 mM EDTA pH 6.0

Protein purification by chromatography

Similar to previous studies (Boland *et al.*, 1972) actinidin was isolated from other proteins, present in GrK by anion exchange chromatography. The sample was injected onto a 5 mL HiLoad™ Q HP column (GE Healthcare). Bound protein was eluted by increasing the concentration of NaCl from 0 to 500 mM over 6 column volumes. The protein eluting from the column was monitored by the absorbance measured at 280 nm and 1 mL fractions were collected in a 96 well plate.

The fractions containing the highest amount of protein (> 1000 mAU), deemed by the absorbance at 280 nm were pooled. The pooled fractions (6 mL) were snapped frozen using liquid nitrogen and stored at -80^{o}C in 250 µL aliquots. A 22% decrease in activity was measured after one month of storage. This appeared to not be minimised by the addition of 10% glycerol.

For further purification and to assess if the protein had aggregated, actinidin was eluted down a size exclusion column. Samples were eluted down a 120 mL HiLoad™ 16/600 Superdex™ 200 pg column (GE Healthcare) with a low salt buffer (Table 9), which had also been used to equilibrate the column. Protein elution was monitored by the absorbance at 280 nm and 1 mL

fractions were collected in a 96 well plate.

Table 9: Buffer composition used during chromatography steps.

Solution	Contents
Actinidin high salt buffer	50 mM $NaPO_4$ 1 mM EDTA 0.5 M NaCl pH 6.0
Actinidin low salt buffer	50 mM $NaPO_4$ pH 6.0

7.2.2 Kiwellin

Protein extraction

Kiwellin was extracted from *Actinidia chinensis* using the salt extraction method as developed previously (Tamburrini *et al.*, 2005). The outer pericarp (flesh) was removed from the outer skin, seeds, and core and mixed with water at a ratio of 2 parts water (mL) to 1 part fruit (g). This mixture was homogenised for 30-60 seconds in a fruit blender. The resulting crude sample was centrifuged for 15 minutes at 17,600 rcf at 4^{o}C. The pellet was resuspended in a basic salt solution and 1 M NaOH was added, drop-wise until the pH reached approximately 8. The pellet was then homogenised again for 15-30 seconds before the sample was centrifuged at 52,600 rcf for 20 minutes. The solution was filtered through a 0.45 µm Minisart® filter (Sigma-Aldrich) and dialysed in 12,000-14,000 MWCO tubing (Medicell International Ltd) overnight against 10 mM Tris-HCl, pH 7.5 buffer.

Table 10: Buffer composition used during protein extraction.

Solution	Contents
Kiwellin salt solution	0.5 M NaCl Adjusted to pH 8.3 with 500 mM NaOH
Kiwellin dialysis buffer	10 mM Tris-HCl Adjusted to pH 7.5 with 5 M NaOH

Protein purification by chromatography

The second step to isolate kiwellin from the other protein constituents was using anion exchange chromatography, in accordance with a previously designed protocol (Tamburrini *et al.*, 2005). The protein sample that had been extracted from kiwifruit and dialysed was injected onto a 5 mL HiLoad™ Q HP column, which had been equilibrated in low salt buffer (Table 11). The bound protein was eluted by a linear gradient of high salt buffer from 0 to 100% over 6 column volumes. Any protein fractions that appeared to contain kiwellin, as shown by SDS-PAGE analysis were pooled for further purification.

Cation exchange chromatography was utilised in the next chromatography step. Buffer exchange into the cation exchange, low salt buffer was conducted by eluting the sample through a 53 mL HiPrep™ 26/10 (GE Healthcare) desalting column that had been equilibrated with the desired buffer. The protein sample was then injected onto a 1 mL HiLoad™ SP HP column (GE Healthcare). Any protein that had bound to the column was eluted by increasing the concentration of the high salt buffer (Table 11) from 0 to 100% over 6 column volumes. Protein fractions (> 800 mAU) corresponding to the highest absorbance at 280 nm were pooled. The purity of the purification throughout the chromatography steps was checked by using SDS-PAGE analysis.

To assess aggregation and to exchange the buffer into a low salt phosphate buffer (Table 11) the pooled sample was eluted through a size exclusion column. The sample was eluted down a 120 mL HiLoad™ 16/600 Superdex™ 200 pg column (GE Healthcare) that had been

equilibrated in low salt phosphate buffer at a flow rate of 1 mL/min. Fractions containing the highest protein concentration, as determined by the absorbance at 280 nm were pooled and concentrated using spin concentrators with a 10,000 MWCO (GE Healthcare).

Table 11: Buffer composition used during chromatography steps.

Solution	**Contents and Instructions**
	Anion exchange chromatography
Kiwellin low salt buffer	10 mM Tris-HCl Adjusted to pH 7.5 with 5 M NaOH
Kiwellin high salt buffer	10 mM Tris-HCl 0.5 M NaCl Adjusted to pH 7.5 with 5 M NaOH
	Cation exchange chromatography
Kiwellin low salt buffer	10 mM Na acetate Adjusted to pH 5.0 with conc HCl
Kiwellin high salt buffer	10 mM Na acetate 0.5 M NaCl Adjusted to pH 5.0 with conc HCl
	Size exclusion chromatography
Kiwellin low salt buffer	50 mM $NaPO_4$ pH 6.0

7.3 Protein concentration

Protein concentration was measured using the Bradford protein assay (Bradford, 1976) throughout the purification and was used to calculate the specific and total activities of actindin from fresh fruit, pulp, and freeze dried powder samples. The stain that was used was the Protein Assay Dye Reagent Concentrate (Bio-Rad), which is a Coomassie Brilliant Blue G-250 stain. Samples were prepared using either the microassay or microtiter plate protocols (Bio-Rad). The microassay procedure used 200 µL of a protein sample and this was added to 800 µL of protein stain, which had not been diluted. The samples were incubated for 10 minutes before the absorbance at 595 nm was measured using a spectrophotometer. Absorbance measurements from 5 dilutions of BSA (Life Technologies) between 2 and 10 µg/mL was used to create a protein standard curve. The microtiter plate procedure used 15 µL of protein sample and 185 µL of protein stain, that had previously been diluted 4 fold. The absorbance at 595 nm was measured on a SpectraMax M5 plate reader after incubation for 10 minutes. The BSA standard curve was created from 10 dilutions over a range of 1 to 15 µg.

The protein concentration of purified protein samples was also measured by the absorbance at 280 nm using a NanoDrop ND 1000 spectrophotometer from Thermo Scientific after blanking with the appropriate buffer. The concentrations were corrected using the calculated extinction coefficients of actinidin (ACT1A) (Nieuwenhuizen *et al.*, 2007), and kiwellin (Tamburrini *et al.*, 2005) which were 54235 and 23335 M^{-1} cm^{-1}, respectively.

7.4 Protein SDS-PAGE

Protein gel electrophoresis was carried out using Bolt® Bis-Tris Plus precast polyacrylamide gels (Invitrogen). Samples were prepared by adding 1 µL of NuPAGE® Sample Reducing Agent (10X) (Invitrogen), 2.5 µL of NuPAGE® LDS Sample Buffer (4X) (Invitrogen), and a suitable amount of protein sample to ensure each lane contained 5-10 µg of protein (typically 5 µL). Water was used to make a final loading volume of 10 µL. The samples were heated in water to above 70 ^{o}C for 5 minutes before being loaded onto the precast gels. 5 µL of Novex® Sharp Pre-Stained Protein Standard (Invitrogen) was pipetted into a lane, which was used as a molecular weight ladder. The gels were run for 35 minutes at a constant voltage of 165 V in 1X NuPAGE® MES SDS Running Buffer. Gels were stained for 30 minutes with a Coomassie stain and destained for approximately one hour. Protein bands were visualised and

photographed using a Syngene Bio Imaging System.

Table 12: Staining and destaining solutions used show protein bands after electrophoresis.

Solution	Contents
Coomassie stain (per 1 L)	1 g Coomassie Brilliant Blue G250 500 mL water 400 mL methanol 100 mL acetic acid
Destain (per 1 L)	500 mL water 400 mL methanol 100 mL acetic acid

7.5 Mass spectroscopy

Samples were prepared for mass spectrometry by dialysing the purified protein into water at a protein concentration of approximately 1 mg/mL. 50 µL was pipetted into mass spectrometry vials before being analysed on a maXis 3G UHR-Qq-TOF mass spectrometer (BrukerDaltonik GmbH, Bremen, Germany) coupled to a Dionex Ultimate 3000 LC system (ThermoFisher) with the expertise of Dr Marie Squire. 5 µL was injected from the sample onto a Zorbax, 300Extend C8 Narrow Bore column at a flow rate of 200 µL/min. This was followed by a ESI-L Low Concentration Tuning Mix (Agilent Technologies) as a calibrant. Samples were eluted by running a gradient of acetonitrile (Scharlau, Multisolvent®, HPLC grade) from 0-50% with water (purified using a MilliQ deionising system) and 0.5% formic acid over 1 minute, followed by an isocratic hold on 50% for 1 minute and then a restoration to 0% over 30 seconds. The method was finished with an isocratic hold on 0% acetonitrile over 4.5 minutes. Mass spectrometer analysis was processed using Compass software (BrukerDaltonik GmbH, Bremen, Germany).

7.6 Temperature data loggers

iButton® temperature data loggers (Maxim Integrated, CA, U.S) supplied by FF Instrumentation Ltd (Christchurch) were placed in a shallow groove cut into frozen kiwifruit pulp just before freeze drying commenced. The frozen pulp was typically cut as slabs at a thickness of 1 cm and the shallow groove was dug to approximately half of this thickness. The four data loggers were distributed evenly across the tray. The tray was placed in the middle of the freeze dryer. Changes in temperature were measured at time intervals of 5 minutes and data was analysed using 1-Wire Net software.

7.7 Differential scanning fluorimetry (DSF)

The thermal stability of actinidin and kiwellin was measured in different buffers by differential scanning fluorimetry (DSF) (Niesen *et al.*, 2007). For each condition a 100 µL stock solution was made up containing: purified protein at either 0.1 mg/mL (actinidin) or 0.5 mg/mL (kiwellin), 1000 fold dilution of SYPRO® Orange (Sigma), and an appropriate amount of buffer to increase the volume to 100 µL. The buffers used for the pH range tested are listed below in Table 13. 25 µL of the stock solution were added to each well and each condition was run as triplicates. The thermal melt was conducted by increasing the temperature to 100^{o}C at increments of 0.5^{o}C per minute from 0^{o}C using an iQ™5 Real-Time PCR Detection System (Bio-Rad). Data was analysed using the iQ™5 software after the run had been completed.

Table 13: Buffers selected to assess the thermal stability of actinidin and kiwellin using DSF.

Buffer	**Contents**	**pH range**
Citric	0.1 M Sodium citrate	1.9-3
	0.1 M HCl	
Citric-phosphate	0.1 M Citric acid	3.6-7.6
	0.2 M Na_2HPO_4	
Tris-base	0.1 M Citric acid	8-9.3
	0.2 M Na_2HPO_4	

7.8 Circular dichroism spectroscopy (CD)

Protein secondary structure was determined by UV circular dichroism spectroscopy (CD) (Greenfield, 2006). Purified protein samples were pipetted into a quartz cuvette, with a cell length of 0.2 cm. To ensure that there was a sufficient amount of light that reached the detector the protein samples were diluted in water until a final protein concentration in the cuvette concentration was 0.08 mg/mL. The cuvette was placed in a JASCO J-815 CD Spectrometer, purged with N_2 gas. A continuous scan from 240 nm to 190 nm was run at a scanning speed of 100 nm/min. Three scans were run for each sample and averaged. The analysis was run using Spectra Manager J-800 Control Driver software (JASCO Corporation). A final spectrum was obtained by subtracting the sample spectrum with the averaged blank spectrum using CCAplus CD Analyser System.

7.9 Size-exclusion chromatography with in-line light scattering (SEC/SLS)

Static light scattering was conducted using a Viscotek 302-040 Triple Detector GPC/SEC system (ATA Scientific), operated at 30^{o}C. 130 µL of the protein sample was injected onto a 24 mL Superdex™ 200 10/300 gel filtration column (GE Healthcare). The column had been equilibrated in phosphate buffer (50 mM $NaPO_4$, 1 mM EDTA, pH 6). Protein was eluted from the column at a flow rate of 0.5 mL/min. Absolute molecular weight, radius of hydration and size distributions was calculated using the refractive index (RI), intrinsic viscosity, and right-angle light scattering (RALS) measurements as the eluted samples passed through the detectors. Measurements were calibrated against a bovine serum albumin (BSA) standard (66.5 kDa, Sigma), which was run at the beginning and end of each sample run. Calibration was carried out using the OmniSEC software as per the manufacturer's instructions.

7.10 Analytical Ultracentrifugation (AUC)

7.10.1 AUC measurements

Sedimentation velocity experiments were used to determined the size distribution of the protein samples. The protein samples that were measured had previously been eluted down a 120 mL HiLoad™ 16/600 Superdex™ pg 200 size exclusion column (GE Healthcare), equilibrated in 50 mM phosphate buffer at pH 6.0. 380 µL of the protein sample along with 400 µL of the phosphate buffer as a reference was used for the experiments. The protein concentration was 0.5 mg/mL and 0.3 mg/mL for kiwellin and actinidin, respectively. The samples were loaded into 12 mm double-sector cells with quartz windows in an eight hole (An-50) rotor. The proteins were centrifuged at 201,600 rcf for 200 scans. UV/Vis scanning optics that were attached to the Beckman Coulter Model XL-I analytical ultracentrifuge was used to monitor the sedimentation of proteins at 285 nm. The experiment was conducted at 20^{o}C under the supervision of Dr Grant Pearce.

7.10.2 AUC data analysis

Parameters such as: buffer density (1.0027 g/mL), buffer viscosity (0.01029 cp), and the partial specific volume of actinidin (0.7232 mL/g) and kiwellin (0.70734 mL/g) were computed using SEDNTERP (Laue, 1992) and used to analyse the data by the *c*(*M*) modelled distribution in SEDFIT (Schuck, 2000).

7.11 Small angle X-ray scattering (SAXS)

7.11.1 SAXS measurements

Purified kiwellin was eluted down a 120 mL HiLoad™ 16/600 Superdex™ 200 pg size exclusion column (GE Healthcare) in preparation for the analysis. The low salt phosphate buffer that was used to equilibrate the column was also used to subtract the background scatter. The protein sample, at 5.11 mg/mL was further eluted down an in-line 3 mL Superdex 200 5/150 gel filtration column (GE Healthcare), to remove any aggregated protein immediately prior to data collection. SAXS measurements were performed at the Australian Synchrotron SAXS/WAXS beamline equipped with a Pilatus 1M detector (170 mm X 170 mm, effective pixel size, 172 X 172 µm) by Dr Grant Pearce. The wavelength of the X-rays

was 1.0332 Å. The sample-detector distance was 1600 mm, which provide a q range of 0.006-0.400 $Å^{-1}$. Data was collected using a 1.5 mm glass capillary at 20°C under a continuous flow in 2 second intervals. 2D intensity plots were radially averaged, normalised to sample transmission, and background-subtracted.

7.11.2 SAXS data analysis

The 2D scattering plots were averaged and background scattering subtracted using *Scatterbrain* software (Maxim V. Petoukhov *et al.*, 2007). The scatter intensity plot, Guinier plot, Porod volume, and Kratky plot were generated using PRIMUS (Konarev *et al.*, 2003). Indirect Fourier transform was performed using GNOM (Svergun, 1992) to yield the real-space function $P(r)$, which gives both the relative probabilities of distances between scattering centres and the maximum dimension of the scattering particle, D_{max}. GASBOR (Svergun, 1992) was used for *ab initio* reconstruction of a 3D envelope model using the SAXS data.

7.12 Crystallography screening

Crystal trays using the sitting drop method were laid down by use of a mosquito® Crystal automated liquid distributer (TTP Labtech) in an attempt to crystallise kiwellin. 300 nL of purified kiwellin at a concentration of 9.4 mg/mL ($Abs_{280\ nm}$) was added drop-wise to each condition. From a 40 µL stock solution of each crystal screen condition 300 nL was taken and added to the protein droplet. The screening conditions chosen were: JSCG, Morpheus, PAC, and Clear Screen 1 (Molecular Dimensions). The 96 well plates were covered and incubated at 20°C. At time intervals of two weeks, one month, and two months the crystal trays were checked to identify any crystal formation by use of light microscopy.

7.13 Actinidin activity kinetics

7.13.1 General methods

The assay used for the kinetic analysis of actinidin has been used extensively in previous studies (Baker *et al.*, 1980; Boland *et al.*, 1972) and was chosen as it gave fast and replicable results. The reagents used in each assay and their respective concentrations are shown in Table 14. Both the reagents, N-α-carbobenzoxy-L-lysine-*p*-nitrophenyl ester (CBZ-Lys-ONP)

and cysteine were prepare using water as fresh solutions each time an activity assay experiment was conducted and were stored on ice. The protein sample, containing actinidin was also stored on ice throughout the assays, unless otherwise stated. Buffer was added to the cuvette until a final volume of 1 mL was reached. The buffer used for all assays was a phosphate buffer (100 mM $NaPO_4$, 1 mM EDTA, pH 6), however during actinidin purification the strength of phosphate was reduced to 50 mM. Neither buffer showed a strong blank rate when CBZ-Lys-ONP was assayed with buffer alone and was pre-incubated at room temperature before it was added to the cuvette. The addition of cysteine to the assay did, however show a concentration dependent degradation of the substrate. A blank rate containing cysteine, buffer, and CBZ-Lys-ONP was subtracted from all activity rates that contained these reagents.

Table 14: Summary of reagents used for most assays and the concentration that were present in the 1 mL assay.

Reagent	**Stock solution**	**Volume added**	**Final cuvette concentration**
Enzyme	Variable	25 or 50 µL	Variable
CBZ-Lys-ONP	8 mM	25 µL	200 µM
Cysteine	100 mM	50 µL	5 mM
Phosphate buffer	100 mM $NaPO_4$	875/900 µL	100 mM $NaPO_4$
	1 mM EDTA		1 mM EDTA
	pH 6		pH 6

The assays were run for 1.5 minutes at 25^{o}C using a Cary 100 Bio UV-Visible Spectrophotometer (Agilient Technologies). The absorbance change at 348 nm was recorded after the reaction was initiated by the addition of CBZ-Lys-ONP. The reaction rate was measured by calculating the gradient of the linear portion of the slope at the start of the reaction, which was between the time points of 10-50 seconds. Assays were run in either duplicates or triplicates.

7.13.2 Kinetic analysis of fresh fruit

The actinidin activity from the fresh fruit obtained from Kiwifruit Processing Company Ltd and the fruit used to measure activity variations between individual fruits was processed and assayed using an analogous method. The fruit was deskinned, deseeded, and the core was

removed, which left the outer pericarp tissue (flesh). The flesh was homogenised for 30-60 seconds in a 2:1 ratio of phosphate buffer (100 mM, pH 6) (mL) and flesh (g). The sample was centrifuged at 10,000 rcf for 10 minutes at 4^{o}C. The supernatant was decanted from the insoluble material and diluted 4 fold. Either 25 or 50 µL of the kiwifruit sample was used for the assays. 5 mM of cysteine was added to the cuvette to prevent any inactivation from occurring. A blank rate of 5 mM cysteine and CBZ-Lys-ONP was measured and subtracted from the activity rate.

7.13.3 Kinetic analysis of samples before and after lyophilisation

To determine whether freeze drying was affecting the retention of actinidin the activity difference between the frozen pulp and freeze dried kiwifruit powder was measured. Pulp and powder samples (4) were taken within the same region as their respective temperature data logger, which was used to measure the temperature throughout the transformation.

Both the pulp (after being defrosted) and kiwifruit powder from Genesis Bio-Lab was weighed out to a kiwifruit dry weight concentration of 100 mg/ml. The water content of kiwifruit at 85% was taken into consideration when calculating the weight needed for the desired concentration of dry weight in the pulp sample. Phosphate buffer (100 mM, pH 6) was added to the sample to obtain the concentration. The samples were then centrifuged at 14,000 rcf for 5 minutes at room temperature before the supernatant was diluted 5 fold and assayed. The assay cuvette contained 5 mM cysteine to prevent inactivation and the blank rate was correctly accounted for.

7.13.4 Michaelis-Menten kinetics

Kinetic parameters for the activity assay were calculated from the relationship between enzymatic activity and substrate concentration. The substrate concentration was increased by pipetting a larger volume of substrate from a 8 mM stock solution. 16 concentrations of the substrate were measured that ranged from 7 µM to 720 µM. The enzyme concentration remained constant for each assay by adding 50 µL of a purified actinidin stock solution of 0.034 mg/mL ($Abs_{280\ nm}$) to each cuvette. This gave a final cuvette concentration of 0.072 µM.

7.13.5 Effect that pH on activity rates

The effect that pH had on the activity was assessed using buffer solutions with a pH range of 2-9. The buffers that were used was either citric, citric-phosphate, or a tris-base buffer (Table 13). A blank rate of buffer and CBZ-Lys-ONP was measured for each pH condition. This rate was subtracted from the activity rate measured in the presence of actinidin before specific activity was calculated. 50 µL of actinidin from a stock solution of 0.12 mg/mL ($Abs_{280\ nm}$) was added to the cuvette, which gave a final cuvette concentration of 0.25 µM.

7.13.6 Time dependent inactivation

The time dependent inactivation measured any loss of actinidin kinetic activity over 120 minutes after the kiwifruit sample was prepared. Freeze dried kiwifruit powder was solubilised in phosphate buffer (100 mM, pH 6) at a concentration of 100 mg/mL. The samples were then centrifuged at 9,700 rcf for 2 minutes at room temperature. The resulting supernatant was diluted 5 fold and assayed immediately using 25 µL of this stock solution. Assays were conducted every 5 minutes thereafter and samples were stored at room temperature.

7.13.7 Effect of vitamin C on activity rates

A concentration range of vitamin C measured the effects that vitamin C had on activity rates. From a 1 M stock solution of vitamin C varying volumes were pipetted into the cuvette to obtain final concentrations of: 0, 1, 10, 20, 40, 60, 80 and 100 mM. The ascorbate dibasic sodium salt was used as opposed to ascorbic acid due to the acidic pH change that occurred when using ascorbic acid. 50 µL of purified actinidin from a stock solution of 0.042 mg/mL ($Abs_{280\ nm}$) gave an assay concentration of 0.088 µM.

7.13.8 Effect of dissolved oxygen on activity rates

Dissolved oxygen present in the buffer was measured to understand whether this could have an impact on actinidin activity. A YSI550A portable dissolved oxygen probe (YSI) was used to measure the dissolved oxygen present in the phosphate buffer before and after it was degassed. The buffer, that was added to the cuvette to make a final volume 1 mL was degassed under a vacuum while a stirring bar was used to release the oxygen for approximately one hour. Oxygen was further released from the buffer by placing the buffer in

a sonicating bath for 5 minutes (not under vacuum). Assays were conducted immediately after 50 µL of purified actinidin was added to the cuvette or after the cuvette, which contained the enzyme was incubated at room temperature for one hour. The cuvette that was incubated either did or did not contain vitamin C at a concentration of 20 mM. The enzyme stock solution concentration was 0.042 mg/mL ($Abs_{280\ nm}$), which gave an assay concentration of 0.088 µM.

7.13.9 Activation of actinidin using reducing agents

The inactivation of actinidin in the powder was reversed by incubating samples in the presence of a reducing agent, prior to the sample being assayed. Dithiothreitol (DTT), cysteine, and β-mercaptoethanol were added to an assay containing kiwifruit powder that was being measured over a period of 120 minutes. The final cuvette concentration for each reducing agent was 5 mM and this was achieved by pipetting 50 µL of the appropriate reducing agent into the cuvette from a 100 mM stock solution. The activity of actinidin present in kiwifruit powder (100 mg/mL) was measured every 30 minutes as a control. After the control sample was measured for its drop in activity the assay was repeated in the presence of the respective reducing agent after a 2 minute incubation period.

7.13.10 Concentration dependent activation of actinidin with cysteine

The concentration effects of cysteine on the activation of actinidin, present in the kiwifruit powder was measured to observe any differences over a 30 hour time period. Cysteine was pipetted into the kiwifruit powder sample (100 mg/mL) from a 100 mM stock solution to give a final concentration of either: 1, 3, 5, 10, 20, 30, or 40 mM. The protective effect of cysteine on actinidin activity was monitored by taking activity measurements at the time points of: 0, 5, 10, 20, 25, and 30 hours.

Chapter Eight : References

Arakawa, T., Prestrelski, S. J., Kenney, W. C., & Carpenter, J. F. (2001). Factors affecting short-term and long-term stabilities of proteins. *Advanced Drug Delivery Reviews, 46*(1-3), 307-326.

Armstrong, D. A., & Buchanan, J. D. (1978). Reaction of O2-, H2O2 and other oxidants with sulfhydryl enzymes. *Photochemistry and Photobiology, 28*(4-5), 743-755.

Baker, E. N. (1980). Structure of actinidin, after refinement at 1.7 A resolution. *J Mol Biol, 141*(4), 441-484.

Baker, E. N., Boland, M. J., Calder, P. C., & Hardman, M. J. (1980). The specificity of actinidin and its relationship to the structure of the enzyme. *Biochim Biophys Acta, 616*(1), 30-34.

Bernardi, M. L., Picone, D., Tuppo, L., Giangrieco, I., Petrella, G., Palazzo, P., et al. (2010). Physico-chemical features of the environment affect the protein conformation and the immunoglobulin E reactivity of kiwellin (Act d 5). *Clin Exp Allergy, 40*(12), 1819-1826.

Boland, M. J., & Hardman, M. J. (1972). Kinetic studies on the thiol protease from Actinidia chinensis. *FEBS Lett, 27*(2), 282-284.

Bonvehi, J. S., Jorda, R. E., & Jaen, J. A. (1997). The ripening process of kiwifruits (Actinidia deliciosa) grown in Catalonia, Spain. *Journal of Food Quality, 20*(5), 371-380.

Boyes, S., Strubi, P., & Marsh, H. (1997). Actinidin levels in fruit of Actinidia species and some Actinidia arguta rootstock scion combinations. *Food Science and Technology-Lebensmittel-Wissenschaft & Technologie, 30*(4), 379-389.

Boyes, S., Strübi, P., & Marsh, H. (1997). Sugar and Organic Acid Analysis ofActinidia argutaand Rootstock–Scion Combinations ofActinidia arguta. *LWT - Food Science and Technology, 30*(4), 390-397.

Bradford, M. M. (1976). Rapid and sensitive method for quantitation of microgram quantities of protein utilizing principle of protein-dye binding *Analytical Biochemistry, 72*(1-2), 248-254.

Brevik, A., Gaivao, I., Medin, T., Jorgenesen, A., Piasek, A., Elilasson, J., et al. (2011).

Supplementation of a western diet with golden kiwifruits (Actinidia chinensis var.'Hort 16A':) effects on biomarkers of oxidation damage and antioxidant protection. *Nutr J, 10*, 54.

Brocklehurst, K., Baines, B. S., & Malthouse, J. P. (1981). Differences in the interaction of the catalytic groups of the active centres of actinidin and papain. Rapid purification of fully active actinidin by covalent chromatography and characterization of its active centre by use of two-protonic-state reactivity probes. *Biochem J, 197*(3), 739-746.

Brocklehurst, K., Willenbrock, F., & Salih, E. (1987). Chapter 2 Cysteine proteinases. In A. Neuberger & K. Brocklehurst (Eds.), *New Comprehensive Biochemistry* (Vol. Volume 16, pp. 39-158).

Bujacz, A. (2012). Structures of bovine, equine and leporine serum albumin. *Acta Crystallogr D Biol Crystallogr, 68*(Pt 10), 1278-1289.

Buttriss, J. L., & Stokes, C. S. (2008). Dietary fibre and health: an overview. *Nutrition Bulletin, 33*(3), 186-200.

Carotti, A., Hansch, C., Mueller, M. M., & Blaney, J. M. (1984). Actinidin hydrolysis of substituted-phenyl hippurates: a quantitative structure-activity relationship and graphics comparison with hydrolysis by papain. *J Med Chem, 27*(11), 1401-1405.

Carpenter, J. F., & Crowe, J. H. (1989). An infrared spectroscopic study of the interactions of carbohydrates with dried proteins. *Biochemistry, 28*(9), 3916-3922.

Carpenter, J. F., Crowe, L. M., & Crowe, J. H. (1987). Stabilization of phosphofructokinase with sugars during freeze-drying-characterization of enhanced protection in the presence of divalent-cations. *Biochim Biophys Acta, 923*(1), 109-115.

Cavic, M., Grozdanovic, M., Bajic, A., Srdic-Rajic, T., Andjus, P. R., & Gavrovic-Jankulovic, M. (2012). Actinidin, a protease from kiwifruit, induces changes in morphology and adhesion of T84 intestinal epithelial cells. *Phytochemistry, 77*, 46-52.

Chan, A. O. O., Leung, G., Tong, T., & Wong, N. Y. H. (2007). Increasing dietary fiber intake in terms of kiwifruit improves constipation in Chinese patients. *World Journal of Gastroenterology, 13*(35), 4771-4775.

Chang, C.-C., Lin, Y.-T., Lu, Y.-T., Liu, Y.-S., & Liu, J.-F. (2010). Kiwifruit improves bowel function in patients with irritable bowel syndrome with constipation. *Asia Pacific Journal of Clinical Nutrition, 19*(4), 451-457.

Ciacci, C., Russo, I., Bucci, C., Iovino, P., Pellegrini, L., Giangrieco, I., Tamburrini, M., & Ciardiello, M. A. (2013). The Kiwifruit Peptide Kissper Displays Anti-Inflammatory

and Antioxidant Effects in In Vitro And Ex Vivo Human Intestinal Models. *Clin Exp Immunol*.

Ciardiello, M. A., Giangrieco, I., Tuppo, L., Tamburrini, M., Buccheri, M., Palazzo, P., Bernardi, M. L., Ferrara, R., & Mari, A. (2009). Influence of the Natural Ripening Stage, Cold Storage, and Ethylene Treatment on the Protein and IgE-Binding Profiles of Green and Gold Kiwi Fruit Extracts. *J Agric Food Chem, 57*(4), 1565-1571.

Ciardiello, M. A., Meleleo, D., Saviano, G., Crescenzo, R., Carratore, V., Camardella, L., et al. (2008). Kissper, a kiwi fruit peptide with channel-like activity: structural and functional features. *J Pept Sci, 14*(6), 742-754.

Crowhurst, R. N., Gleave, A. P., MacRae, E. A., Ampomah-Dwamena, C., Atkinson, R. G., Beuning, L. L., et al. (2008). Analysis of expressed sequence tags from Actinidia: Applications of a cross species EST database for gene discovery in the areas of flavor, health, color and ripening. *Bmc Genomics, 9*.

Cruz-Castillo, J. G., Baldicchi, A., Frioni, T., Marocchi, F., Moscatello, S., Proietti, S., Battistelli, A., & Famiani, F. (2014). Pre-anthesis CPPU low dosage application increases 'Hayward' kiwifruit weight without affecting the other qualitative and nutritional characteristics. *Food Chem, 158*(0), 224-228.

D'Avino, R., Bernardi, M. L., Wallner, M., Palazzo, P., Camardella, L., Tuppo, L., et al. (2011). Kiwifruit Act d 11 is the first member of the ripening-related protein family identified as an allergen. *Allergy, 66*(7), 870-877.

Datson, P. M., & Ferguson, A. R. (2011). Actinidia. In C. Kole (Ed.), *Wild Crop Relatives: Genomic and Breeding Resources* (pp. 1-20).

Drossman, D. A. (2006). The functional gastrointestinal disorders and the Rome III process. *Gastroenterology, 130*(5), 1377-1390.

Du, G., Li, M., Ma, F., & Liang, D. (2009). Antioxidant capacity and the relationship with polyphenol and Vitamin C in Actinidia fruits. *Food Chem, 113*(2), 557-562.

Edmunds, S. J., Roy, N. C., Davy, M., Cooney, J. M., Barnett, M. P. G., Zhu, S., Park, Z., Love, D. R., & Laing, W. A. (2012). Effects of kiwifruit extracts on colonic gene and protein expression levels in IL-10 gene-deficient mice. *British Journal of Nutrition, 108*(1), 113-129.

Edmunds, S. J., Roy, N. C., Love, D. R., & Laing, W. A. (2011). Kiwifruit extracts inhibit cytokine production by lipopolysaccharide-activated macrophages, and intestinal epithelial cells isolated from IL10 gene deficient mice. *Cellular Immunology, 270*(1),

70-79.

Eshamah, H., Han, I., Naas, H., Acton, J., & Dawson, P. (2014). Antibacterial effects of natural tenderizing enzymes on different strains of Escherichia coli O157:H7 and Listeria monocytogenes on beef. *Meat Sci*(0).

FAOSTAT. (2012). Food and Agriculture Organization of the United Nations. (7 July 2014). Retrieved from http://faostat3.fao.org/faostat-gateway/go/to/download/Q/QC/E

Ferguson, A. R. (2004). 1904 - the year that kiwifruit (Actinidia deliciosa) came to New Zealand. *New Zealand Journal of Crop and Horticultural Science, 32*(1), 3-27.

Ferrandino, A., & Lovisolo, C. (2014). Abiotic stress effects on grapevine (Vitis vinifera L.): Focus on abscisic acid-mediated consequences on secondary metabolism and berry quality. *Environmental and Experimental Botany, 103*, 138-147.

Fiorentino, A., D'Abrosca, B., Pacifico, S., Mastellone, C., Scognamiglio, M., & Monaco, P. (2009). Identification and Assessment of Antioxidant Capacity of Phytochemicals from Kiwi Fruits. *J Agric Food Chem, 57*(10), 4148-4155.

Fukal, L., Kas, J., & Rauch, P. (1984). Inactivation of papain proteolytic activity in the presence of ascorbic acid and Cu++ ions. *Journal of the Institute of Brewing, 90*(2), 73-76.

Gasteiger, E., Hoogland, C., Gattiker, A., Duvaud, S. e., Wilkins, M., Appel, R., & Bairoch, A. (2005). Protein Identification and Analysis Tools on the ExPASy Server. In J. Walker (Ed.), *The Proteomics Protocols Handbook* (pp. 571-607).

Gavrovic-Jankulovic, M., cIrkovic, T., Vuckovic, O., Atanaskovic-Markovic, M., Petersen, A., Gojgic, G., Burazer, L., & Jankov, R. M. (2002). Isolation and biochemical characterization of a thaumatin-like kiwi allergen. [Research Support, Non-U.S. Gov't]. *J Allergy Clin Immunol, 110*(5), 805-810.

Gerasopoulos, D., & Drogoudi, P. D. (2005). Summer-pruning and preharvest calcium chloride sprays affect storability and low temperature breakdown incidence in kiwifruit. *Postharvest Biology and Technology, 36*(3), 303-308.

Gorinstein, S., Zemser, M., Friedman, M., Rodrigues, W. A., Martins, P. S., Vello, N. A., Tosello, G. A., & ParedesLopez, O. (1996). Physicochemical characterization of the structural stability of some plant globulins. *Food Chem, 56*(2), 131-138.

Greenfield, N. J. (2006). Using circular dichroism spectra to estimate protein secondary structure. *Nature Protocols, 1*(6), 2876-2890.

Grozdanovic, M., Popovic, M., Polovic, N., Burazer, L., Vuckovic, O., Atanaskovic-

Markovic, M., Lindner, B., Petersen, A., & Gavrovic-Jankulovic, M. (2012). Evaluation of IgE reactivity of active and thermally inactivated actinidin, a biomarker of kiwifruit allergy. [Research Support, Non-U.S. Gov't]. *Food Chem Toxicol, 50*(3-4), 1013-1018.

Grozdanovic, M. M., Ostojic, S., Aleksic, I., Andjelkovic, U., Petersen, A., & Gavrovic-Jankulovic, M. (2014). Active actinidin retains function upon gastro-intestinal digestion and is more thermostable than the E-64-inhibited counterpart. *J Sci Food Agric*.

Gudkov, S. V., Karp, O. E., Garmash, S. A., Ivanov, V. E., Chernikov, A. V., Manokhin, A. A., Astashev, M. E., Yaguzhinsky, L. S., & Bruskov, V. I. (2012). Generation of reactive oxygen species in water under exposure to visible or infrared irradiation at absorption bands of molecular oxygen. *Biophysics, 57*(1), 1-8.

Ha, M., Bekhit, A. E.-D., & Carne, A. (2014). Effects of L- and iso-ascorbic acid on meat protein hydrolyzing activity of four commercial plant and three microbial protease preparations. *Food Chem, 149*, 1-9.

Ha, M., Bekhit, A. E., Carne, A., & Hopkins, D. L. (2013). Characterisation of kiwifruit and asparagus enzyme extracts, and their activities toward meat proteins. *Food Chem, 136*(2), 989-998.

Ha, M., Bekhit, A. E. A., Carne, A., & Hopkins, D. L. (2012). Characterisation of commercial papain, bromelain, actinidin and zingibain protease preparations and their activities toward meat proteins. *Food Chem, 134*(1), 95-105.

Hedoux, A., Paccou, L., Achir, S., & Guinet, Y. (2013). Mechanism of protein stabilization by trehalose during freeze-drying analyzed by in situ micro-raman spectroscopy. *Journal of Pharmaceutical Sciences, 102*(8), 2484-2494.

Kamphuis, I. G., Drenth, J., & Baker, E. N. (1985). Thiol proteases. Comparative studies based on the high-resolution structures of papain and actinidin, and on amino acid sequence information for cathepsins B and H, and stem bromelain. *J Mol Biol, 182*(2), 317-329.

Kamphuis, I. G., Kalk, K. H., Swarte, M. B. A., & Drenth, J. (1984). Structure of papain refined at 1.65 Å resolution. *J Mol Biol, 179*(2), 233-256.

Kanazawa, H., Fujimoto, S., & Ohara, A. (1994). On the mechanism of inactivation of active papain by ascorbic-acid in the presence of cupric ions. *Biological & Pharmaceutical Bulletin, 17*(6), 789-793.

Karlsen, A., Svendsen, M., Seljeflot, I., Laake, P., Duttaroy, A. K., Drevon, C. A., Arnesen, H., Tonstad, S., & Blomhoff, R. (2013). Kiwifruit decreases blood pressure and whole-blood platelet aggregation in male smokers. *Journal of Human Hypertension, 27*(2), 126-130.

Katsaros, G. I., Tavantzis, G., & Taoukis, P. S. (2010). Production of novel dairy products using actinidin and high pressure as enzyme activity regulator. *Innovative Food Science and Emerging Technologies, 11*(1), 47-51.

Kaur, L., Rutherfurd, S. M., Moughan, P. J., Drummond, L., & Boland, M. J. (2010a). Actinidin enhances gastric protein digestion as assessed using an in vitro gastric digestion model. *J Agric Food Chem, 58*(8), 5068-5073.

Kaur, L., Rutherfurd, S. M., Moughan, P. J., Drummond, L., & Boland, M. J. (2010b). Actinidin enhances protein digestion in the small intestine as assessed using an in vitro digestion model. *J Agric Food Chem, 58*(8), 5074-5080.

Kitts, D. D., & Weiler, K. (2003). Bioactive proteins and peptides from food sources. Applications of bioprocesses used in isolation and recovery. *Current Pharmaceutical Design, 9*(16), 1309-1323.

Kiwifruit-Vine-Health. (2014). Kiwifruit Vine Health Psa Statistics. Retrieved from http://www.kvh.org.nz/vdb/document/453

Ko, S. H., Choi, S. W., Ye, S. K., Cho, B. L., Kim, H. S., & Chung, M. H. (2005). Comparison of the antioxidant activities of nine different fruits in human plasma. *Journal of Medicinal Food, 8*(1), 41-46.

Konarev, P. V., Volkov, V. V., Sokolova, A. V., Koch, M. H. J., & Svergun, D. I. (2003). PRIMUS: a Windows PC-based system for small-angle scattering data analysis. *Journal of Applied Crystallography, 36*, 1277-1282.

Konno, K., Hirayama, C., Nakamura, M., Tateishi, K., Tamura, Y., Hattori, M., & Kohno, K. (2004). Papain protects papaya trees from herbivorous insects: role of cysteine proteases in latex. *Plant Journal, 37*(3), 370-378.

Laue, T. M. S., B.D. Ridgeway, T.M. Pelletier, S.L. (1992). *Analyticall Ultracentrifugation in Biochemistry and Polymer Science*: Royal Society of Chemistry.

Lee, Y. J., & Park, K. S. (2014). Irritable bowel syndrome: Emerging paradigm in pathophysiology. *World Journal of Gastroenterology, 20*(10), 2456-2469.

Lewis, D. A., & Luh, B. S. (1988). Development and distribution of actinidin in kiwifruit (Actinidia-chinensis) and its partial characterization. *Journal of Food Biochemistry,*

12(2), 109-116.

Lin, W. S., Armstrong, D. A., & Gaucher, G. M. (1975). Formation and repair of papain sulfenic acid. *Canadian Journal of Biochemistry, 53*(3), 298-307.

Lin, W. S., Clement, J. R., Gaucher, G. M., & Armstrong, D. A. (1975). Repairable and nonrepariable inactivation of irradiated aqueous papain: effects of OH, O2-, eaq-, and H2O2. *Radiation Research, 62*(3), 438-455.

Luo, D. Y., Smith, S. W., & Anderson, B. D. (2005). Kinetics and mechanism of the reaction of cysteine and hydrogen peroxide in aqueous solution. *Journal of Pharmaceutical Sciences, 94*(2), 304-316.

Maddumage, R., Nieuwenhuizen, N. J., Bulley, S. M., Cooney, J. M., Green, S. A., & Atkinson, R. G. (2013). Diversity and relative levels of actinidin, kiwellin, and thaumatin-like allergens in 15 varieties of kiwifruit (Actinidia). *J Agric Food Chem, 61*(3), 728-739.

Matsubara, T., Fujita, R., Sugiyama, S., & Kawashiro, K. (2006). Stability of protease in organic solvent: Structural identification by solid-state NMR of lyophilized papain before and after 1-propanol treatment and the corresponding enzymatic activities. *Biotechnology and Bioengineering, 93*(5), 928-933.

Mazzaglia, A., Studholme, D. J., Taratufolo, M. C., Cai, R. M., Almeida, N. F., Goodman, T., Guttman, D. S., Vinatzer, B. A., & Balestra, G. M. (2012). Pseudomonas syringae pv. actinidiae (PSA) Isolates from Recent Bacterial Canker of Kiwifruit Outbreaks Belong to the Same Genetic Lineage. *PLoS One, 7*(5).

Meleleo, D., Gallucci, E., Notarachille, G., Sblano, C., Alessandra, S., & Micelli, S. (2012). Studies on the Effect of Salts on the Channel Activity of Kissper, a Kiwi Fruit Peptide. *The Open Nutraceuticals Journal, 5*, 136-145.

Miller, S. A., Broom, F. D., Thorp, T. G., & Barnett, A. M. (2001). Effects of leader pruning on vine architecture, productivity and fruit quality in kiwifruit (Actinidia deliciosa cv. Hayward). *Scientia Horticulturae, 91*(3–4), 189-199.

Ministry-of-Health. (2003). Food and Nutrition Guidelines for Healthy Adults: A background paper. Retrieved from https://www.health.govt.nz/system/files/documents/publications/foodandnutritionguidelines-adults.pdf

Mishra, S., & Monro, J. (2012). Kiwifruit remnants from digestion in vitro have functional attributes of potential importance to health. *Food Chem, 135*(4), 2188-2194.

Montoya, C. A., Hindmarsh, J. P., Gonzalez, L., Boland, M. J., Moughan, P. J., & Rutherfurd, S. M. (2014). Dietary Actinidin from Kiwifruit (Actinidia deliciosa cv. Hayward) Increases Gastric Digestion and the Gastric Emptying Rate of Several Dietary Proteins in Growing Rats. *Journal of Nutrition, 144*(4), 440-446.

Morimoto, K. T., M. Tonomura, B (2002). The steady-state and the pre-steady-state kinetic analysis of the hydrolysis of *N*-α-Cbz-L-Lysine *p*-nitrophenyl ester catalysed by actinidain isozymes. *Memoirs of the School of B.O.S.T.*(10), 29-37.

Motohashi, N., Shirataki, Y., Kawase, M., Tani, S., Sakagami, H., Satoh, K., et al. (2002). Cancer prevention and therapy with kiwifruit in Chinese folklore medicine: a study of kiwifruit extracts. *Journal of Ethnopharmacology, 81*(3), 357-364.

MPI. (2014). Situation and Outlook for Primary Industries. Retrieved from http://www.mpi.govt.nz/news-resources/publications.aspx?title=Situation+and+Outlook+for+Primary+Industries&keywords=SOPI&2012

Nagaoka, Y., Otsu, K., Okada, F., Sato, K., Ohba, Y., Kotani, N., & Fujii, J. (2005). Specific inactivation of cysteine protease-type cathepsin by singlet oxygen generated from naphthalene endoperoxides. *Biochemical and Biophysical Research Communications, 331*(1), 215-223.

Niesen, F. H., Berglund, H., & Vedadi, M. (2007). The use of differential scanning fluorimetry to detect ligand interactions that promote protein stability. *Nature Protocols, 2*(9), 2212-2221.

Nieuwenhuizen, N. J., Beuning, L. L., Sutherland, P. W., Sharma, N. N., Cooney, J. M., Bieleski, L. R. F., Schröder, R., MacRae, E. A., & Atkinson, R. G. (2007). Identification and characterisation of acidic and novel basic forms of actinidin, the highly abundant cysteine protease from kiwifruit. *Functional Plant Biology, 34*(10), 946-961.

Nieuwenhuizen, N. J., Maddumage, R., Tsang, G. K., Fraser, L. G., Cooney, J. M., De Silva, H. N., Green, S., Richardson, K. A., & Atkinson, R. G. (2012). Mapping, complementation, and targets of the cysteine protease actinidin in kiwifruit. *Plant Physiol, 158*(1), 376-388.

Notredame, C., Higgins, D. G., & Heringa, J. (2000). T-Coffee: A novel method for fast and accurate multiple sequence alignment. *J Mol Biol, 302*(1), 205-217.

NZ-Statistics. (2007). Agricultural Production Statistics. Retrieved from

http://www.stats.govt.nz/~/media/Statistics/Browse%20for%20stats/AgriculturalProduction/HOTPJun07final/agriculturalproductionstatisticsfinaljun07hotp.pdf

Offer, T., Mohsen, M., & Samuni, A. (1998). An SOD-mimicry mechanism underlies the role of nitroxides in protecting papain from oxidative inactivation. *Free Radical Biology and Medicine, 25*(7), 832-838.

Ozawa, K., Tanaka, S., & Ohnishi, T. (1962). Activation and inhibition of papain. *J Biochem, 51*(5), 372-374.

Petoukhov, M. V., Konarev, P. V., Kikhney, A. G., & Svergun, D. I. (2007). ATSAS 2.1 - towards automated and web-supported small-angle scattering data analysis. *Journal of Applied Crystallography, 40*, S223-S228.

Petoukhov, M. V., Svergun, D. I., Konarev, P. V., Ravasio, S., van den Heuvel, R. H. H., Curti, B., & Vanoni, M. A. (2003). Quaternary structure of Azospirillum brasilense NADPH-dependent glutamate synthase in solution as revealed by synchrotron radiation x-ray scattering. *Journal of Biological Chemistry, 278*(32), 29933-29939.

Podivinsky, E., Forster, R. L., & Gardner, R. C. (1989). Nucleotide sequence of actinidin, a kiwi fruit protease. *Nucleic Acids Res, 17*(20), 8363.

Préstamo, G. (1995). Actinidin in kiwifruit cultivars. *Zeitschrift für Lebensmittel-Untersuchung und -Forschung, 200*(1), 64-66.

Prestrelski, S. J., Tedeschi, N., Arakawa, T., & Carpenter, J. F. (1993). Dehydration-induced conformational transitions in proteins and their inhibition by stabilizers. *Biophysical Journal, 65*(2), 661-671.

Putnam, C. D., Hammel, M., Hura, G. L., & Tainer, J. A. (2007). X-ray solution scattering (SAXS) combined with crystallography and computation: defining accurate macromolecular structures, conformations and assemblies in solution. *Quarterly Reviews of Biophysics, 40*(3), 191-285.

Rawlings, N. D., Barrett, A. J., & Bateman, A. (2012). MEROPS: the database of proteolytic enzymes, their substrates and inhibitors. *Nucleic Acids Res, 40*(D1), D343-D350.

Reid, J. D., Hussain, S., Sreedharan, S. K., Bailey, T. S. F., Pinitglang, S., Thomas, E. W., Verma, C. S., & Brocklehurst, K. (2001). Variation in aspects of cysteine proteinase catalytic mechanism deduced by spectroscopic observation of dithioester intermediates, kinetic analysis and molecular dynamics simulations. *Biochemical Journal, 357*, 343-352.

Riaz, M. N., Asif, M., & Ali, R. (2009). Stability of Vitamins during Extrusion. *Crit Rev*

Food Sci Nutr, 49(4), 361-368.

Ritenour, M. A., Crisosto, C. H., Garner, D. T., Cheng, G. W., & Zoffoli, J. P. (1999). Temperature, length of cold storage and maturity influence the ripening rate of ethylene-preconditioned kiwifruit. *Postharvest Biology and Technology, 15*(2), 107-115.

Rodrigues, S., & Fernandes, F. A. N. (2012). Advances in Fruit Processing Technologies Retrieved from http://canterbury.eblib.com.au/patron/FullRecord.aspx?p=919021

Rush, E. C., Patel, M., Plank, L. D., & Ferguson, L. R. (2002). Kiwifruit promotes laxation in the elderly. *Asia Pacific Journal of Clinical Nutrition, 11*(2), 164-168.

Russo, I., Luciani, A., De Cicco, P., Troncone, E., & Ciacci, C. (2012). Butyrate Attenuates Lipopolysaccharide-Induced Inflammation in Intestinal Cells and Crohn's Mucosa through Modulation of Antioxidant Defense Machinery. *PLoS One, 7*(3).

Rutherfurd, S. M., Montoya, C. A., Zou, M. L., Moughan, P. J., Drummond, L. N., & Boland, M. J. (2011). Effect of actinidin from kiwifruit (Actinidia deliciosa cv. Hayward) on the digestion of food proteins determined in the growing rat. *Food Chem, 129*(4), 1681-1689.

Sagar, V. R., & Kumar, S. P. (2010). Recent advances in drying and dehydration of fruits and vegetables: a review. *Journal of Food Science and Technology-Mysore, 47*(1), 15-26.

Sandler, R. S., Everhart, J. E., Donowitz, M., Adams, E., Cronin, K., Goodman, C., et al. (2002). The burden of selected digestive diseases in the United States. *Gastroenterology, 122*(5), 1500-1511.

Schuck, P. (2000). Size-distribution analysis of macromolecules by sedimentation velocity ultracentrifugation and lamm equation modeling. *Biophys J, 78*(3), 1606-1619.

Singletary, K. (2012). Kiwifruit: Overview of Potential Health Benefits. *Nutrition Today, 47*(3), 133-147.

Steinmetz, K. A., & Potter, J. D. (1996). Vegetables, fruit, and cancer prevention: A review. *Journal of the American Dietetic Association, 96*(10), 1027-1039.

Sugiyama, S., Ohtsuki, K., Sato, K., & Kawabata, M. (1997). Enzymatic properties, substrate specificities and pH-activity profiles of two kiwifruit proteases. *J Nutr Sci Vitaminol (Tokyo), 43*(5), 581-589.

Svergun, D. I. (1992). Determination of the regularization parameter in indirect-transform methods using perceptual criteria. *Journal of Applied Crystallography, 25*, 495-503.

Tamburrini, M., Cerasuolo, I., Carratore, V., Stanziola, A. A., Zofra, S., Romano, L.,

Camardella, L., & Ciardiello, M. A. (2005). Kiwellin, a novel protein from kiwi fruit. Purification, biochemical characterization and identification as an allergen. *Protein Journal, 24*(7-8), 423-429.

Tello-Solis, S. R., Valle-Guadarrama, M. E., & Hernandez-Arana, A. (1995). Purification and circular dichroism studies of multiple forms of actinidin from Actinidia chinensis (kiwifruit). *Plant Science, 106*(2), 227-232.

Tommaso, P., Moretti, S., Xenarios, I., Orobitg, M., Montanyola, A., Chang, J. M., Taly, J. F., & Notredame, C. (2011). T-Coffee: a web server for the multiple sequence alignment of protein and RNA sequences using structural information and homology extension. *Nucleic Acids Res, 39*, W13-W17.

Tuppo, L., Giangrieco, I., Palazzo, P., Bernardi, M. L., Scala, E., Carratore, V., Tamburrini, M., Mari, A., & Ciardiello, M. A. (2008). Kiwellin, a modular protein from green and gold kiwi fruits: evidence of in vivo and in vitro processing and IgE binding. *J Agric Food Chem, 56*(10), 3812-3817.

USDA. (2011). USDA National Nutrient Database for Standard Reference Release 24. from http://www.ars.usda.gov/ba/bhnrc/ndl

van der Hoorn, R. A. L. (2008). Plant proteases: From phenotypes to molecular mechanisms. *Annual Review of Plant Biology, 59*, 191-223.

Warrington, I. J., Weston, G. C., & Science, N. Z. S. f. H. (1990). *Kiwifruit: Science and Management*: Ray Richards.

Xian, M., Chen, X. C., Liu, Z. Y., Wang, K., & Wang, P. G. (2000). Inhibition of papain by S-nitrosothiols - Formation of mixed disulfides. *Journal of Biological Chemistry, 275*(27), 20467-20473.

Yoon, S. L., Grundmann, O., Koepp, L., & Farrell, L. (2011). Management of irritable bowel syndrome (IBS) in adults: conventional and complementary/alternative approaches. *Altern Med Rev, 16*(2), 134-151.

Yue, S. T., Steinberg, T. H., Patton, W. F., Cheung, C. Y., & Haugland, R. P. (2003). For detecting and quantifying peptides, polypeptides and proteins; sensitive, facile and does not require use of organic solvents: Google Patents.

Zespri. (2013-2014). Zespri Annual Review. Retrieved from https://www.zespri.com/ZespriInvestorPublications/Annual-Review-2013-14.pdf